THESIS

OPTIMIZING ENERGY CONVERSION EFFICIENCY OF A PROTON EXCHANGE MEMBRANE GREEN HYDROGEN GENERATION SYSTEM WHILE INCORPORATING BALANCE OF PLANT MODELING

Submitted by

Nikolas Landin

Department of Mechanical Engineering

In partial fulfillment of the requirements

For the Degree of Master of Science

Colorado State University

Fort Collins, Colorado

Summer 2023

Master's Committee:

Advisor: Bret Windom

Thomas Bradley
David Montgomery

ABSTRACT

OPTIMIZING ENERGY CONVERSION EFFICIENCY OF A PROTON EXCHANGE MEMBRANE GREEN HYDROGEN GENERATION SYSTEM WHILE INCORPORATING BALANCE OF PLANT MODELING

Hydrogen has the potential to decarbonize several difficult to decarbonize sectors of the U.S. energy economy such as medium- and heavy-duty transportation, energy storage, and industrial processes such as steel making. Currently most of the hydrogen produced globally is produced with steam methane reforming and has a carbon intensity associated with partially burning natural gas. An alternative way of producing hydrogen is using electrolysis and renewable energy to split water into hydrogen and oxygen. Hydrogen produced in this way is called “green” hydrogen. The devices that are used to produce green hydrogen are electrolyzers and the most prominent type of electrolyzer today is the proton exchange membrane (PEM) electrolyzer. Most PEM systems are designed for continuous operation with a constant input of electricity. When PEM electrolyzers are coupled with renewable energy such as wind turbines and solar photovoltaics, the input electricity to the electrolyzer may follow the same variable and intermittent profile as renewable energy generation. System modeling while including balance of plant components can be used to optimize the green hydrogen generation system for the highest energy conversion efficiency across the range of possible operating conditions with renewable energy input.

This work is focused on creating a system model of a PEM green hydrogen generation system including the balance of plant components such as power electronics, electrolyzer stack, hydrogen purification, hydrogen compression/storage, and system cooling. Literature primarily focuses on modeling the electrolyzer stack and ignores the balance of plant components. Some recent publications create system models with the balance of plant included but are

unnecessarily complex. The model created in this work includes the balance of plant and reduces the complexity of recently published balance of plant models while maintaining the model's functionality in system optimization studies. Limited experimental data available in literature is used to verify and validate the model. The model is scaled to represent a utility scale system which would include multiple electrolyzer stacks and power electronics. A case study of wind and solar generation in Texas is used to demonstrate the model's capability in optimization studies.

The model results show the effects of varying operating conditions such as electrolyzer cathode pressure and electrolyzer current density on the overall system efficiency for a single 120-kW electrolyzer green hydrogen generation system. At low electrolyzer power, the system energy conversion efficiency drops off significantly which is mainly driven by the increase in specific hydrogen loss in the balance of plant. Increasing the electrolyzer cathode pressure decreases the system efficiency and operating range but may provide benefit by allowing the hydrogen compressor to be removed from the system. Two different electrolyzer "loading" strategies were imposed on the multi-electrolyzer stack model with the Texas case study and show that there is a slight benefit in efficiency if the strategy maximizes the electrolyzer power and minimizes the amount of electricity that is wasted within the system. Other tradeoffs such as average electrolyzer power and the number of electrolyzer shutdowns are evaluated between the two loading strategies. If a minimum electrolyzer power is selected at 50% of the rated power, the parallel loading scheme produces 9,000 kg more hydrogen than the series loading scheme with the same input power profile. The model developed in this work is a valuable tool to optimize the production of green hydrogen by identifying and optimizing the interactions of different components within the system to maximize the energy conversion efficiency. Optimizing the green hydrogen generation system will improve the economic feasibility and accelerate the adoption of green hydrogen at a large scale.

ACKNOWLEDGEMENTS

There are many people who have supported me through this research and who I owe a great deal of thanks to. Dr. Bret Windom has been all one could hope for in an advisor, he has provided countless insights and suggestions on how to push my research further and create meaningful conclusions. Dr. Windom has inspired me to always pursue rewarding research and to go the extra mile to achieve a deeper understanding of the mechanical world around me. My committee members, Dr. Dave Montgomery and Dr. Thomas Bradley, have added their guidance on how to reap the most benefit out of my research and have greatly increased the quality of this work. Dr. Montgomery has given me the opportunity to expand my learning into industry and is an exemplary model of what an industry expert looks like. All my colleagues at the Powerhouse Energy Campus have been around the clock advisors and have provided rapid response feedback and troubleshooting throughout my research. My fiancé Renee has been my support from home, always willing to hear about my struggles and work with me on solutions. My parents and grandparents have allowed me to pursue higher education and get to this point in the first place. I am eternally grateful for everyone that I have mentioned who has allowed me to accomplish what I have to date and to pursue a career in energy research and development. Thank you for all the invaluable support along this journey!

TABLE OF CONTENTS

LIST OF FIGURES

CHAPTER 1: INTRODUCTION AND LITERATURE REVIEW

1.1: INTRODUCTION

Hydrogen is the most common element in the universe, but it is rarely found as pure hydrogen gas, instead it exists within molecules such as methane (CH_4) or water (H_2O). Pure hydrogen can be produced by either stripping hydrogen from hydrocarbons such as methane or by splitting water into hydrogen and oxygen. In the United States, the primary method of producing hydrogen is steam methane reforming (SMR) which has the carbon emissions associated with burning natural gas, this type of hydrogen is called “grey” hydrogen. Natural gas is a strategic and low-cost resource for the U.S. which has led to its popularity as a hydrogen feedstock. Coal gasification is another method of producing hydrogen, this hydrogen is called “black” hydrogen. Coal is an abundant and cheap resource and therefore is popular in many developing countries. Black hydrogen, much like coal fired power plants, can be the most carbon intense methods of producing hydrogen or electricity. Hydrogen produced from SMR that utilizes carbon capture is called “blue” hydrogen. While carbon capture can greatly reduce the carbon intensity of the produced hydrogen, it still must account for the upstream emissions associated with producing natural gas such as methane leakage which is more difficult to prevent and has a greater greenhouse effect compared to carbon dioxide. Another aspect of blue hydrogen that must be discussed is the maturity of the carbon capture technology and the added cost. While some solutions exist today, they are not commercially mature and often carbon capture projects run into the issue of offloading the captured carbon. If a dedicated carbon pipeline and storage facility are not available, trucks may be required to remove captured carbon and bring it to an established storage site which will add cost to the product hydrogen. Water electrolysis is a method of producing hydrogen by splitting water into hydrogen and oxygen using electrical current. Electrolyzers are the devices used to carry out the electrolysis reaction. Electrolyzers that are powered with nuclear energy produce hydrogen

which is called “pink” hydrogen. Nuclear power generation facilities operate in a very continuous fashion and therefore pink hydrogen benefits from high electrolyzer utilization factors which avoid unused expensive capital equipment. If the electrolysis process uses electricity from the grid, the resulting hydrogen is called “yellow” hydrogen. Electrolyzers used in producing yellow hydrogen can operate in a continuous fashion like pink hydrogen and can take advantage of the economic benefit of a high utilization factor. Some areas of the U.S. grid have lower carbon intensities than other areas based on the mix of energy generation sources. Some areas of the grid that are heavily coal dependent will transmit that carbon intensity to the produced yellow hydrogen. The hydrogen produced using electrolysis and renewable energy (RE) is called “green” hydrogen and has zero direct carbon emissions. Typically, green hydrogen has the lowest carbon intensity of the different hydrogen production routes depending on how the RE generators are made and how the hydrogen is transported. As it stands currently, the levelized cost to produce green hydrogen (LCOH) is estimated at around $5 per kilogram [1]. The International Energy Agency reports that the production carbon intensity of grey, blue, and green hydrogen are 10-13, 0.8-6.2, and 0 kg CO_2-eq/kg H_2 respectively [2]. In the same report, the International Energy Agency states that currently blue and green hydrogen account for less than 1% of global hydrogen production. Figure 1 shows the relative production carbon emissions intensity of each “color” of hydrogen mentioned. The carbon intensity is represented as a carbon dioxide equivalent which factors in other greenhouse gas emissions such as nitrous oxide and methane which are much more potent than CO_2.

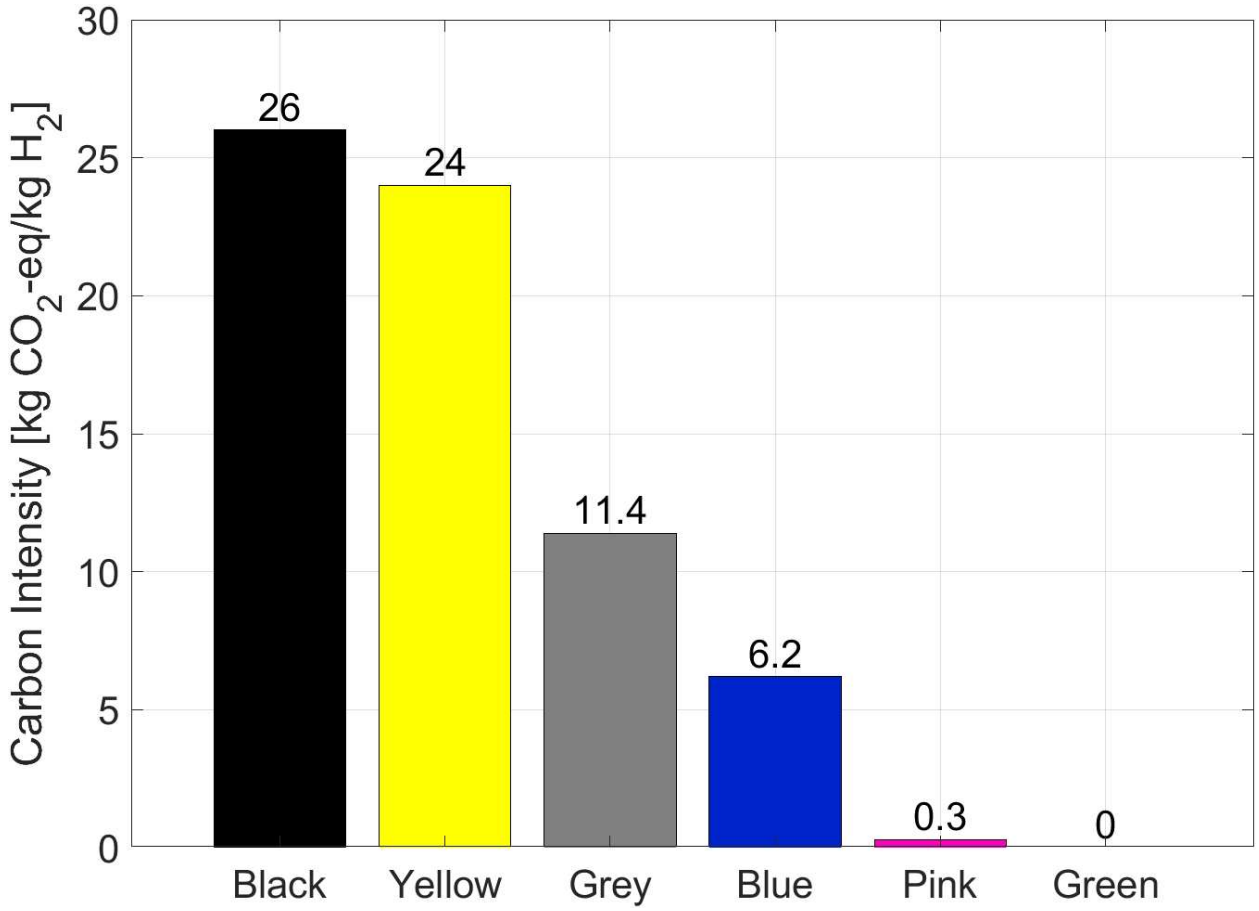

Figure 1: Carbon intensity of different hydrogen production pathways [2].

As can be seen in figure 1, using grid electricity with the average U.S. grid carbon intensity produces more carbon emissions than from SMR. For hydrogen to truly decarbonize certain hard-to-decarbonize sectors it must be produced with the lowest carbon intensity and as economically as possible. The lowest carbon intensive method of producing hydrogen is green hydrogen which uses RE to power electrolyzers. Currently PEM electrolyzers are an expensive technology and have not been deployed at scale. As electrolyzer manufacturers increase their production volumes, electrolyzers will become less expensive if the cost of the raw materials such as platinum and iridium doesn't increase dramatically. This scaling of electrolyzer production will make green hydrogen more economical and available. Other than significantly scaling electrolyzer production, optimizing green hydrogen production systems will help to make green hydrogen more economical.

Today, hydrogen is used primarily in the industrial sector to refine petroleum products, produce chemicals such as ammonia and methanol, and in treating metals [3]. Using green hydrogen specifically instead of grey hydrogen is attractive to help decarbonize the industrial sector because it is already a feedstock to large industrial applications. Additionally, green hydrogen can be utilized for seasonal energy storage. With the share of RE generation growing in the U.S. electricity grid, it is important to have enough energy storage to withstand the large fluctuations in generation seen with wind and solar photovoltaics (PV). Many states now have legislation that requires a certain amount, sometimes up to 100%, of electricity generation must come from renewable or net zero sources. Studies have shown that gaps in wind and solar generation can span multiple days and, in the worst cases, weeks [4]. Reliability and resiliency must be a major focus of developing future energy gids that will not be able to rely on fossil fuel-based generators, leading to the necessity of long duration storage that can cover multiple days and even weeks of missing generation.

Historically, batteries have been used in the case of small-scale rooftop solar and RE installations, but the economics of large-scale battery storage prevent them from being adopted for long duration storage. Figure 2 shows the energy capacity at rated discharge power and the rated discharge power of different types of energy storage technologies [5]. Hydrogen falls into the thermochemical type of energy storage which is best suited for applications where the required discharge power is high and the discharge time at rated power can reach into months of duration such as in a seasonal energy storage scenario. Batteries scale practically linearly with duration meaning that 16 hours of storage would require two 8-hour battery systems with the same amount of capital cost. Hydrogen energy storage on the other hand can keep the same rated power and increase the amount of hydrogen storage on site to reach the required discharge duration. This means that instead of requiring two 8-hour hydrogen systems, the 8-hour hydrogen system can be adapted to increase the amount of thermochemical storage of hydrogen without increasing the electrolyzer and fuel cell rating.

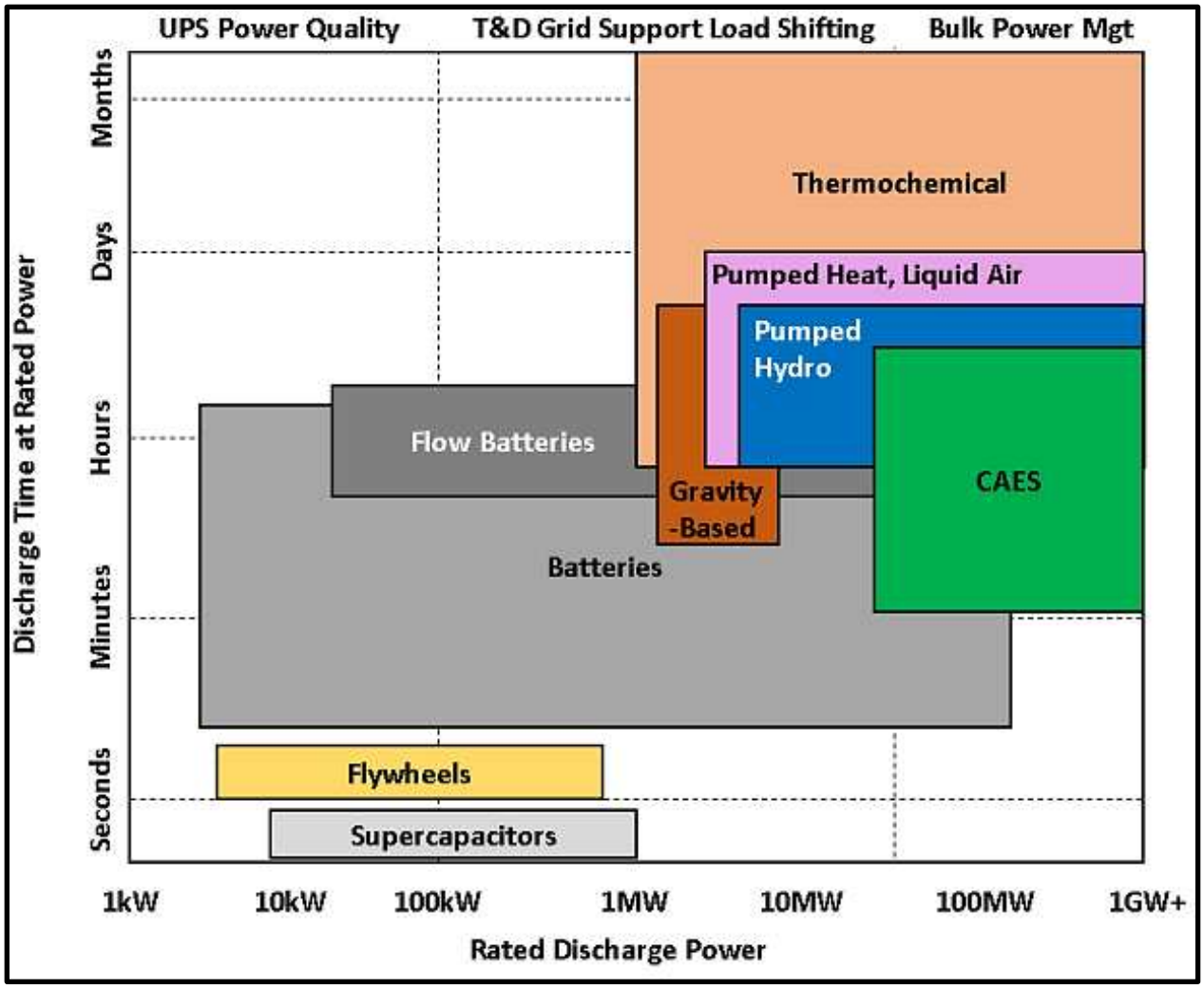

Figure 2: Discharge time at rated power vs rated discharge power comparison of energy storage technologies [5].

Most of the energy storage capacity in the U.S. is in the form of pumped hydro storage (PHS) which stores energy by pumping water to a higher elevation and then uses gravity to recover that potential energy when needed. PHS suffers from geological constraints that limit where the technology can be applied. Because green hydrogen generation systems do not experience the same economy of scale as batteries do, they are a promising solution for long duration storage.

The working principle of water electrolysis is where a current flow between electrodes separates water into hydrogen and oxygen and selectively outputs hydrogen. Commercial

electrolyzers utilize three different technologies: proton exchange membrane (PEM), alkaline, and solid oxide electrolyzers (SOEC). The three technologies have different approaches with how they selectively transmit hydrogen or oxygen and even what working fluid they use. The two reactions that allow water electrolysis to occur are the oxygen evolution reaction (OER) which generates molecular oxygen and hydrogen evolution reaction (HER) which generates molecular hydrogen. The OER occurs at the anode while the HER occurs at the cathode.

PEM electrolyzers operate by selectively transmitting positive hydrogen ions between the anode and cathode. For PEM electrolysis the OER is represented as chemical equation 1.

$$H_2O \rightarrow {}^{1}/_{2}\, O_2 + 2H^+ + 2e^- \qquad \text{Eq. 1}$$

Where one water molecule (H_2O) is broken up into half of an oxygen molecule (${}^{1}/_{2}\, O_2$), two positive hydrogen ions (H^+), and two electrons (e^-). The HER for PEM is represented as chemical equation 2.

$$2H^+ + 2e^- \rightarrow H_2 \qquad \text{Eq. 2}$$

Where the two positive hydrogen ions (H^+) recombine with two electrons (e^-) to form one hydrogen molecule (H_2). PEM electrolyzers are stacks of individual cells arranged in series. The cells are typically constructed with bi-polar plates (BPP), current collectors, and the membrane electrode assembly (MEA). The BPPs are conductive plates, normally with grooves, and have two functions: to conduct current to the adjacent cells and separate the hydrogen and oxygen from other cells. The current collectors are a porous conducting material that function by allowing water and gas to flow through them while applying current to the electrodes. The PEM electrolyzer systems developed to date are primarily focused on continuous hydrogen generation and use a stable input of grid electricity. For example, many hydrogen refueling stations are controlled by monitoring the amount of hydrogen available for refueling. If the station needs hydrogen, it sends a signal to the electrolyzer system to turn on and produce hydrogen at a constant set power. PEM electrolyzers can respond to load changes rapidly (on

the second and minute time scales) which makes them ideal for use in grid services such as demand response and in RE applications where the incoming generation can change rapidly [6].

Alkaline electrolyzers have traditionally used a liquid alkaline solution to conduct negative hydroxide ions between the anode and cathode. The OER for an alkaline electrolyzer is represented as chemical equation 3.

$$2OH^- \rightarrow {}^1/_2\, O_2 + H_2O + 2e^- \quad \text{Eq. 3}$$

Where two molecules of negatively charged hydroxide ions (OH^-) react to form half of an oxygen molecule (O_2), one water molecule (H_2O), and two electrons (e^-). The HER is represented as chemical equation 4.

$$2H_2O + 2e^- \rightarrow H_2 + 2OH^- \quad \text{Eq. 4}$$

Where two molecules of water (H_2O) react with two electrons (e^-) to form one hydrogen molecule (H_2) and two molecules of negatively charged hydroxide ions (OH^-). The main components of the alkaline electrolyzer cell are the liquid alkaline solution, hydroxide ion conducting diaphragm, cathode, and anode. When the proper voltage is applied the reduction reaction occurs and the negatively charged hydroxide ion acts as the charge carrier by passing through the diaphragm from the cathode to the anode. Alkaline electrolyzers are limited to lower current densities compared to PEM electrolyzers because of the liquid electrolyte and therefore experience lower hydrogen production rates. Additionally, the liquid electrolyte reduces their ability to respond to load changes as fast as with PEM electrolyzers. Alkaline electrolyzers are more technologically mature than the other technologies and therefore commonly have a lower capital cost than the other technologies.

Solid oxide electrolyzers utilize solid oxide electrolytes which conduct negative oxygen ions from a normally composite ceramic cathode and mixed oxide anode. The materials used in a solid oxide electrolysis stack allow it to be operated in high temperatures, usually being paired with waste heat. The OER for a solid oxide electrolyzer is represented as chemical equation 5.

$$O^{2-} \rightarrow {}^{1}/_{2}\, O_2 + 2e^{-}$$ Eq. 5

Where a negative oxygen ion (O^{2-}) forms half of an oxygen molecule (O_2) and two electrons (e^{-}). The HER for a solid oxide electrolyzer is represented as chemical equation 6.

$$H_2O + 2e^{-} \rightarrow H_2 + O^{2-}$$ Eq. 6

Where one molecule of water (H_2O) react with two electrons (e^{-}) to form one molecule of hydrogen (H_2) and a negative oxygen ion (O^{2-}). The working fluid in solid oxide electrolyzers is steam instead of liquid water used in PEM and alkaline. Having some of the energy required to split water being supplied by heat means that solid oxide electrolyzers can operate at higher efficiencies when compared to PEM and alkaline. The thermal load of solid oxide electrolyzers make them undesirable for use with variable input electricity like what is seen with RE because they are slow to start up/shutdown and cannot respond to load changes as rapidly as PEM electrolyzers.

Typically, PEM green hydrogen generation systems include balance of plant (BOP) components such as power electronics, electrolyzer stacks, PSA dryers, hydrogen compressors, and a system cooling circuit. The power electronics convert alternating current (AC) into direct current (DC) that can be used by the electrolyzer to split water. The electrolyzer stack electrochemically splits water into hydrogen ions and oxygen and selectively transports hydrogen ions to be reduced into hydrogen gas. The PSA dryer removes any water present in the produced hydrogen using pressure swings and adsorbent materials. The hydrogen compressor increases the volumetric density of hydrogen and allows bulk storage in the quantities needed for vehicle refueling or other high pressure hydrogen applications. The system cooling circuit is used to reject waste heat from the different components. To effectively simulate the process of generating green hydrogen with variable amounts of power, it is necessary to include all components of the system and how they interact at different load conditions.

There are several demonstrations and modeling projects focusing on the direct connection of solar PV and DC wind turbines to electrolyzer systems [7]–[9]. The direct connection configuration allows for the reduction or elimination of the power conversion subsystem of the green hydrogen production facility which will benefit future installations. This work is focused on modeling hydrogen generation systems that utilize current renewable energy installations that are designed for grid production and therefore produce AC power that is ready for grid export. Additionally, green hydrogen production systems that provide grid services will be required to have AC/DC conversion equipment to interface with the grid.

1.2: GREEN HYDROGEN GENERATION SYSTEM MODELLING LITERATURE REVIEW

A recent review on PEM electrolyzer modelling was published by Falcão and Pinto in 2020 and summarized the methodology of 23 publications on electrolyzer modeling [10]. The review covered both empirical and semi-empirical models such as the model developed in this work. Most of the models use the same methodology that the model developed in this work uses to calculate the cell voltage of the PEM electrolyzer. Different empirical equations and constants are used between the models but typically most models use the Nernst equation, Butler-Volmer equation, and Ohms Law to calculate the total cell voltage. Some models include a mass transport overpotential, but it is stated that the mass transport overpotential is only observed at higher current densities. Only a few models contained a thermal portion of the model where the electrolyzer heat generation and temperature were calculated. The review did not include any methodology on how to model the BOP of a green hydrogen generation system utilizing a PEM electrolyzer such as the power electronics, hydrogen purification, compression/storage, or system cooling and did not mention any of the models having capability to include these subsystems.

One of the most cited electrolyzer models was developed by Øystein Ulleberg in 2003 to simulate advanced alkaline electrolyzers [11]. Although the model is meant for alkaline electrolyzer technology, the methodology for calculating the cell voltage is the same as for PEM

electrolyzers but uses different empirical equations specialized for alkaline technology. The model focused on the electrochemical and thermal behavior of the electrolyzer. The cell voltage was calculated using an empirical equation. The empirical equation is a good way to predict the performance of an electrolyzer at the same operating conditions used to produce the experimental data but lacks the ability to predict changes in the performance of the electrolyzer if some operating conditions are changed such as cathode pressure. The thermal portion of the model was based on a lumped capacitance assumption where the heat generated in the electrolyzer was determined by multiplying the difference in total cell voltage and thermo-neutral cell voltage by the current applied to the electrolyzer cell. The model was validated against an experimental alkaline electrolyzer. The electrolyzer model did not account for any of the BOP such as the power electronics, hydrogen purification, hydrogen compression/storage, or system cooling.

Another highly cited model in literature was developed by Marangio *et al.* in 2009 and focused on a high pressure PEM electrolyzer for hydrogen production [12]. The model focused on the voltage-current relationship in the electrolyzer cell as well as the gas production and transport between the electrodes. The voltage-current relationship was modeled similarly to the model developed in this work and included a mix of empirical and semi-empirical equations and constants. The model only accounted for the transport of water in the cell and uses Fick's law of diffusion and an electro-osmotic drag coefficient to calculate a net water transport between the electrodes. This model included an in-depth analysis of the electric and ionic resistance of the electrolyzer cell which accounted for the physical dimensions of the membrane and end plates. The model was validated against an experimental PEM electrolyzer setup. The BOP of the system was not included in the model such as power electronics, hydrogen purification, hydrogen compression/storage, or system cooling.

A model focusing on PEM electrolyzers operating in a domestic microgrid was developed by Valverde *et al.* in 2012 [13]. The experimental microgrid being modeled consisted

of a power source, electric load, PEM electrolyzer, metal hydride hydrogen storage, PEM fuel cell, battery pack, and water purification system. The authors exclude the hydrogen purification and system cooling subsystems of the hydrogen system. The model includes semi empirical equations to calculate the current produced from a PV array given irradiance data. The method used to model the electrolyzer voltage-current relationship is like the method presented in previous literature and the method used in this work where the cell voltage is a combination of the open circuit voltage, activation overpotential, and ohmic overpotential. The model also solves a differential equation to calculate the electrolyzer temperature using a lumped thermal capacitance assumption. The authors validated the model with experimental data recorded from a pilot microgrid with a 6-kW power source.

Yigit and Selamet developed a PEM electrolyzer model similar to this work in 2016 but did not include all of the necessary BOP or the necessary losses within the system [14]. The model included calculations for the voltage-current relationship, power electronics, water pump, cooling fan, and hydrogen compressor. The heat generation of the system was calculated by assuming all the losses within the system generate heat. The model did not include any calculations on the purification of hydrogen and therefore did not include any hydrogen loss associated with the hydrogen purification process. The model also did not calculate any hydrogen transport within the electrolyzer. The model was validated against experimental voltage and current data from a single electrolyzer cell.

A PEM electrolyzer system model which includes the BOP subsystems was developed by Olivier *et al.* in 2017. This model was developed using the bond graph approach which provides a visual representation of all the important system parameters being solved. After reviewing the literature on PEM electrolyzer modeling, the authors concluded that none of the models they studied were able to simulate the entire green hydrogen generation system and did not include the BOP. The model methodology covered the power conversion subsystem, electrolyzer stack, water circulation pumps, hydrogen/oxygen separators, and cooling system.

The method used in the model to calculate the voltage-current relationship is very similar to the methodology utilized in this work where the cell voltage is broken down into the open-circuit voltage, activation overpotential, and ohmic overpotential. The thermal portion of the model utilized a lumped capacitance approach like the other models presented. The heat generation from the electrolyzer stack was determined by multiplying the difference between the cell voltage and thermo-neutral voltage by the current applied to the stack. The model also calculated the gas diffusion and water transport between the electrodes. The power electronics portion of the model utilized an empirical curve fit to calculate the conversion efficiency. The inefficiency of the power electronics was not included in the heat generation of the system. The hydrogen purification system was modeled by calculating the flowrate of separated water using thermodynamic equations. The purification portion of the model also calculated the amount of hydrogen that is vented from the purification system to the atmosphere. The system cooling was modeled using an effectiveness-NTU prediction of the work required to drive the rejected heat flow. The model was validated against a 27-kW PEM electrolyzer system and some of the empirical constants used in the model were derived from the measured data. The presented model covered two electrolyzer stacks that combined to a total of 27-kW and did not explore the performance impact of independently controlling the power level of each stack. Currently PEM electrolyzer manufacturers offer electrolyzer stacks with around a 1.25-MW power rating. If green hydrogen is to become widely available, there needs to be MW/GW size facilities that will include arrays of electrolyzer stacks which offer the possibility of optimizing how the system is loaded with varying amounts of power.

Another model that includes the BOP of the PEM hydrogen generation system was developed by Sood *et al.* and published in 2020 [15]. The model uses the same bond graph approach as [16] but attempts to modularize the system model so it can be easily adopted for different system configurations. The modeling methodology of the two bond graph models is

essentially the same. The authors state that this modeling methodology is suitable for future studies on controls and diagnosis studies.

Ipsakis *et al.* [17] studied power management strategies for a RE/PEM electrolyzer system similar to this work but used a significantly simplified model for the electrolyzer system and did not model the electrical load of the cooling system or take into account the hydrogen loss due to gas permeation and purification. The model uses an empirical equation to predict the voltage-current relationship of the electrolyzer and then uses a constant efficiency to calculate the amount of hydrogen produced. The lack of BOP in the model means that any losses or power consumption originating from the BOP are not taken into effect when developing power management strategies. The resulting strategies run the risk that energy losses in the BOP are not mitigated and therefore the green hydrogen production system is not truly optimized.

The simplified electrolyzer models that only focus on the voltage-current relationship in the stack are better suited for modeling PEM electrolyzers being used for dedicated hydrogen production where the input power is not varied. Two recent publications developed system models using the bond graph approach which, like the model developed in this work, include BOP subsystems such as power electronics and PSA dryer, however, the models were not scaled to model a multi-stack generation system. Both bond graph models are complex and calculate several parameters that are not of interest if the goal is to optimize a multi-electrolyzer stack green hydrogen generation system [15], [16].

With the objective of optimizing the energy conversion efficiency of a green hydrogen generation system, the only factors that are of interest are accurately predicting the current-voltage relationship, accounting for all electrical consumption within the system, and accounting for all energy “loss” in the system whether that be in the form of heat generation in the electrolyzer or physical hydrogen loss in the PSA. The model developed in this paper expands beyond the modeling that has been done in literature to include the BOP of the green hydrogen

generation system as well as reduce the complexity of the bond graph system models. The developed model is used to analyze the performance of a scaled system operating with a theoretical case study of RE generation in Texas and is notably suited for system optimization studies and high-level controls development. Here we demonstrate this capability by investigating the system energy conversion efficiency with different electrolyzer cathode pressures and stack load management strategies for a utility scale multi-electrolyzer green hydrogen generation system. The results show that a sample green hydrogen generation system can be optimized using the system model developed in this work to produce the most amount of hydrogen given a profile of RE generation. The model developed in this work is a valuable tool to optimize the production of green hydrogen by identifying and using the interactions of different components within the system to maximize the amount of hydrogen produced. Optimizing the green hydrogen generation system will improve the economic feasibility and is imperative to accelerate the adoption of green hydrogen at scale.

CHAPTER 2: MODEL DEVELOPMENT

2.1: BASELINE SINGLE ELECTROLYZER SYSTEM MODEL

The system model was developed using Matlab Simulink and has a modular structure to include a separate module for each BOP subsystem. Figure 3 shows the block diagram of the green hydrogen generation system and the 5 modules that make up the system model. The model can predict the performance of the PEM green hydrogen generation system given either a time series of RE input power or a steady state input power and system parameters such as hydrogen pressure, electrolyzer cell area, and electrolyzer temperature. Any one of the modules can be run independently by removing the input connections from other modules and imposing the inputs of interest. The modular structure allows each module to be updated without running the whole system model. As the model is expanded to include other technologies and system configurations, the modular structure allows for certain Simulink subsystems to be edited, added, or removed. The model results can be viewed either by adding scope blocks to the outputs of certain blocks in the model or by having the Simulink model write a time series of data to a MAT file. The MAT file approach is used in this work to easily store and manipulate output data within a Matlab script to generate output plots.

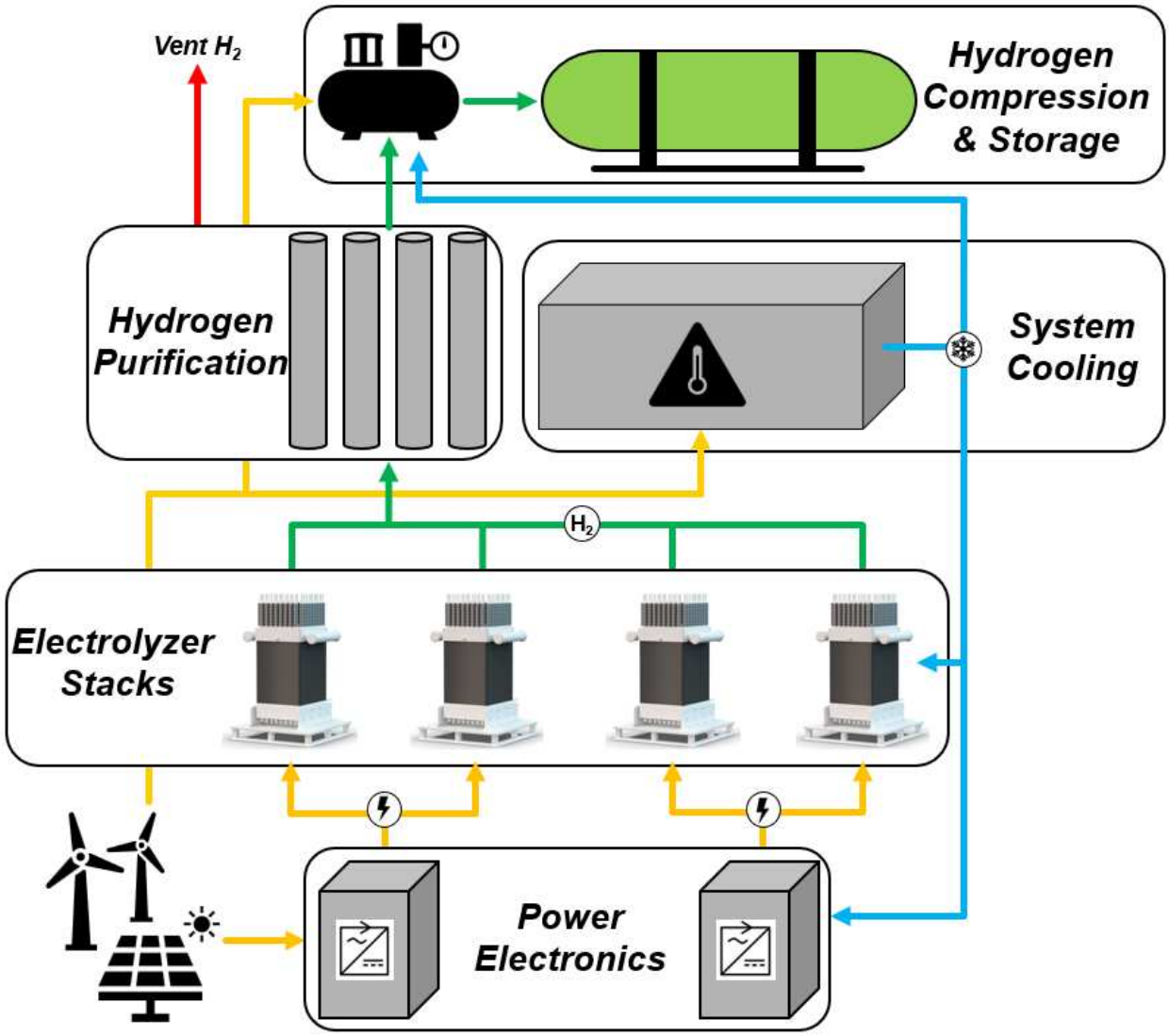

Figure 3: Green hydrogen generation system block diagram with all 5 major subsystems: power electronics, electrolyzer stacks, hydrogen purification, compression/storage, and system cooling.

The Simulink model can be run by selecting the simulation time and solver method within the Simulink program. Alternatively, the Simulink model can be called within a Matlab script which is particularly useful when sweeping parameters such as electrolyzer power. The Matlab script method of running the model is also useful when tuning and scaling the system parameters because “for”, “if”, and “while” loops can be used to run the model until a certain criteria is achieved. Many results shown in this work are produced using a Matlab script with

“for” loops to iterate through a certain set of inputs or operating strategies and change model parameters using the script rather than manually.

2.1.1: Power Electronics Module

The power electronics module predicts the conversion losses of turning AC power into DC power. An insulated-gate bipolar transistor (IGBT) rectifier is commonly used for PEM green hydrogen generation systems and experience energy loss due to fast switching and imperfect conductors. The power electronics module uses a regression model of measured conversion efficiency data for a 73-kW IGBT rectifier to predict the conversion efficiency based on the fraction of the rated AC power [18]. The difference in the incoming AC power and the output DC power due to inefficiencies is assumed to generate heat that must be removed by the system’s cooling circuit. Figure 4 shows the experimental conversion data and the logarithmic linear regression model. The logarithmic regression model fits the data with an R squared value of 0.871.

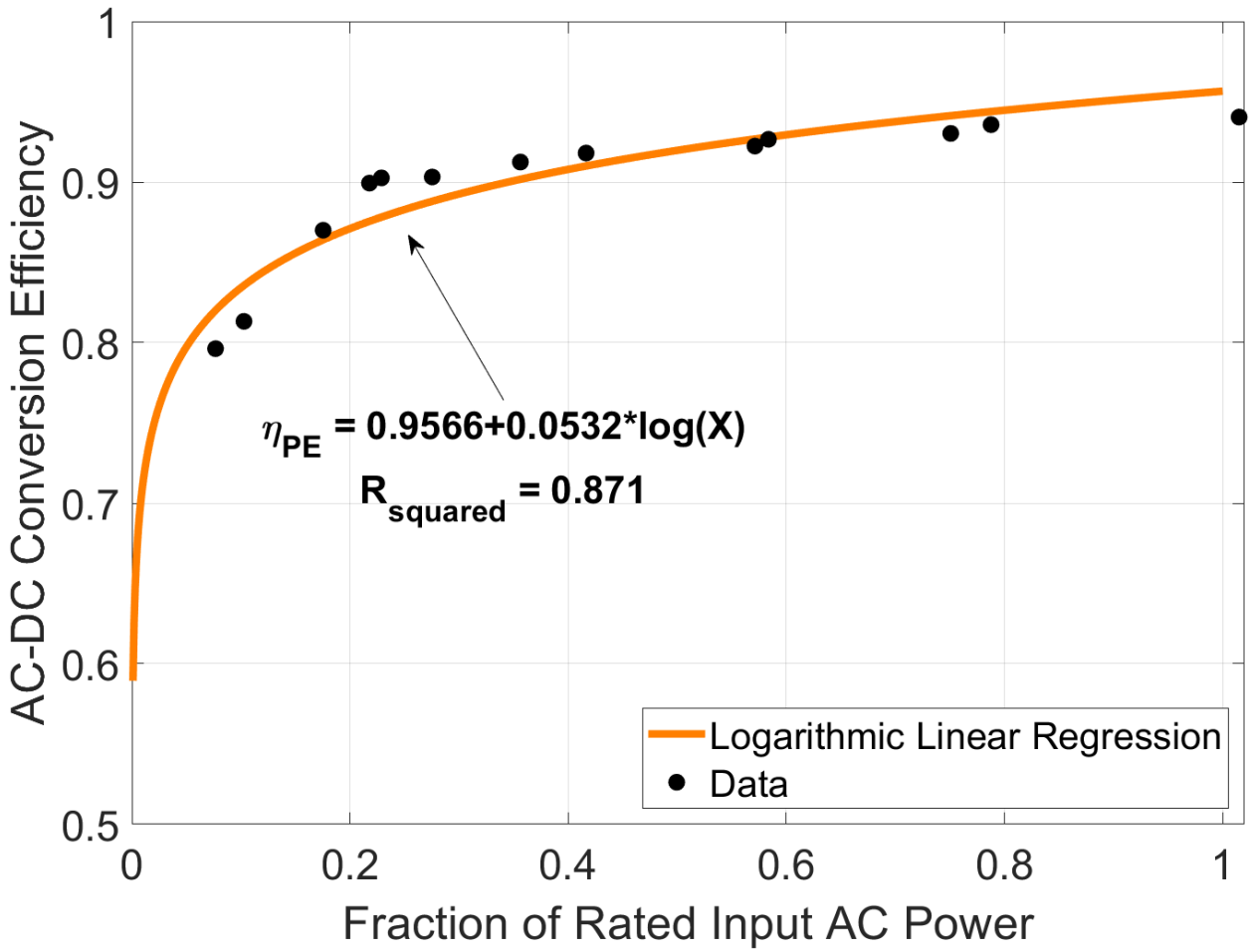

Figure 4: Logarithmic linear regression of energy conversion efficiency data from a 73-kW IGBT rectifier [18].

The limited amount of experimental data appears to have two distinct linear trends depending on if the fraction of rated input power is above or below 0.22, therefore a piecewise regression model is also presented in figure 5. The piecewise regression model has the risk of overparameterizing the system due to the low amount of datapoints. The piecewise model would result in a higher system energy conversion efficiency compared to the logarithmic regression model for AC-DC conversion efficiency.

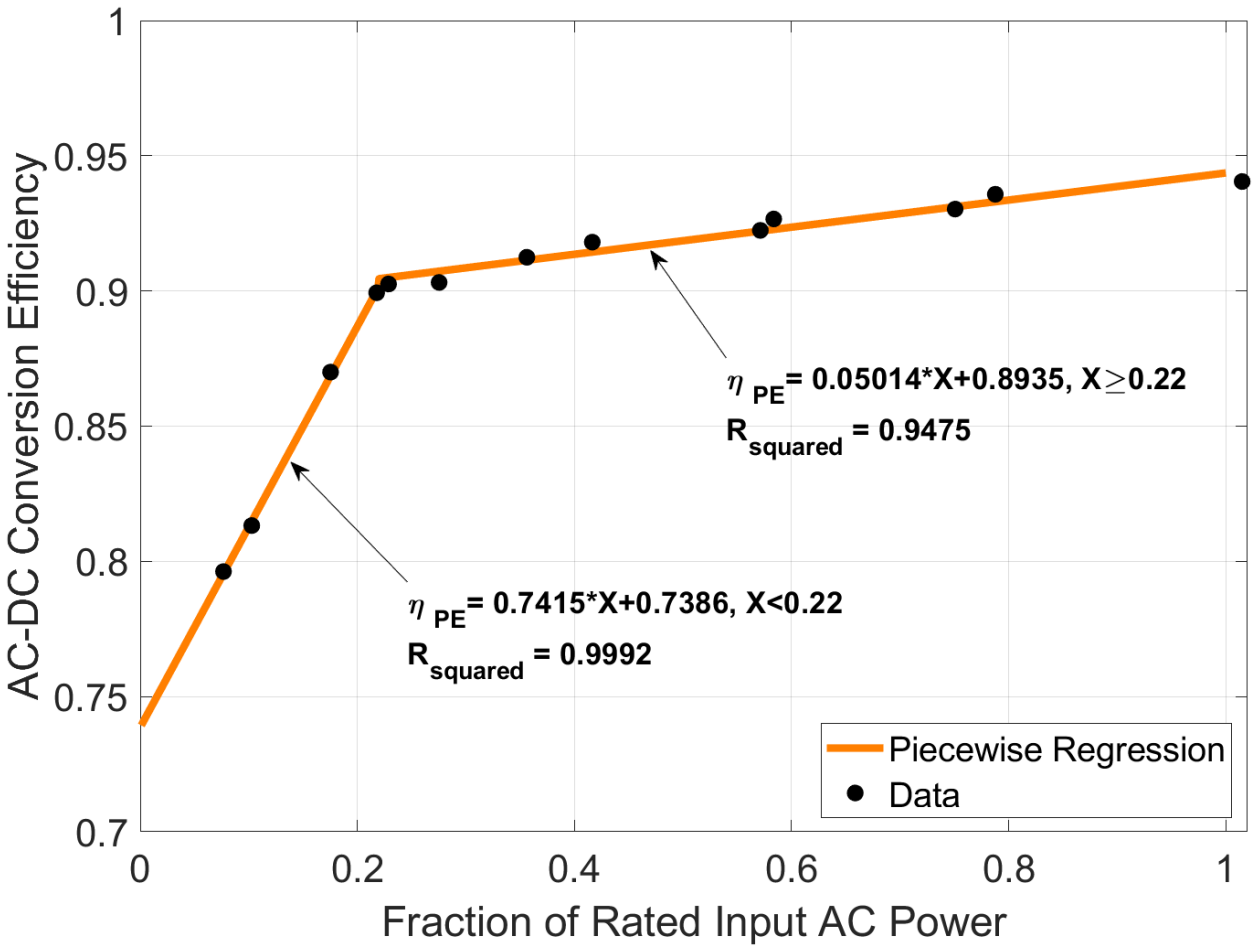

Figure 5: Piecewise regression of energy conversion efficiency data from a 73-kW IGBT rectifier [18].

The logarithmic regression model is selected to represent the rectifier efficiency in the green hydrogen generation system model, as more experimental measurements become available, the regression model can be tuned to increase the accuracy of the model. If the RE generation site allows for it, the power electronics module can be simplified or eliminated to represent the case where the DC electricity generated from the solar PV, or a DC wind turbine, can be fed directly to the electrolyzer stack with minimal power conversion.

2.1.2: PEM Electrolyzer Stack Module

The electrolyzer module predicts the generation of hydrogen and oxygen; the hydrogen gas crossover; and the voltage-current relationship of each cell. The generation of hydrogen at the cathode and oxygen at the anode is described by Faraday's law of electrolysis which states

that the generation of elements at an electrode is proportional to the current applied to the cell and the valency of the corresponding ions. Faraday's law of electrolysis for the generation of hydrogen and oxygen are represented by equations 7 and 8 respectively.

$$\dot{N}_{H_2} = \frac{I}{F \cdot 2} \cdot \eta_F \quad \text{Eq. 7}$$

$$\dot{N}_{O_2} = \frac{I}{F \cdot 4} \cdot \eta_F \quad \text{Eq. 8}$$

Where $\dot{N}_{H_2}$ and $\dot{N}_{O_2}$ are the molar generation rates of hydrogen and oxygen, I is the current applied to the cell, F is faraday's constant which is equal to 96,485 coulombs per mole, and η_F is the faradaic efficiency. Almost every model reviewed in literature uses Faraday's law of electrolysis to predict the generation of hydrogen within the electrolyzer. Some models in literature omit the faradaic efficiency entirely [13], [16]. The models in literature that do not use Faraday's law of electrolysis instead use a simple assumption of constant electrolyzer energy conversion efficiency and use that to calculate the produced hydrogen energy content based on the input power [19], [20].

The gas crossover of hydrogen from the cathode to the anode is described by Fick's law of diffusion coupled with the diffusion permeability of hydrogen gas across Nafion membranes [21]. Hydrogen gas crossover has been shown to be independent of pressure differentials and so hydrogen permeation due to pressure gradients has been neglected in this model [22]. Fick's law rewritten with partial pressure and diffusion permeability is represented by equation 9.

$$\dot{N}_{H_2,diff} = \frac{\varepsilon_{H_2,diff}}{A \cdot \delta_{mem}} \left(P_{H_2,C} - P_{H_2,A}\right) \quad \text{Eq. 9}$$

Where $\dot{N}_{H_2,diff}$ is the molar flow rate of hydrogen, $\varepsilon_{H_2,diff}$ is the diffusion permeability of Nafion 117 which is a common membrane used in PEM electrolyzers, A is the active area of the membrane, δ_{mem} is the membrane thickness, $P_{H_2,C}$ is the partial pressure of hydrogen at the cathode, and $P_{H_2,A}$ is the partial pressure of hydrogen at the anode. The membrane active area and thickness is taken from a 60-kW Nel Hydrogen C10 hydrogen generator evaluated in [21].

The reviewed electrolyzer models in literature use Fick's law or empirical equations to model gas diffusion within the electrolyzer. The partial pressure of hydrogen at the cathode is calculated using equation 10.

$$P_{H_2,C} = P_C - P_{H_2O,C} \quad \text{Eq. 10}$$

Where P_C is the total pressure in the cathode and $P_{H_2O,C}$ is the saturated water vapor pressure in the cathode. The saturated water vapor pressure in the cathode and anode is calculated with empirical equation 11 used in [21].

$$P_{H_2O,sat} = 6.1078 \times 10^{-3} \exp\left[17.2694\left(\frac{T - 273.15}{T - 34.85}\right)\right] \quad \text{Eq. 11}$$

Where T is the electrolyzer operating temperature. The model assumes that any hydrogen entering the anode is immediately vented from the anode alongside the oxygen and excess water, therefore, $P_{H_2,A}$ is assumed to be equal to zero.

Water is transported between the anode and cathode through several mechanisms including diffusion, permeation, and electro-osmotic drag. The diffusion of water across the membrane is described using Fick's law and the Bruggeman equation to correct the diffusion coefficient in the presence of the porous Nafion membrane. Equation 12 shows Fick's law for water diffusion across the membrane.

$$\dot{N}_{H_2O,diff} = \frac{A \cdot D_{eff}}{\delta_{mem}}\left(C_{H_2O,C} - C_{H_2O,A}\right) \quad \text{Eq. 12}$$

Where $\dot{N}_{H_2O,diff}$ is the molar flowrate of water due to diffusion, D_{eff} is the effective water diffusion coefficient, $C_{H_2O,C}$ is the concentration of water at the cathode, and $C_{H_2O,A}$ is the concentration of water at the anode. The effective water diffusion coefficient is calculated using the Bruggeman equation represented as equation 13.

$$D_{eff} = \varepsilon^{1.5} \cdot D_w \quad \text{Eq. 13}$$

Where ε is a dimensionless constant and D_w is the water diffusivity. The dimensionless constant ε is calculated using the void fraction of the membrane in equation 14.

$$\varepsilon = \frac{1}{1-\varphi} \quad \text{Eq. 14}$$

Where φ is the void fraction of the membrane. Literature reports values for the void fraction of Nafion 117 to be equal to 0.3 [23],[24],[25]. The diffusivity of water is a function of temperature and is calculated using empirical equation 15.

$$D_w = 0.256 \times 10^{-4} \left(\frac{T}{273.15}\right)^{1.823} \quad \text{Eq. 15}$$

Water transport due to permeation or pressure differences is calculated using Darcy's law which is represented as equation 16.

$$\dot{N}_{H_2O,perm} = \frac{\rho_{H_2O} \cdot A \cdot K_D \cdot \nabla P}{\mu_{H_2O}} \quad \text{Eq. 16}$$

Where $\dot{N}_{H_2O,perm}$ is the flowrate of water caused by permeation, ρ_{H_2O} is the density of water, K_D is Darcy constant, ∇P is the pressure gradient, and μ_{H_2O} is the dynamic viscosity of water. The Darcy constant is taken as $5.49 \times 10^{-16}\ cm^2 \times 10^{16}$ as published in literature for Nafion 115 at 60° C [26]. The dynamic viscosity of water is calculated using empirical equation 17.

$$\mu_{H_2O} = 0.6612(T - 229)^{-1.562} \quad \text{Eq. 17}$$

Water transport due to electro-osmotic drag is caused by water molecules attaching to ions being transferred between the anode and cathode and is calculated using an electro-osmotic drag coefficient and the current, or rate of ion transfer, in equation 18.

$$\dot{N}_{H_2O,eod} = n_{eod} \frac{I}{F} \quad \text{Eq. 18}$$

Where $\dot{N}_{H_2O,eod}$ is the flowrate of water due to electro-osmotic drag and n_{eod} is the electro-osmotic drag coefficient which is calculated using empirical equation 19.

$$n_{eod} = 0.0029 \cdot \lambda_m^2 + 0.05 \cdot \lambda_m - 3.4 \times 10^{-19} \quad \text{Eq. 19}$$

Where λ_m is the membrane water content. Literature reports that a fully hydrated Nafion 117 membrane has a water content of 22 [27]. Although the model calculates the expected

molar flowrate of water transport within the cell, it is not used in predicting the performance of the system. The water transport within the electrolyzer cell may become useful if the consumption of water is included in the system performance calculations or if the PSA dryer methodology changes to a thermodynamics-based approach where it is necessary to know the water vapor content in the product hydrogen.

PEM electrolyzer cells do not have a linear current-voltage relationship like other devices such as resistors. The cell voltage across each electrolyzer cell can be broken down into the sum of the thermo-neutral cell potential or open circuit voltage, activation overpotential, and ohmic overpotential. The thermo-neutral cell potential is the minimum potential across the PEM cell to satisfy the thermodynamics of the water splitting reaction assuming that all the energy required to split water comes from electricity and not external heat. The thermo-neutral potential is governed by the operational aspects of the cell such as electrolyzer temperature, cathode pressure, and species concentrations. The Nernst equation is used to calculate the thermo-neutral cell potential and is represented in equation 20.

$$V_{th} = E_0 + \frac{RT}{nF} ln\left(\frac{P_{H_2} \cdot P_{O_2}^{0.5}}{P_{H_2O}}\right) \quad \text{Eq. 20}$$

Where V_{th} is the thermo-neutral cell potential, E_0 is the reversible cell potential at standard conditions, R is the universal gas constant, n is the number of electrons exchanged in the electrolysis reaction, P_{H_2} is the partial pressure of hydrogen in the cathode, P_{O_2} is the partial pressure of oxygen in the anode, and P_{H_2O} is the partial pressure of water vapor. Empirical equation 21 has been used to calculate the reversible cell potential [28].

$$E_0 = 1.228 - 0.9 \times 10^{-3}(T - 298) \quad \text{Eq. 21}$$

For electrolysis to begin, a voltage above the thermo-neutral cell potential must be applied to overcome the resistance to the non-spontaneous reaction of splitting water into hydrogen and oxygen. The activation overpotential is the additional potential that must be applied to the cell to start the electrolysis reaction and is determined by the physical properties

of the electrodes and catalysts. The Butler-Volmer equation is used to predict the activation overpotential and is represented in equation 22.

$$\eta_{act} = \frac{RT}{\alpha_A F} sinh^{-1}\left(\frac{i}{2 \cdot i_{0,A}}\right) + \frac{RT}{\alpha_C F} sinh^{-1}\left(\frac{i}{2 \cdot i_{0,C}}\right) \quad \text{Eq. 22}$$

Where η_{act} is the activation overpotential, α_A is the anode charge transfer coefficient, i is the current density applied to the cell, $i_{0,A}$ is the anode exchange current density, α_C is the cathode charge transfer coefficient, and $i_{0,C}$ is the cathode exchange current density. Values for the charge transfer coefficients and exchange current densities were empirically derived in [21].

The PEM electrolyzer operates by passing hydrogen ions between the anode and cathode. The ohmic overpotential must be applied to the electrolyzer cell to overcome the overall resistance of the cell to ionic transfer. The electrolyzer membrane has an inherent resistance to passing hydrogen ions across it that is governed by the conductivity of the membrane. Ohms law is used to calculate the ohmic overpotential that is required to overcome the ionic resistance and is represented in equation 23.

$$\eta_{ohm} = \left(\frac{\delta_{mem}}{\sigma_{mem}}\right) \cdot i \quad \text{Eq. 23}$$

Where η_{ohm} is the ohmic overpotential and σ_{mem} is the membrane conductivity. The empirical equation 24 is used to calculate the membrane conductivity of a Nafion 117 membrane given water uptake and temperature [29].

$$\sigma_{mem} = 0.005139 \cdot \lambda_m - 0.0326 \cdot \left[1268 \cdot \left(\frac{1}{303} - \frac{1}{T}\right)\right] \quad \text{Eq. 24}$$

Simulink iteratively solves for the electrolyzer stack current, cell voltage, and gas transport given the amount of incoming DC power and the thermodynamic properties of the electrochemical reaction. The activation and ohmic overpotentials are multiplied by the stack current to calculate the inefficiency of the electrolyzer which is assumed to generate heat that must be removed by the system's cooling circuit. Once the current is known, the amount of hydrogen produced in the electrolyzer can be calculated. The net amount of hydrogen produced

by the stack and sent to the hydrogen purification subsystem is equal to the hydrogen crossover subtracted from the amount of hydrogen generated using Faraday's law of electrolysis.

2.1.3: Hydrogen Purification Module

The gas produced in the electrolyzer stack has some amount of water vapor that must be removed for proper utilization of the product hydrogen. Normally the hydrogen will move through heat exchangers and phase separators, but to produce higher quality hydrogen, the system utilizes a PSA dryer as well. The PSA process requires a purge gas to remove impurities from the system. Typically, some of the purified hydrogen is used as purge gas which represents a loss in the overall green hydrogen generation system. Figure 6 shows the PSA purification cycle of a system using 4 separate adsorbing bays [30]. The system constantly cycles through a set of phases where one adsorbent bay is actively removing impurities while the other adsorbent bays go through a regeneration step where the purge gas is used. In the figure, PP denotes the step where one adsorber bay "provides a purge" to regenerate another bay. The purge gas is purified hydrogen which comes from an adsorber bay that has finished an adsorption phase and is depressurizing to change the equilibrium content of impurities in the adsorbent material. The lower pressure causes a lower equilibrium content and allows for the impurities to be quickly reabsorbed into the purge gas and removed from the bay which can then be repressurized and continue the adsorption process.

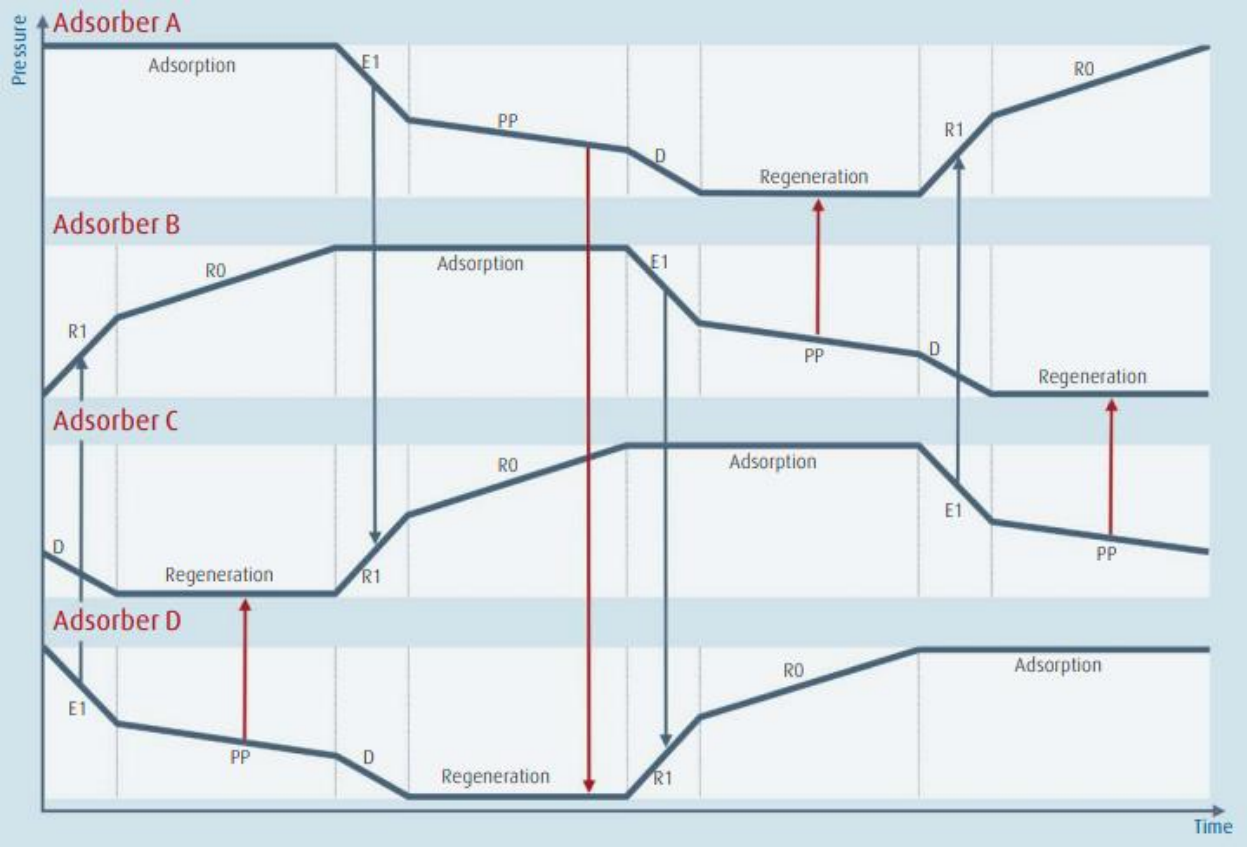

Figure 6: Purification cycle of a theoretical 4-bay PSA dryer on a pressure vs time plot showing the various stages of adsorption and regeneration [30].

Most PSA dryers in green hydrogen generation systems use a fixed orifice to provide the purge hydrogen. The fixed orifice provides a constant flow of purge hydrogen directed at the regenerating PSA bay given a constant cathode pressure. The PSA system module uses an analytical equation and average PSA uptime to predict the constant flowrate of purge hydrogen based on pressure [21]. The choked flowrate of purge hydrogen is calculated using equation 25.

$$\dot{m}_{H_2,purge} = \eta_{PSA} \cdot C_d \cdot A_O \cdot P_C \sqrt{\left(\frac{k \cdot g_c \cdot M_{H_2}}{R \cdot T}\right) \cdot \left(\frac{2}{k+1}\right)^{\left(\frac{k+1}{k-1}\right)}} \qquad \text{Eq. 25}$$

Where $\dot{m}_{H_2,purge}$ is the mass flowrate of purge hydrogen used in the PSA, η_{PSA} is the fraction of PSA uptime, C_d is the coefficient of discharge for the orifice, A_O is the orifice area, k is the ratio of specific heats for hydrogen, g_c is the gravitational constant, and M_{H_2} is the

molecular weight of hydrogen. Values for the PSA uptime and orifice discharge coefficient are measured from a PEM hydrogen generating system in [21]. If the predicted purge hydrogen flowrate and hydrogen diffusion flowrate exceed the amount of hydrogen generated at the cathode, the electrolyzer is shut down.

2.1.4: Hydrogen Compressor Module

The hydrogen compressor module predicts the electric power consumption and cooling requirement of the high-pressure hydrogen compressor. The module assumes the compression process is a 2-stage polytropic compression of an ideal gas and uses thermodynamic equations to calculate the compression work required and heat transfer for intercooling between compression stages. The compression work is translated into electrical power consumption using a constant AC motor efficiency. Equation 26 is used to calculate the compression work required to compress the hydrogen to vehicle refueling storage pressures of 880 barg.

$$W_{comp} = \dot{m}_{H_2} \frac{n \cdot R \cdot T_1}{\eta_{comp}(n-1)} \left[\left(\frac{P_2}{P_1} \right)^{(n-1)/n} - 1 \right] \quad \text{Eq. 26}$$

Where W_{comp} is the compression work of the hydrogen compressor, $\dot{m}_{H_2}$ is the flowrate of hydrogen, n is the polytropic index, T_1 is the temperature of the incoming hydrogen, η_{comp} is the compressor efficiency, P_1 is the pressure of the incoming hydrogen, and P_2 is the final pressure for the compression stage. The polytropic index is taken as 1.609. Values for the compressor efficiency and AC motor efficiency are taken from [31]. The model assumes that ample storage is available and does not include modeled hydrogen offtake and therefore the energy consumption of the compressor is only dependent on the flowrate of hydrogen coming from the electrolyzer. The state of charge of the hydrogen storage will influence the required pressure coming out of the compressor and alter the energy consumption. For example, if the state of charge of the hydrogen storage is low, the hydrogen coming out of the compressor will expand rapidly and may require additional cooling. On the other hand, if the state of charge of the hydrogen storage is high, the hydrogen compressor may experience a higher back pressure

and require more electricity consumption. If hydrogen demand and offtake is added to the system model in the future, the hydrogen compressor module can be updated with an empirical model to predict the required compressor work as it relates to the state of charge of the hydrogen storage and flowrate of hydrogen.

2.1.5: System Cooling Circuit Module

The green hydrogen generation system cooling circuit module predicts the amount of electric power the cooling system consumes to remove the waste heat from the system. The power electronics, electrolyzer stacks, and the hydrogen compressor each produce waste heat that must be removed to maintain functionality and remain within the thermal limits of the components. The system cooling circuit model calculates the electrical power consumed based on the amount of incoming waste heat using a constant coefficient of performance for an R407C chiller system. Equation 27 is used to calculate the electrical load required to run the system's cooling circuit.

$$COP = \frac{Q_{th}}{Q_e} \quad \text{Eq. 27}$$

Where COP is the coefficient of performance, Q_{th} is the total amount of thermal energy to reject, and Q_e is the electrical power consumption of the cooling circuit. The constant coefficient of performance for an R407C chiller is taken as 3.265 from [32].

2.1.6: System Performance Metrics

The system model calculates several key performance metrics of a green hydrogen generation system such as the system wide specific energy consumption, energy conversion efficiency, and the influence of each subsystem on the total system performance. The specific energy consumption of the green hydrogen generation system is defined as the amount of energy needed in kWh to produce 1 kg of usable green hydrogen. Equation 28 is used to calculate the specific energy consumption.

$$E_{kg\ H_2} = \frac{E_{AC,in} + E_{comp} + E_{cool}}{N_{H_2,net}} \quad \text{Eq. 28}$$

Where $E_{kg\ H_2}$ is the specific energy consumption of the system, $E_{AC,in}$ is the total amount of energy input to the system, E_{comp} is the energy used to compress the hydrogen, E_{cool} is the energy used to cool the system, and $N_{H_2,net}$ is the net amount of hydrogen produced by the system after any hydrogen loss is taken into account. The overall system conversion efficiency is defined as the efficiency of converting the electric energy consumed by the system into the energy content of the delivered hydrogen. Equation 29 is used to calculate the system conversion efficiency.

$$\eta_{sys} = \frac{1}{E_{kg\ H_2}} \cdot \left(\frac{HHV_{H_2}}{3.6}\right) \quad \text{Eq. 29}$$

Where η_{sys} is the system energy conversion efficiency and HHV_{H_2} is the higher heating value of hydrogen. It is important to note that the system energy conversion efficiency calculated using the higher heating value will be greater than the system energy conversion efficiency calculated with the lower heating value of hydrogen because of the assumption that the product water is not condensed when the hydrogen is used in a fuel cell, and that energy is not released. The difference in the two methods of calculation is the latent heat of condensation for the product water.

2.2: MODEL VERIFICATION AND VALIDATION

Any model must be verified and validated to claim that its results reflect the reality of whatever system is being modeled. The model developed in this work integrates many methodologies that have been published and individually validated in literature. During the model development, the model predictions were constantly checked for unrealistic values. Some unit conversion errors originating from combining multiple different semi-empirical models from literature were found and corrected. Simulink prints warnings and errors whenever the software is used incorrectly or is in danger of providing false results. For example, incorrect

connections between Simulink objects and unbounded signals can cause warnings and errors preventing the model from running. Each occurrence of a warning message was evaluated and the root cause in the model was fixed. The Simulink model was stress tested with a full range of realistic operating parameters to verify that no warnings are generated from the software. Because the system model runs with no warnings generated and each module has been examined for any unit conversion errors or unrealistic values, the system model developed in this work is considered verified. Validation requires some comparison of the model prediction to a set of experimental data or expected value. While original experimental data is not available for this work, experimental data found in literature has been used to individually validate portions of the model. This section provides the method used to verify and validate each portion of the system model.

2.2.1: Power Electronics Verification and Validation

The power electronics module uses a regression model of experimentally measured conversion efficiencies of a 73-kW IGBT based rectifier. The experimental conversion efficiency dataset consists of 13 measurements at various output powers of the rectifier. The logarithmic regression model has an R squared value of 0.871. The limited amount of experimental datapoints used to create the regression model introduces the risk of not representing the true efficiency of that system. The logarithmic regression model can be compared to the efficiency data of a 6 kW system published in [33]. The experimental measurement of the overall AC-DC conversion efficiency for the 6-kW system is shown in figure 7.

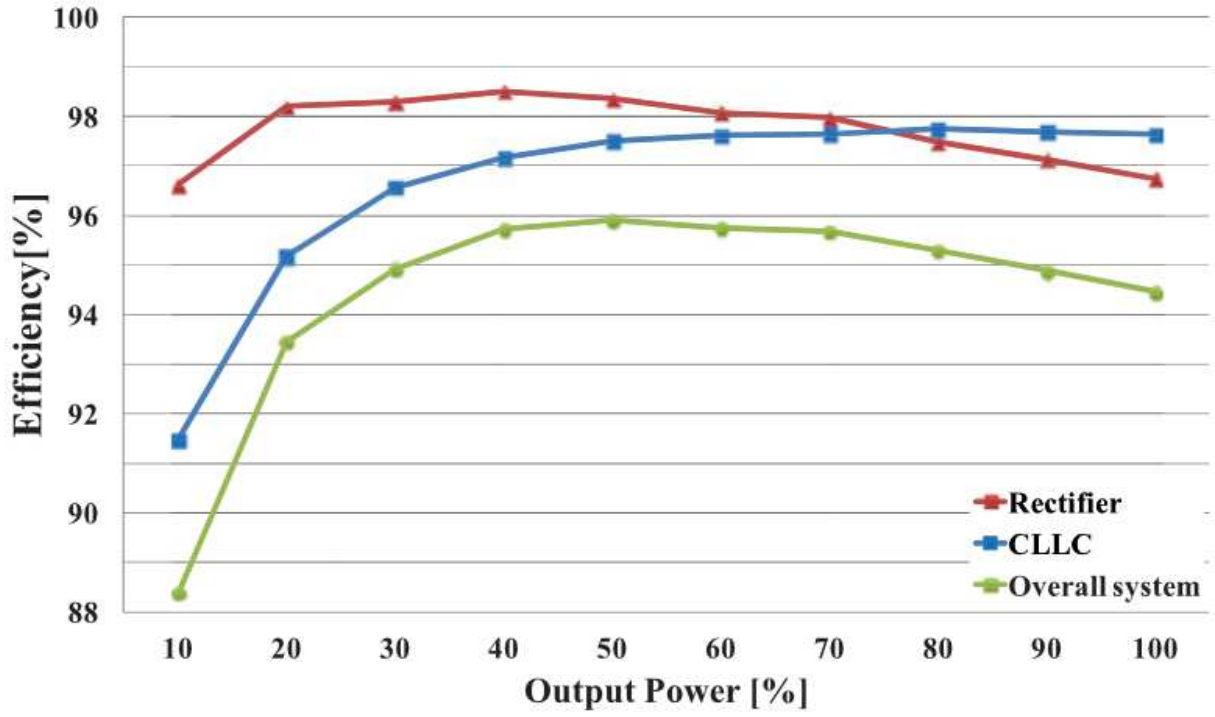

Figure 7: Power conversion efficiency of a 6-kW IGBT bidirectional AC-DC rectifier, DC-DC converter, and overall system in rectification mode [33].

The 6-kW system shows the same behavior of a steep efficiency decrease at low rated output power percentages. At higher rated output percentages, the 6-kW system experiences an efficiency decrease but remains around 94% efficient like what is recorded for the 73-kW system. Although the regression model used in this work does not reflect an efficiency decrease at high output power, it is considered validated because the 73-kW rectifier is specifically designed for use in a PEM electrolyzer based hydrogen refueling station and the regression model exhibits an acceptable agreement to the limited number of experimental measurements. IGBT based rectifiers are the standard power conversion technology for PEM electrolyzers at both the kW and MW scale therefore the same method of predicting power conversion efficiencies is used regardless of the model's electrolyzer scale.

2.2.2: Electrolyzer Module Verification and Validation

The electrolyzer module utilizes a set of semi-empirical and physics-based equations to predict the performance of the electrolyzer. Some of the equations used have been pulled from

literature where they have been independently validated, usually at the benchtop scale with single cell electrolyzers. Some of the important assumptions within the model can be verified with hand calculations. The Simulink model uses an algebraic loop to iteratively solve the current/voltage/species concentration within the cell at each time step. The algebraic loop requires the assumption that the partial pressure of hydrogen in the anode is assumed to be 0 in equation 9 for the loop to resolve. The thermo-neutral cell potential calculated in equation 20 relies on the species concentrations of the reactants and products in the electrolysis reaction. The assumption of having negligible hydrogen partial pressure in the anode means that the oxygen partial pressure would be equal to the anode total pressure minus the water vapor pressure and is not affected by the hydrogen diffusion to the anode. This assumption of having a negligible amount of hydrogen in the anode can be verified by solving equation 20 by hand in two ways and comparing the difference in calculated thermo-neutral cell voltage. Practically all PEM electrolyzers automatically shut down if the hydrogen volume fraction in the anode exhaust reaches 25% of the lower explosion limit (LEL) of hydrogen in air, this corresponds to 1% hydrogen by volume. The difference in calculated open circuit voltage between using the worst case of 1% hydrogen in the anode by volume and assuming negligible hydrogen partial pressure is 0.072 mV. The small voltage difference with and without the assumption verifies the assumption that the small amount of hydrogen diffusion does not meaningfully affect the calculated performance of the electrolyzer.

The method of calculating the amount of hydrogen that diffuses from the cathode to the anode can be verified by measuring the predicted volume percentage of hydrogen in the anode and comparing that to the operation of PEM electrolyzers in the field where any hydrogen volume percentage in the anode above 1% causes the system to shut down for safety. The system model calculates a maximum hydrogen percentage by volume of 1.39% at the minimum electrolyzer power (10% of the rated power) and with a cathode pressure of 30 barg. The model likely overestimates the diffusion of hydrogen to the anode. The modeled diffusion rate of

hydrogen can be tuned to future experimental datasets by fitting a different value for the diffusion permeability coefficient. Due to the lack of experimental data on hydrogen diffusion for a similar scale PEM electrolyzer and because the intent of this work is to analyze general system interactions and trends in performance, the current method of modeling the hydrogen diffusion is acceptable and verified.

The voltage-current relationship of the electrolyzer stack calculated in the system model can be validated with experimental measurements that were obtained from a 60-kW PEM electrolyzer system developed by Nel Hydrogen that was evaluated at UC Irvine [21]. The electrolyzer system operated in a power-to-gas application utilizing onsite RE generation. A polarization curve of the 60-kW electrolyzer was digitized using an online digitization program to produce a set of 56 experimental datapoints of current density and cell voltage to compare the model to. The digitized current densities were imposed on the model to predict the corresponding cell voltage. A regression model of the digitized data was used to compare the model's predicted values of cell voltage to the experimental cell voltage. Figure 8 depicts the agreement between the analytical voltage-current relationship from the model and the digitized experimental voltage-current relationship with the simultaneous 95% confidence interval (SCI) of the experimental data.

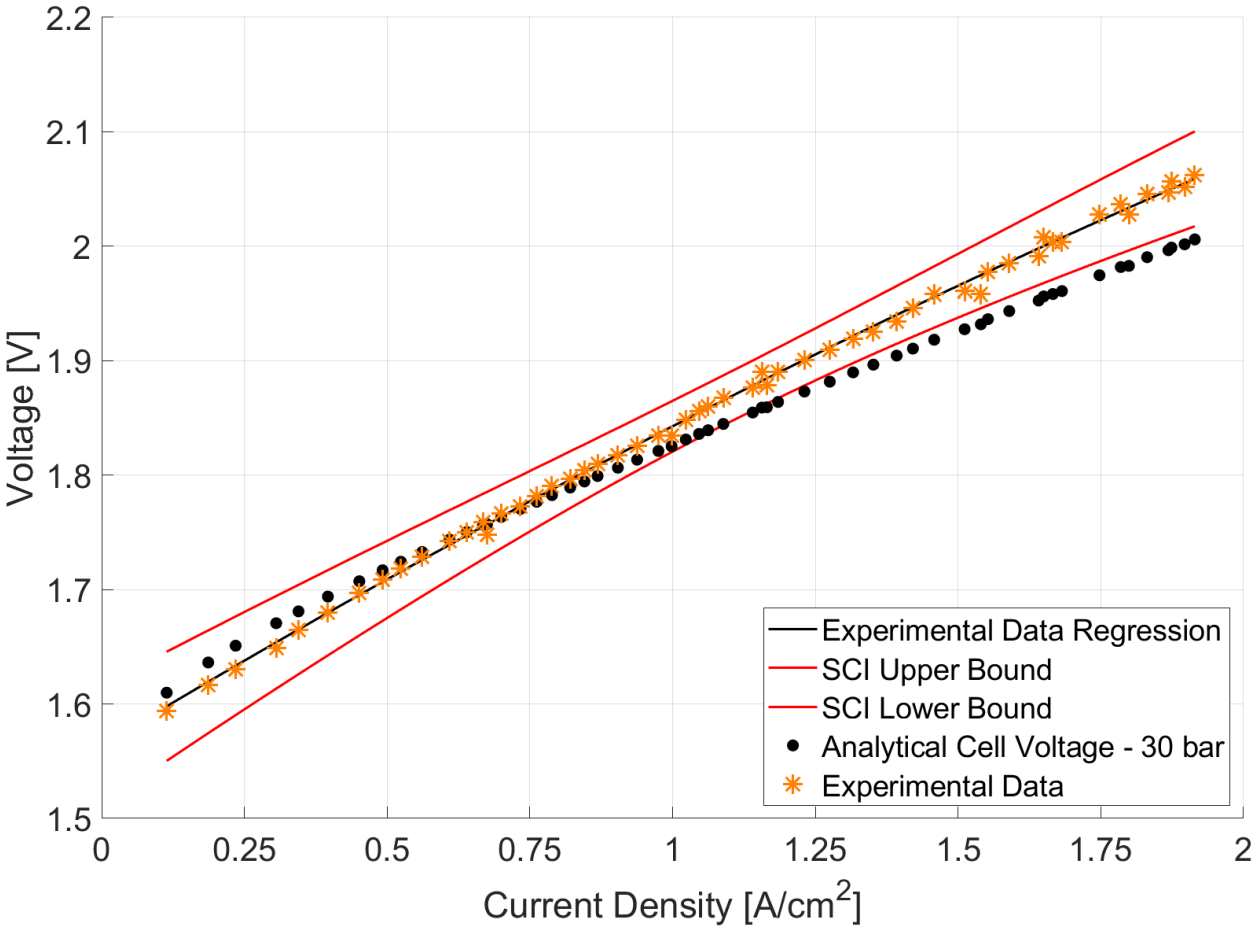

Figure 8: Modeled voltage-current relationship compared to digitized experimental data from a 60-kW PEM electrolyzer system at 60 °C and 30 barg cathode pressure [21].

The system model can predict the voltage-current relationship with an average model to experiment relative error of 13.41%. The figure used to produce the digitized dataset contains a high volume of datapoints which is difficult to properly digitize and contributes to the overall error. The model fit can be improved if a larger set of experimental data is obtained. Originally produced datasets will have less measurement error compared to a digitized set of data. A higher quality and more extensive dataset produced in-house could be used to tune the empirical equations and variables used in calculating the voltage-current relationship such as the conductivity of the membrane which could change the slope of the polarization curve to better align with the experimental data. The data available in literature for tuning and validation

is limited in size and quality, and therefore, the model fit is adequate to analyze general system interactions at different operating conditions and configurations.

The electrolyzer module can be verified by comparing its performance to the specification sheet of a Nel Hydrogen C20 series hydrogen generation system which shares the physical parameters of the C10 system evaluated in [21]. Table 1 shows the specifications of the hydrogen generation system [34]. The model was scaled to include one 120-kW PEM electrolyzer to equal the rated electrolyzer capacity of the C20 hydrogen generator and was run at the full electrolyzer rated power. At the full electrolyzer power, the model predicts a specific energy consumption of just the electrolyzer at 70 kWh/kg and a hydrogen flowrate of 1.82 kg/hr compared to the specified specific energy consumption of 66.7 kWh/kg and hydrogen flowrate of 1.8 kg/hr taken from the C20 specification sheet. The faradaic efficiency used in the model was tuned until the predicted production rate of hydrogen matched the production rate of the C20 system. The resulting faradaic efficiency was 83.5%. The tuned faradaic efficiency is lower than the faradaic efficiencies reported in literature which are between 90 and 100% [35]. The lower faradaic efficiency is due to the imperfect match of the voltage-current relationship which slightly overpredicts the current at higher electrolyzer power which leads to a lower tuned faradaic efficiency to produce the same hydrogen production rate as defined in table 1.

Table 1: Nel Hydrogen C20 specifications and ratings [34].

Power Electronics Rating	146	kW
Electrolyzer Rating	120	kW
Electrolyzer Cathode Pressure	30	Barg
Electrolyzer Specific Energy Consumption	66.7	kWh/kg
Maximum Hydrogen Flowrate	1.8	kg/hr
Electrolyzer Temperature	60	°C
Hydrogen Storage Pressure	880	Barg

2.2.3: Hydrogen Purification Verification and Validation

Experimental measurements from a hydrogen PSA dryer system could not be found in literature with which to validate the purification module. From conversation with researchers at the National Renewable Energy Laboratory who have empirically modeled PEM electrolyzer systems, it is found that they have assumed 6% of the rated hydrogen production of a PEM electrolyzer is lost in a PSA dryer due to the regeneration process where pure hydrogen is used as the purge gas. The method of calculating the choked flow of an orifice was individually validated in [21] using predicted hydrogen flowrate out of the system versus the calculated flowrate after the purge hydrogen is vented. Using the current methodology, the system model predicts that 6.4% of the rated hydrogen production for a modeled 120-kW PEM electrolyzer system is lost due to hydrogen crossover and loss in the PSA dryer at 30 barg cathode pressure which is around what other modelers have assumed. The combination of the methodology being individually validated in literature and the agreement of the percentage of hydrogen loss to the assumption of other modelers results in the hydrogen purification module being verified and validated.

2.2.4: Hydrogen Compressor Verification and Validation

Most of the models in literature that were reviewed for this work used the assumption of a polytropic compression of an ideal gas to obtain the required compression work. The compressor module can be validated by comparing the predicted energy consumption in the model to measured energy consumption values published in a Department of Energy (DOE) report on hydrogen compressors [31]. In the DOE report, a range of experimental specific energy consumption for hydrogen compressors operating up to 880 barg was found to be 1.7 to 6.4 kWh/kg. The hydrogen compressors studied in the report included a wide range of pressures and applications which account for the variability in the measured range of energy consumption. The system model calculates a compressor specific energy consumption of 4.0 kWh/kg using a final hydrogen pressure of 880 barg. Because the model prediction is well within

the range of measured values, it can be assumed that the compressor module is validated to actual hydrogen compressors operating in the field.

2.2.5: System Cooling Module Verification and Validation

Experimental measurements of coolant flowrate or energy consumption for a PEM electrolyzer system cooling circuit is not available in literature. With the absence of data on the green hydrogen generation system cooling circuit, the cooling system module must be verified and validated against a comparable system in literature. A hydrogen refueling station utilizing a 120-kW PEM electrolyzer uses an R407C chiller to provide cooling to the rectifiers, electrolyzer stack, and hydrogen compressor. A similar chiller system was thermodynamically evaluated in [32] and had a COP of 3.265. Because the two systems use the same refrigerant and thermodynamic cycle, this work assumes that the electrolyzer cooling system will also have a COP of 3.265. Measurements of an actual electrolyzer system cooling circuit are required to validate the system cooling methodology.

2.3: MULTI-ELECTROLYZER SYSTEM MODEL AND SCALING

If green hydrogen is to become widely available, large-scale green hydrogen generation systems will need to be deployed alongside RE generation facilities in the multi-MW or GW scale. The state-of-the-art PEM electrolyzer stacks have power ratings of around 1.25-MW per electrolyzer stack. A green hydrogen generation system that utilizes RE generation from a utility scale facility will have to have a total power rating in the multi-MW or GW scale meaning that multiple PEM electrolyzer stacks will have to be included as part of the system. The model developed in this work is uniquely scalable due to the simplicity and modular structure of the BOP model. Individual component modules can be duplicated to represent the configuration of the utility scale system. To evaluate the utility scale green hydrogen generation system, the model based on the 120-kW Nel Hydrogen C20 was scaled up to a multi-stack system comprised of 10 state-of-the-art 1.25-MW electrolyzer stacks which utilize 10 separate power

electronic units and a centralized hydrogen purification, compression/storage, and cooling circuit.

The power electronics rating was scaled using the rectifier efficiency at its maximum rated output to determine the new rectifier rating based on the required maximum electrolyzer power. At 100% of its rated DC power output, the 73-kW IGBT rectifier has a power conversion efficiency of 94.1%. The required AC power rating of the scaled IGBT rectifier is obtained by dividing the scaled electrolyzer power rating by the rectifier efficiency at full DC power output. The state-of-the-art MW scale PEM electrolyzer systems typically use the same IGBT rectifier technology and therefore the same AC-DC power conversion efficiency regression model is used with the scaled rectifier units.

The electrolyzer stack module is scaled from 120-kW to 1.25-MW per stack by iteratively increasing the cell area while keeping the same number of cells per stack. The physical parameters of the 120-kW electrolyzer were kept constant such as the membrane thickness and conductivity. The cell area was iteratively increased until the electrolyzer power equaled 1.25-MW at a current density of 1.9 A/cm^2. The same method of predicting the performance of each electrolyzer stack is used with the increased cell area which produces the same current/voltage relationship but with higher amounts of current flowing through the electrolyzer stack. The current density of 1.9 A/cm^2 was selected because that was the highest current density achieved by the 60-kW C10 system in [21]. The current density is limited by the physical construction of the PEM electrolyzer. It is assumed that the 1.25-MW electrolyzer stack would have the same current density limit of 1.9 A/cm^2 as the 60-kW electrolyzer because the cell construction would be the same. If the same current density limit is applied, the only way to increase the power rating of the electrolyzer stack is to either increase the number of cells per stack or increase the area of each cell. If the number of cells per stack is increased the total voltage requirement of the power electronics would have to increase dramatically. In the interest of using the same power electronics technology it was decided to keep the original number of

cells per stack and increase the cell area to keep the original voltage requirements of the rectifiers. Electrolyzer manufacturers most likely scale their technology using a combination of increased cell area and number of cells per stack but without knowing the balance between the two methods, the area scaling method is acceptable. The goal of scaling the power rating of the electrolyzer while keeping the same voltage-current relationship is achieved.

It is assumed that the utility scale green hydrogen generation system would utilize a centralized purification system to avoid purchasing multiple smaller systems. The PSA dryer used in the 120-kW electrolyzer model was scaled by assuming that the new PSA dryer would increase the size of the adsorbent bays and therefore need to increase the amount of purge gas used to remove impurities. To scale the amount of purge gas used, the PSA orifice diameter was iteratively increased to maintain the same loss percentage as the 120-kW system at its full production capacity (6.4%). The same empirical discharge coefficient and uptime of the PSA dryer were used with the scaled system due to the lack of experimental data on larger scale systems of which new discharge coefficients and uptime coefficients can be derived from.

The utility scale green hydrogen generation system is assumed to utilize a large centralized two-stage compressor to compress all the hydrogen coming from each electrolyzer stack to the same vehicle refueling pressure of 880 barg. The hydrogen compressor module is inherently scaled when the electrolyzer module is scaled. Equation 26 is used to calculate the compression work based on the starting and final pressures as well as the hydrogen flowrate. The scaled model assumes the same assumptions can be made to treat the product hydrogen as an ideal gas. The compressor isentropic efficiency is assumed to stay the same with the higher hydrogen flowrate. The compression work is then only dependent on the hydrogen flowrate which is determined by the current in the electrolyzer which has already been scaled by increasing the power rating and cell area of the electrolyzer stack.

The utility scale green hydrogen generation system is assumed to use a larger R407C cooling circuit to cool the 10 power electronics, 10 electrolyzer stacks, and centralized hydrogen

compressor. The system cooling circuit is inherently scaled when the power electronics, electrolyzer, and hydrogen compressor modules are scaled because their inefficiencies produce a higher amount of heat generation. The scaled model assumes that the larger cooling circuit has the same COP as the 120-kW system. The larger scale system will battle with added heat loss as the coolant is routed to a larger system and will most likely see a decreased COP. Without experimental data from a large-scale system to measure COP, this assumption is acceptable for this analysis. Table 2 shows the scaled specifications of the 12.5 MW multi-electrolyzer stack system with 10 electrolyzer stacks fed by 10 power electronics and a centralized hydrogen purification, hydrogen compressor, and system cooling.

Table 2: Utility scale system specifications utilizing multiple electrolyzer stacks.

Power Electronics Rating	10 X 1.31 = 13.1	MW
Electrolyzer Rating	10 X 1.25 = 12.5	MW
Electrolyzer Cell Active Area	5,950	cm^2
Electrolyzer Cathode Pressure	30	barg
Electrolyzer Temperature	60	°C
Hydrogen Storage Pressure	880	barg
PSA Purge Gas Orifice Diameter	0.494	mm

2.4: GREEN HYDROGEN GENERATION SYSTEM LOADING STRATEGIES

When operating a multi-electrolyzer green hydrogen generation system with a variable and intermittent power source such as wind and solar PV, it is necessary to develop a strategy on how power is distributed to each electrolyzer stack. For this model analysis, two “loading” strategies are developed to control the flow of power to each electrolyzer in the system. For both strategies, a minimum electrolyzer power is specified so that the system can avoid any efficiency losses experienced at low electrolyzer loads. The first loading scheme is named the series loading (SL) scheme where the total amount of incoming excess RE generation is used

to “load” the system in a series fashion. The first electrolyzer stack is loaded up to its rated maximum power and then the next stack is loaded if the leftover RE generation can load the second stack beyond the selected minimum electrolyzer power. This is repeated until all 10 stacks are loaded up to their maximum power rating. If the total amount of excess RE generation is less than the selected minimum electrolyzer power or it is higher than 10 stacks can take at full rated power, it is curtailed or wasted. Figure 9 shows the flowchart for how the system loads each electrolyzer with the SL strategy. The system model calculates the AC power input to the rectifier at the minimum electrolyzer power and uses logic objects in Simulink to impose an “operating factor” on each rectifier. The rectifier operating factor controls the amount of DC power sent to each electrolyzer stack.

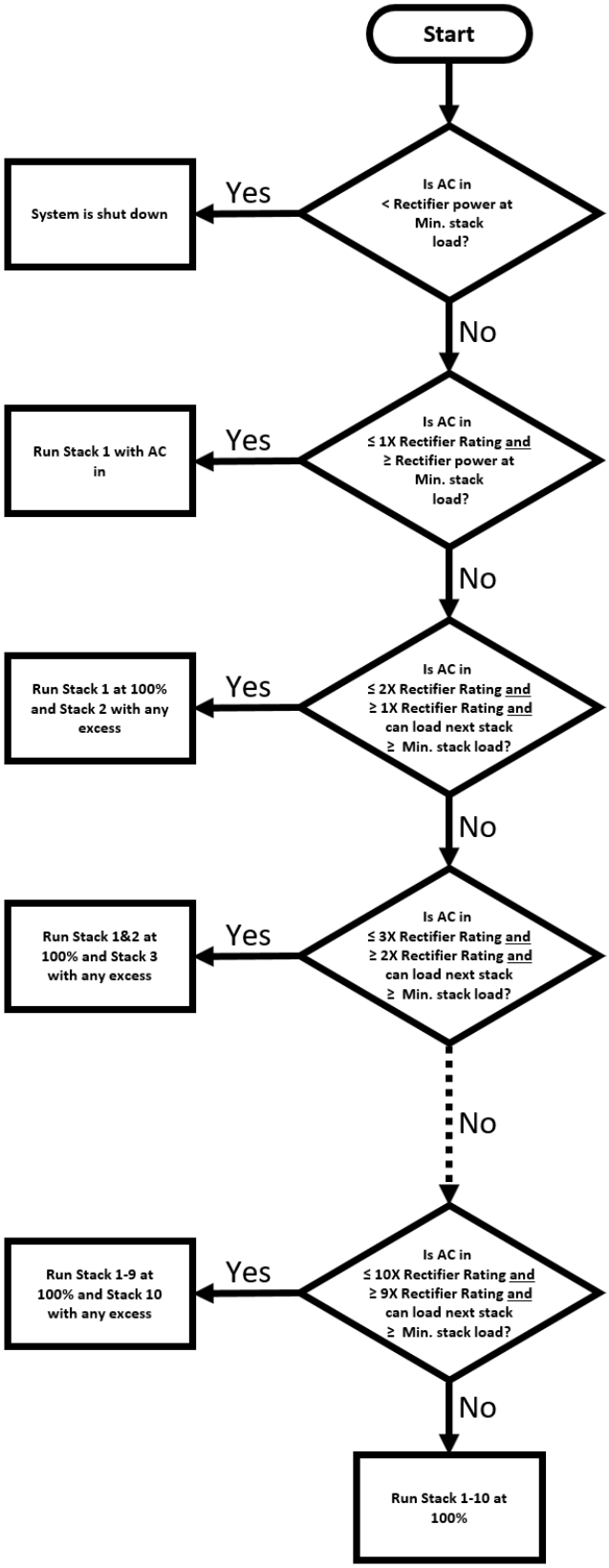

Figure 9: Series loading strategy flowchart.

The second loading scheme is named the parallel loading (PL) scheme where the total amount of incoming excess RE generation is split evenly in parallel between several electrolyzer stacks. Based on the selected minimum electrolyzer power, this scheme calculates how many electrolyzer stacks can be operated above the selected range with the amount of excess RE generation available and splits the “load” evenly among those electrolyzer stacks. If the total amount of excess RE generation is less than the selected minimum electrolyzer power or it is higher than 10 stacks can take at full power, it is curtailed. If the incoming power is less than what is needed to run two electrolyzers at the selected minimum electrolyzer power, then one stack is loaded up to its rated power and any excess is curtailed. Figure 10 shows the flowchart for how the system loads each electrolyzer with the PL strategy. Similar logic objects are used to calculate the operating factor of each rectifier. The Simulink model contains a manual switch which determines what loading strategy is used. Before the model is run, it is important to manually select the operating strategy.

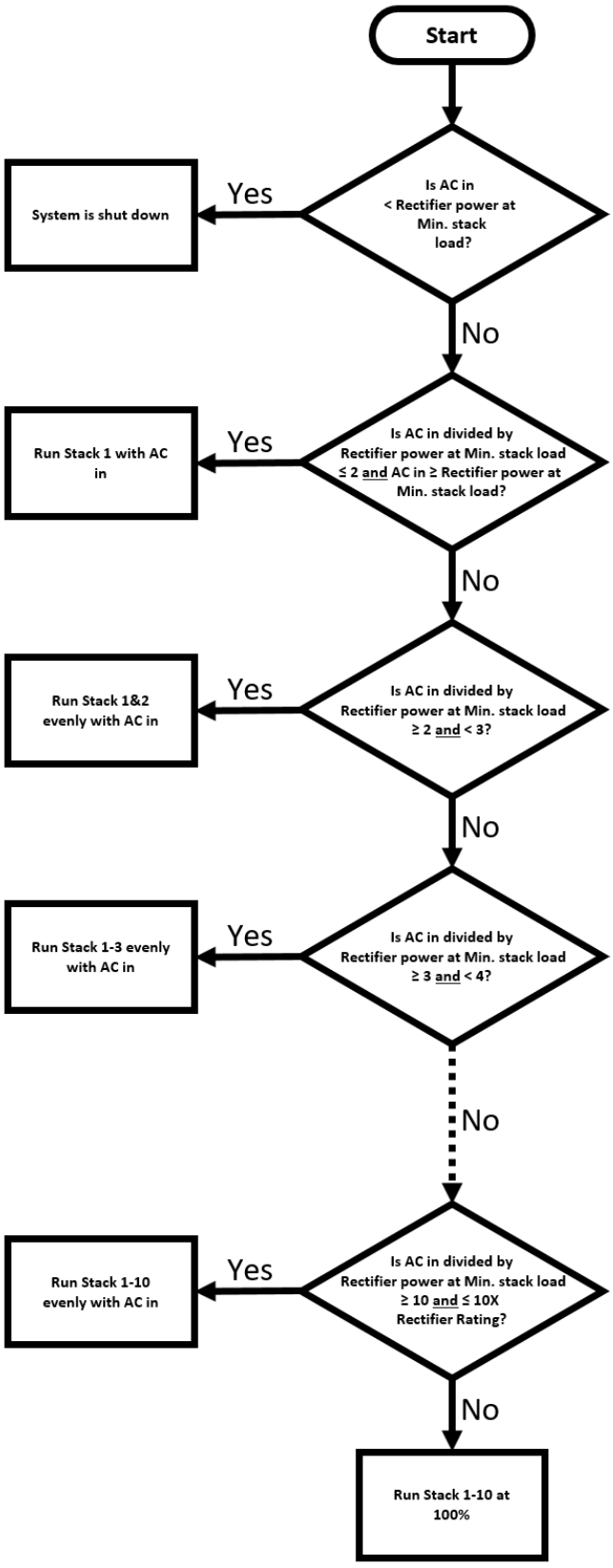

Figure 10: Parallel loading strategy flowchart.

Figure 11 depicts how a sample of incoming AC power is distributed between the multi-electrolyzer system using the two different loading strategies. The principle of the parallel loading strategy is that low electrolyzer power conditions can be avoided by spreading power between multiple stacks instead of trying to load any one stack to its full rated power and the next stack with any leftover.

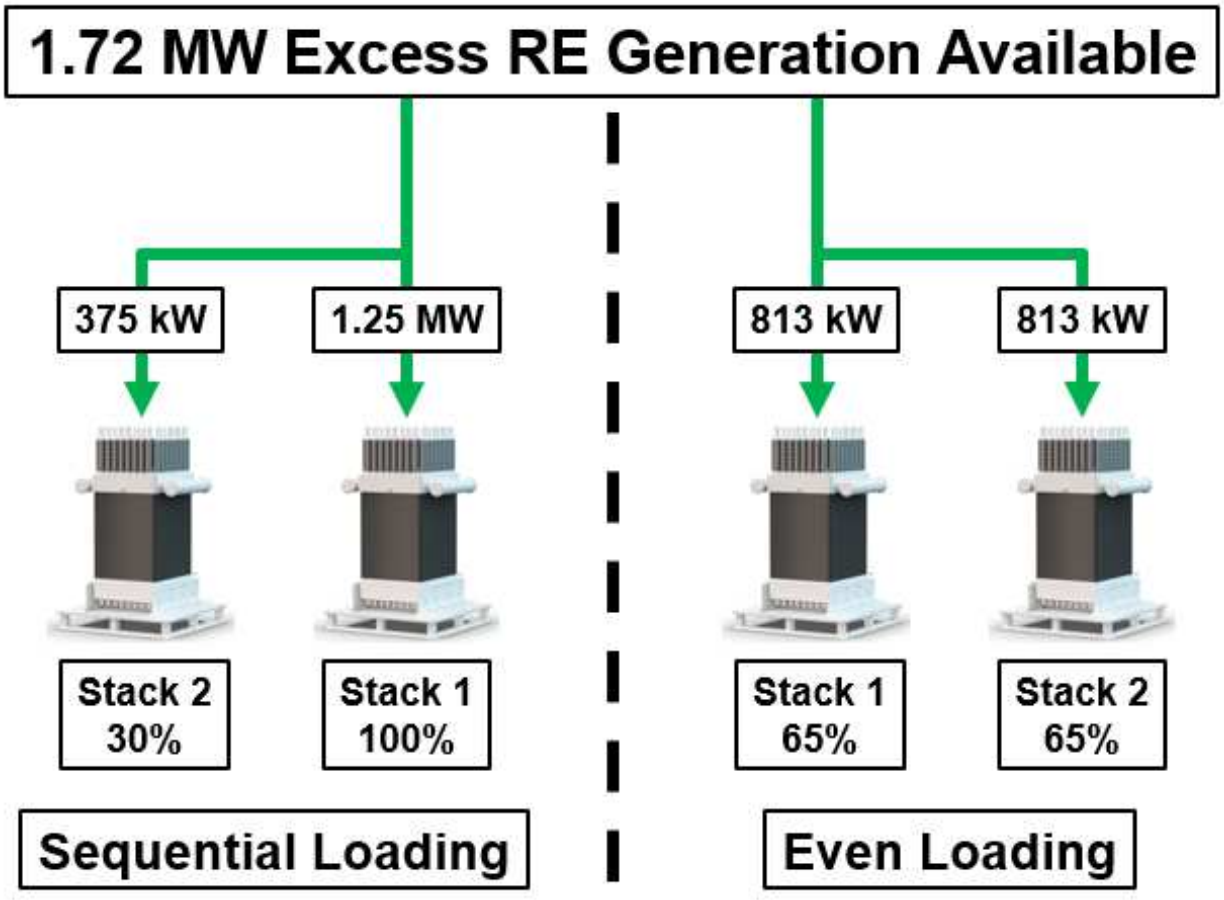

Figure 11: Example of electrolyzer power distribution with series and parallel loading schemes.

3.1: SINGLE ELECTROLYZER SYSTEM RESULTS AND DISCUSSION

The Nel Hydrogen C20 system specifications were used in the model to represent a baseline green hydrogen generation system utilizing a single 120-kW electrolyzer stack. The model was run at steady state from 10% to 100% of the rated electrolyzer power with 5% load steps from 10% to 30% of rated load and 10% load steps from 30% to 100%. Figure 12 shows the predicted specific energy consumption and energy conversion efficiency of the single electrolyzer stack system.

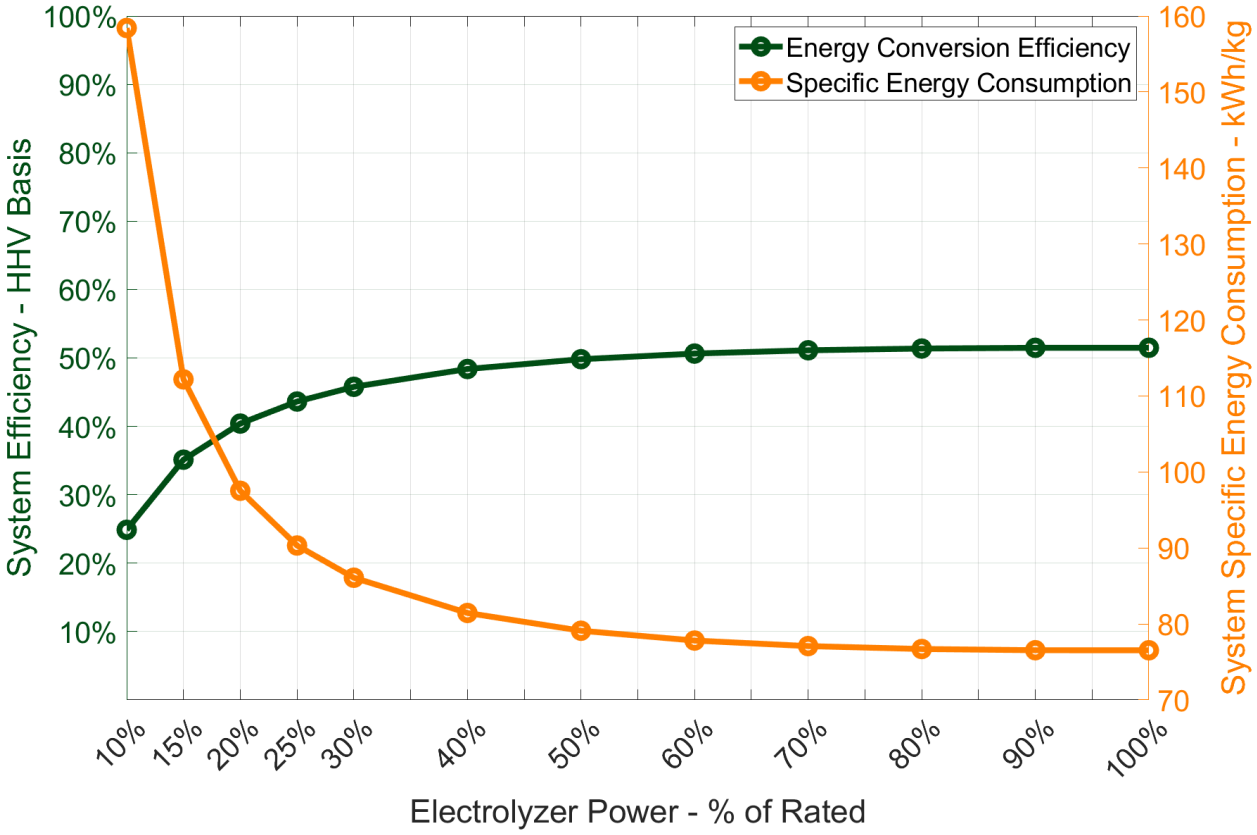

Figure 12: Specific energy consumption and energy conversion efficiency at part electrolyzer load for a 120-kW electrolyzer system at 60 °C and 30 barg cathode pressure.

The system energy conversion efficiency dramatically decreases below 40% of the electrolyzer power. Above 40% of the electrolyzer power, the system energy conversion efficiency stabilizes and hits a maximum of approximately 50% at the 100% of the rated

electrolyzer power load condition. Figure 13 explains the logarithmic behavior of the system energy conversion efficiency which is caused by the rapidly increasing specific hydrogen loss and the decaying electrolyzer voltage efficiency. The specific hydrogen loss increases dramatically because of the combination of the reduced flowrate of hydrogen produced in the electrolyzer due to the decreased current flow and the constant flowrate of purged hydrogen in the PSA that is demanded because of the constant hydrogen pressure and orifice diameter.

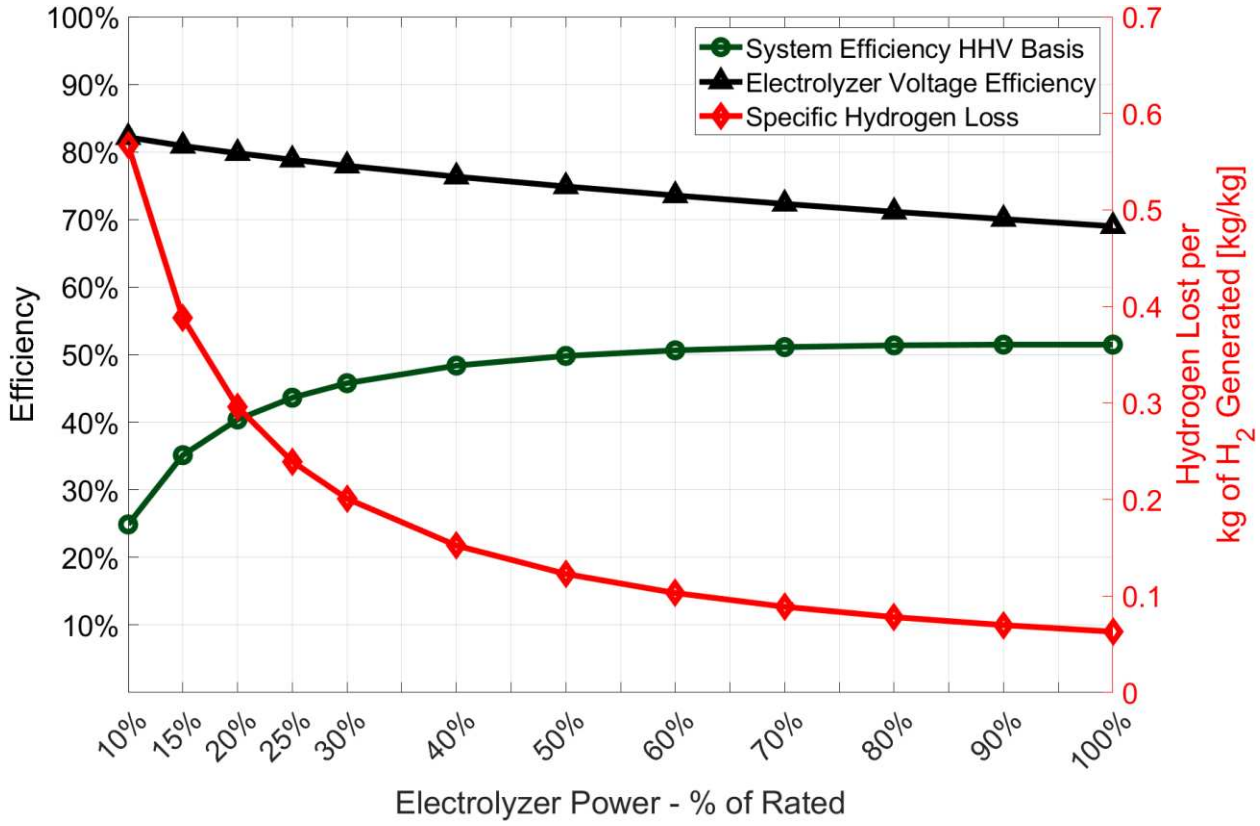

Figure 13: System conversion efficiency, electrolyzer voltage efficiency, and specific hydrogen loss at part electrolyzer load for a 120-kW electrolyzer system at 60 °C and 30 barg cathode pressure.

The BOP energy consumption remains relatively low across the range of electrolyzer power compared to the energy consumed by the electrolyzer. Figure 14 shows the electrolyzer, compressor, and cooling system energy consumption normalized to the amount of hydrogen which is generated in the electrolyzer stack. The normalized cooling system energy consumption is practically constant across the range of electrolyzer power because it is tied

directly to the amount of hydrogen that is being generated in the electrolyzer stack. The normalized electrolyzer energy consumption increases with electrolyzer power because of the increased overpotentials at high current densities which causes a decrease in voltage efficiency. The normalized compressor energy consumption dips at low electrolyzer power because it is reliant on the flowrate of hydrogen leaving the PSA dryer which dramatically decreases at low electrolyzer power.

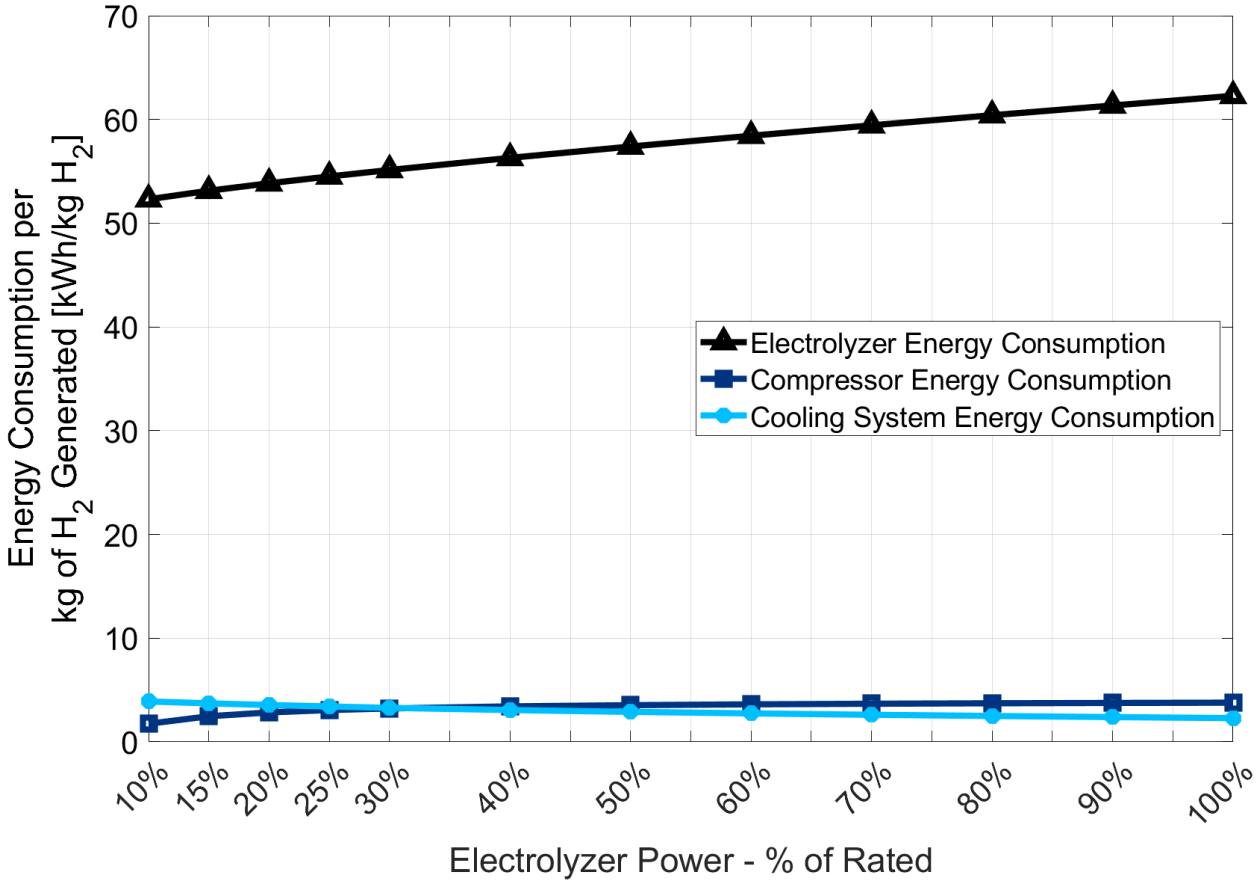

Figure 14: Electrolyzer, compressor, and cooling system energy consumption normalized to the hydrogen generated in the electrolyzer.

Figure 14 also shows that the electrolyzer is the dominant energy consumer in the green hydrogen generation system. Electrolyzer efficiency gains can have a significant impact on the specific energy consumption and energy conversion efficiency. Further scaling of PEM electrolyzers will enable technological advances in the PEM electrolyzer efficiency such as reducing ionic resistance and ohmic overpotentials within the cell by innovating cell construction

and materials selection. Advances in electrode and catalyst technology can help to reduce the activation overpotential and promote higher electrolyzer efficiencies as well.

The experimental current densities from [21] were used to calculate the predicted thermo-neutral cell potential and overpotentials using the analytical voltage-current relationship model. Figure 15 shows the cell voltage breakdown between the thermo-neutral cell potential, activation overpotential and ohmic overpotential. The reason that the electrolyzer voltage efficiency decreases as the electrolyzer power increases is due to an increase in the overpotentials that must be applied to the electrolyzer cell. As the current density increases, the thermo-neutral cell potential does not change if it is assumed that the thermodynamic conditions of the reaction do not change. The activation overpotential increases slightly as the current density increases but the ohmic overpotential experiences a liner increase with current density and is the primary factor of a decreased electrolyzer voltage efficiency with higher current densities.

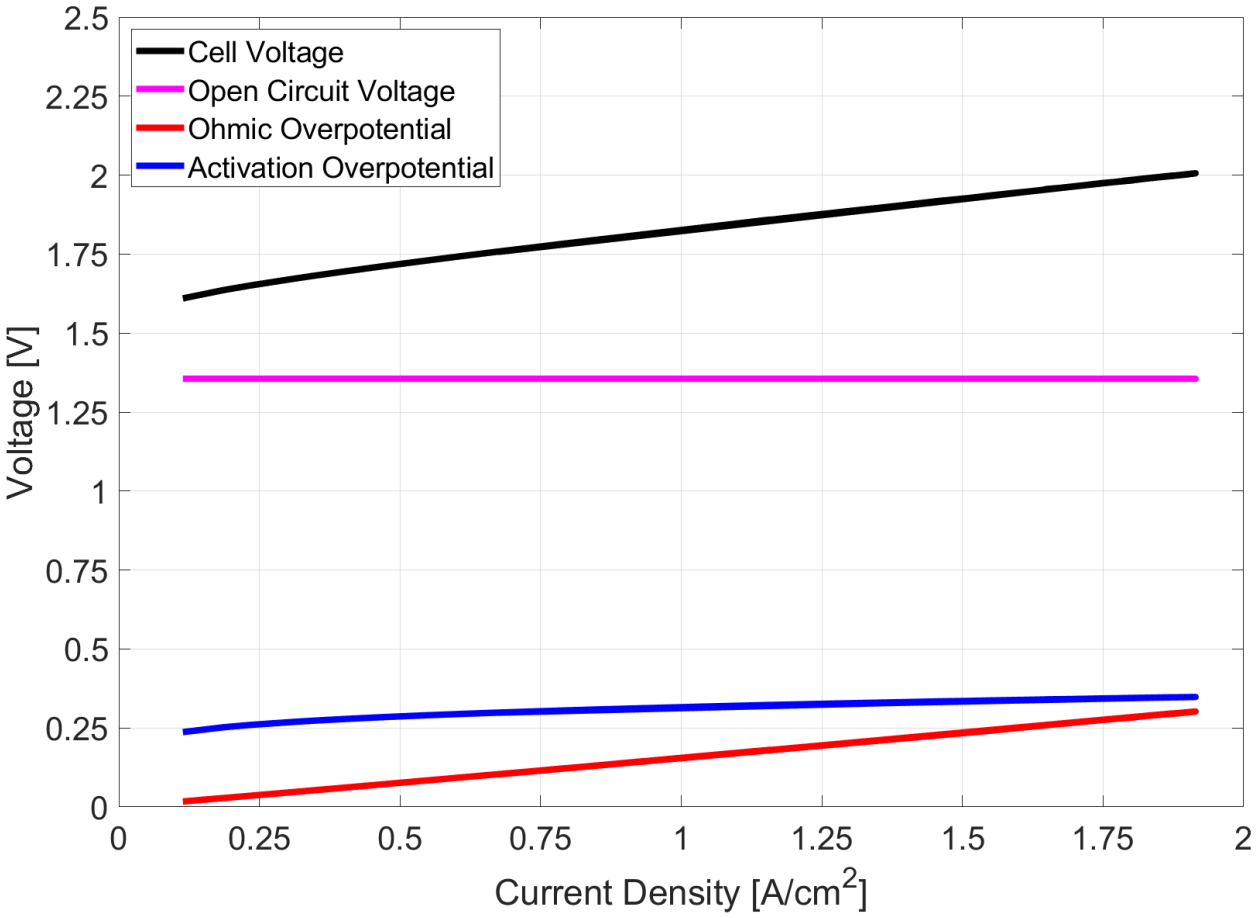

Figure 15: Electrolyzer cell voltage breakdown into the open circuit voltage, activation overpotential, and ohmic overpotential for a 120-kW electrolyzer system at 60 °C and 30 barg cathode pressure.

The voltage efficiency of the electrolyzer stack is shown to decrease with electrolyzer power in figure 13. On the other hand, the IGBT rectifier becomes more efficient with increased electrolyzer power because the rectifier is operating closer to its designed DC output rating. Figure 16 shows the electrolyzer voltage efficiency and AC-DC conversion efficiency as the electrolyzer power is varied.

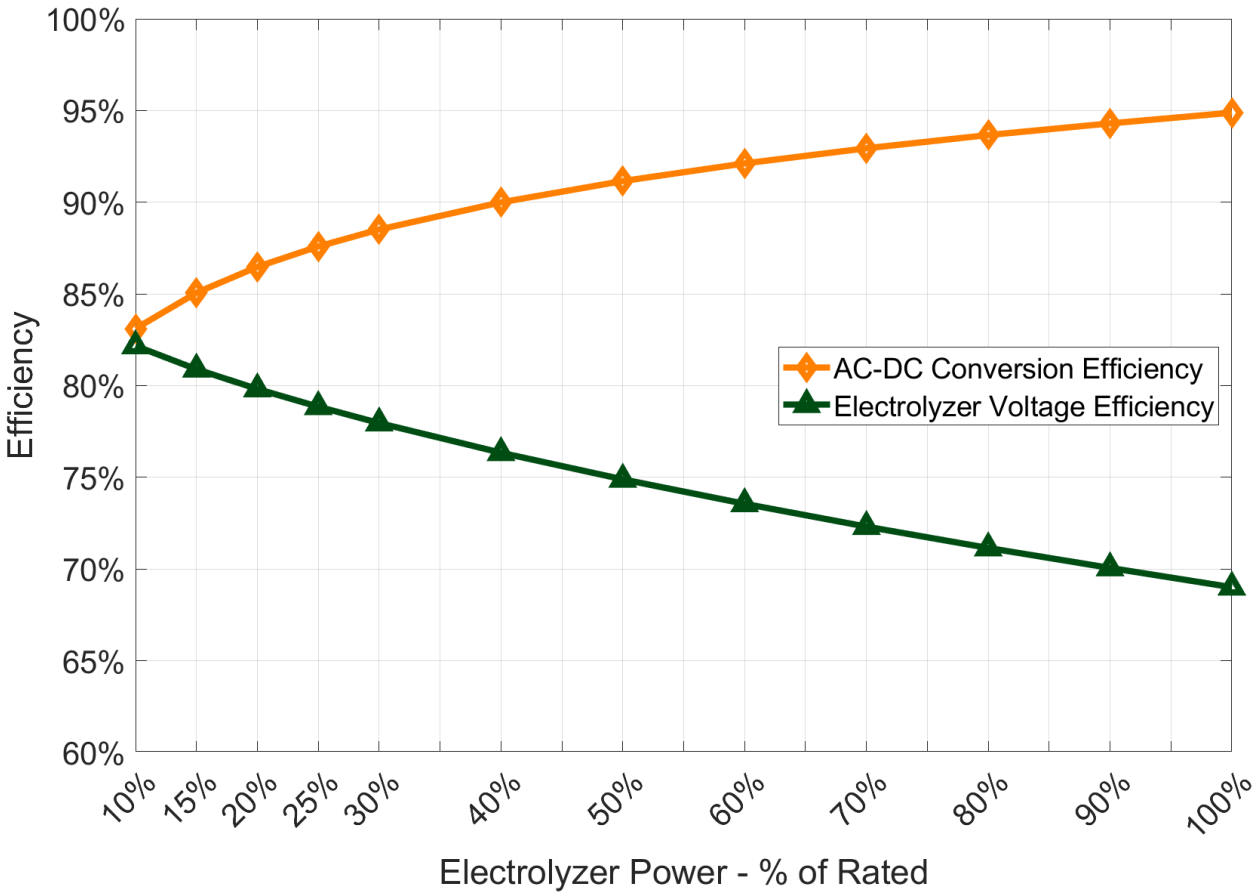

Figure 16: Electrolyzer voltage efficiency and AC-DC power conversion efficiency vs. electrolyzer power.

The single 120-kW electrolyzer system model based on a Nel Hydrogen C20 was run at steady state for the same load range of 10% to 100% of the rated electrolyzer power but at 30, 60, and 90 barg cathode pressure in the electrolyzer. Figure 17 shows the system specific energy consumption and system energy conversion efficiency for the 3 different cathode pressure conditions.

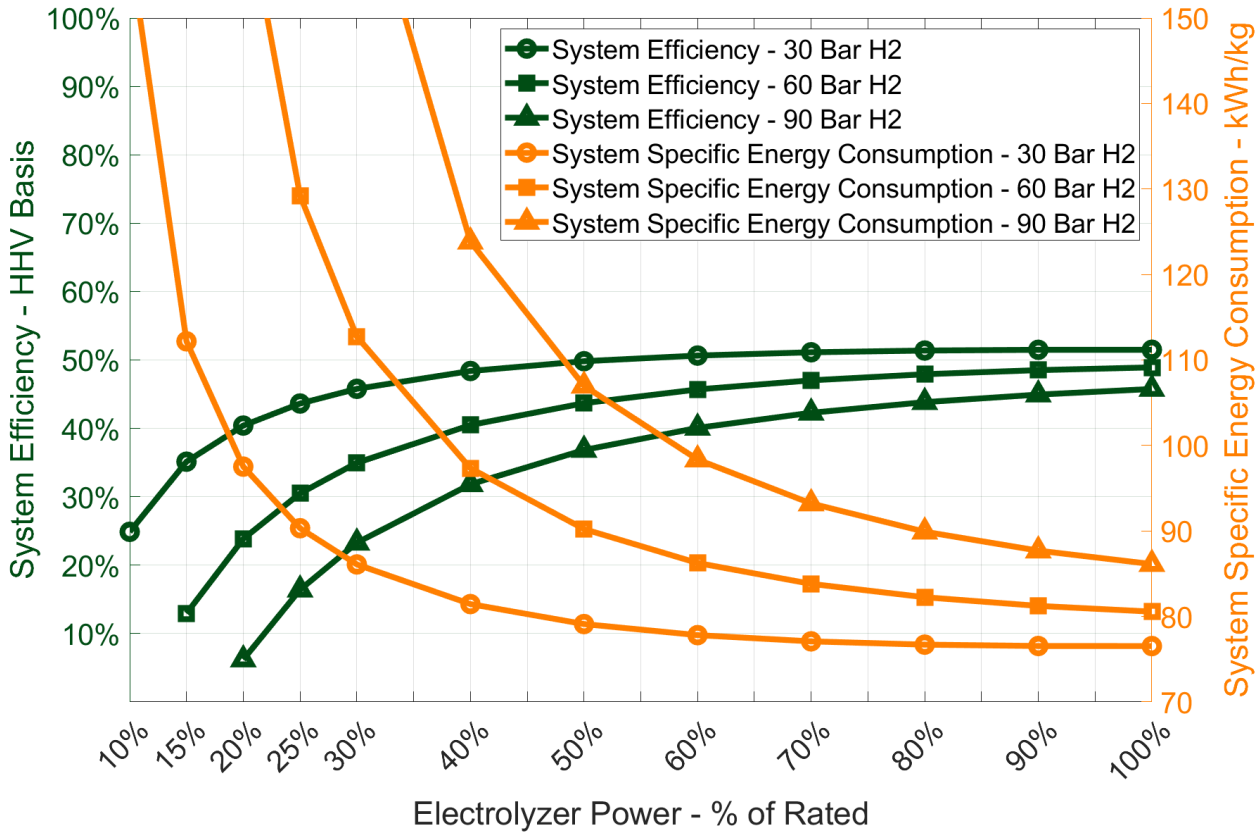

Figure 17: Specific energy consumption and energy conversion efficiency at part electrolyzer load for a 120-kW electrolyzer system at 60 °C and with electrolyzer cathode pressures of 30, 60, and 90 barg.

The increasing electrolyzer cathode pressure causes an increase in system specific energy consumption and decrease in system energy conversion efficiency. This increase in specific energy consumption is primarily caused by an increase in hydrogen loss. As electrolyzer cathode pressure is increased, the constant flowrate of hydrogen used to purge the PSA dryer is increased because of the fixed orifice. An increase in electrolyzer cathode pressure also changes the voltage-current relationship of the PEM electrolysis cell and increases the voltage requirement.

Combining the results from the load sweep and pressure study, it can be concluded that the electrolyzer system energy conversion efficiency begins to decrease rapidly below 40% of the rated electrolyzer power and that increasing the cathode pressure decreases energy conversion efficiency across the range of electrolyzer load. It is also important to note that

increasing the cathode pressure causes a narrowing of the operating range of the electrolyzer from 10-100% for 30 barg to 20-100% for 60 barg because of the increased hydrogen loss. The relationships identified within the single electrolyzer stack system between the energy conversion efficiency and the operating conditions of the system such as cathode pressure and current density suggest that green hydrogen generation systems can be optimized between specific applications by avoiding low electrolyzer power and high cathode pressures.

3.2: RENEWABLE ENERGY GENERATION PROFILE

One of the objectives and capabilities of the system model is to predict the system's performance when it is operated with a variable and intermittent time series of electricity input. This is useful when analyzing green hydrogen generation systems coupled with wind and solar PV power generation facilities as the generated power from these facilities has a highly variable and intermittent profile. On-site RE generation data in Fort Collins is unavailable for this work, instead, the Electric Reliability Council of Texas (ERCOT) publishes generation and load data in 1-hour snapshots for the whole state of Texas that can be used to mimic the input to a real green hydrogen generation system. This model analysis uses the RE generation and grid load data from ERCOT for the entire year of 2022 and scales this data down to a utility scale. The multi-electrolyzer green hydrogen generation system being analyzed consists of 10 x 1.25-MW PEM electrolyzers being fed with 60-MW of wind turbines and 20-MW of solar PV. The multi-electrolyzer system contains a separate rectifier system for each electrolyzer which means that each electrolyzer stack can be loaded individually. The RE generation facility experiences a load from the grid which is derived by scaling down the ERCOT grid load until it averages around 12.5-MW. The electricity generation from the wind turbines and solar PV is calculated using the recorded capacity factors and the scaled down RE capacity. The RE capacity was determined by iteratively decreasing the combined wind and solar capacity in Texas until the total amount of excess RE generation for the year was equal to the amount of insufficient RE

generation. Figure 18 depicts the scaled RE generation and scaled grid load from January 1st to January 7th, 2022.

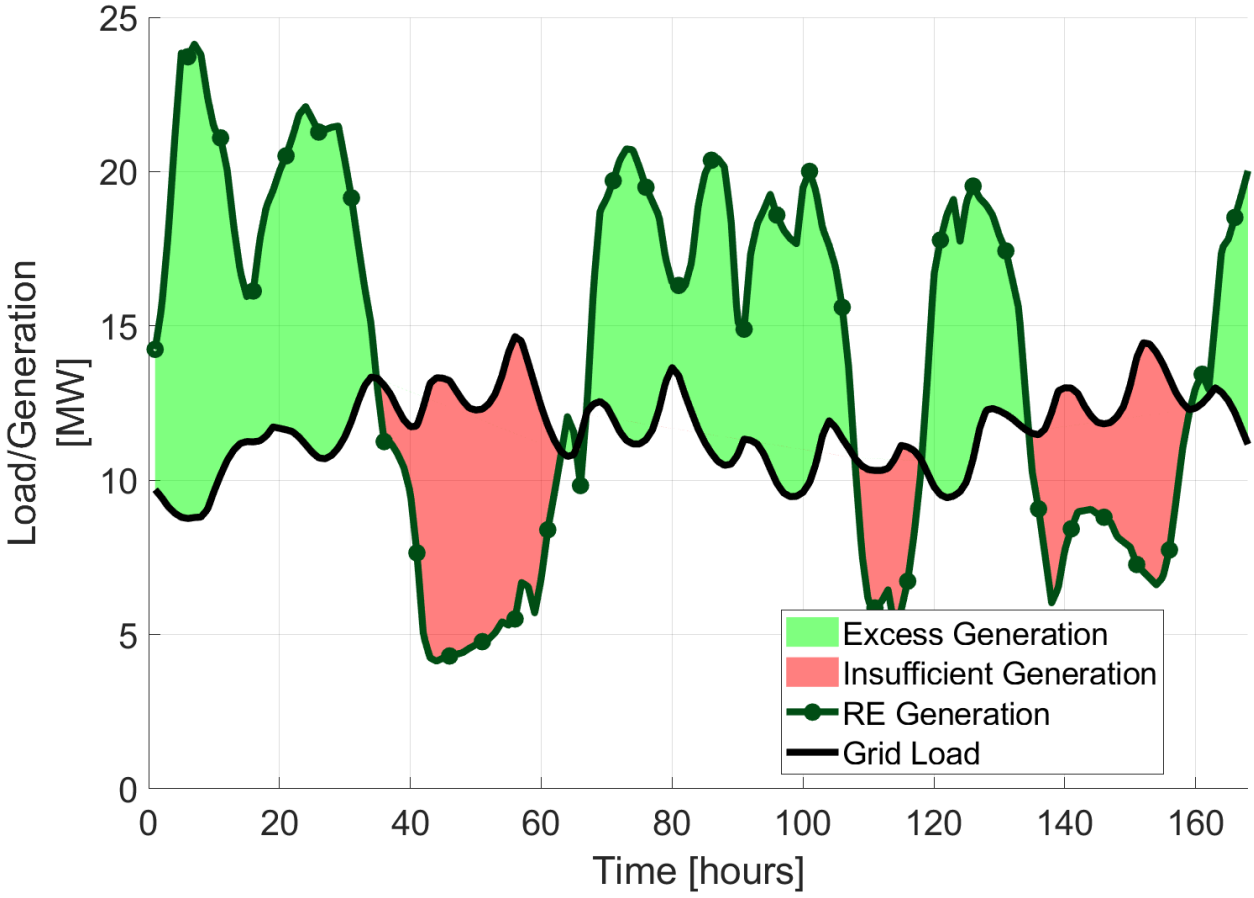

Figure 18: Scaled ERCOT combined wind and solar generation and grid load for Jan 1st to Jan 7th, 2022 [36].

The green shaded area in figure 18 represents the electricity that would be available for the green hydrogen generation system in a RE storage scenario. Figure 19 shows the excess RE generation from the scaled ERCOT data that is used as the input to the multi-electrolyzer green hydrogen generation system model.

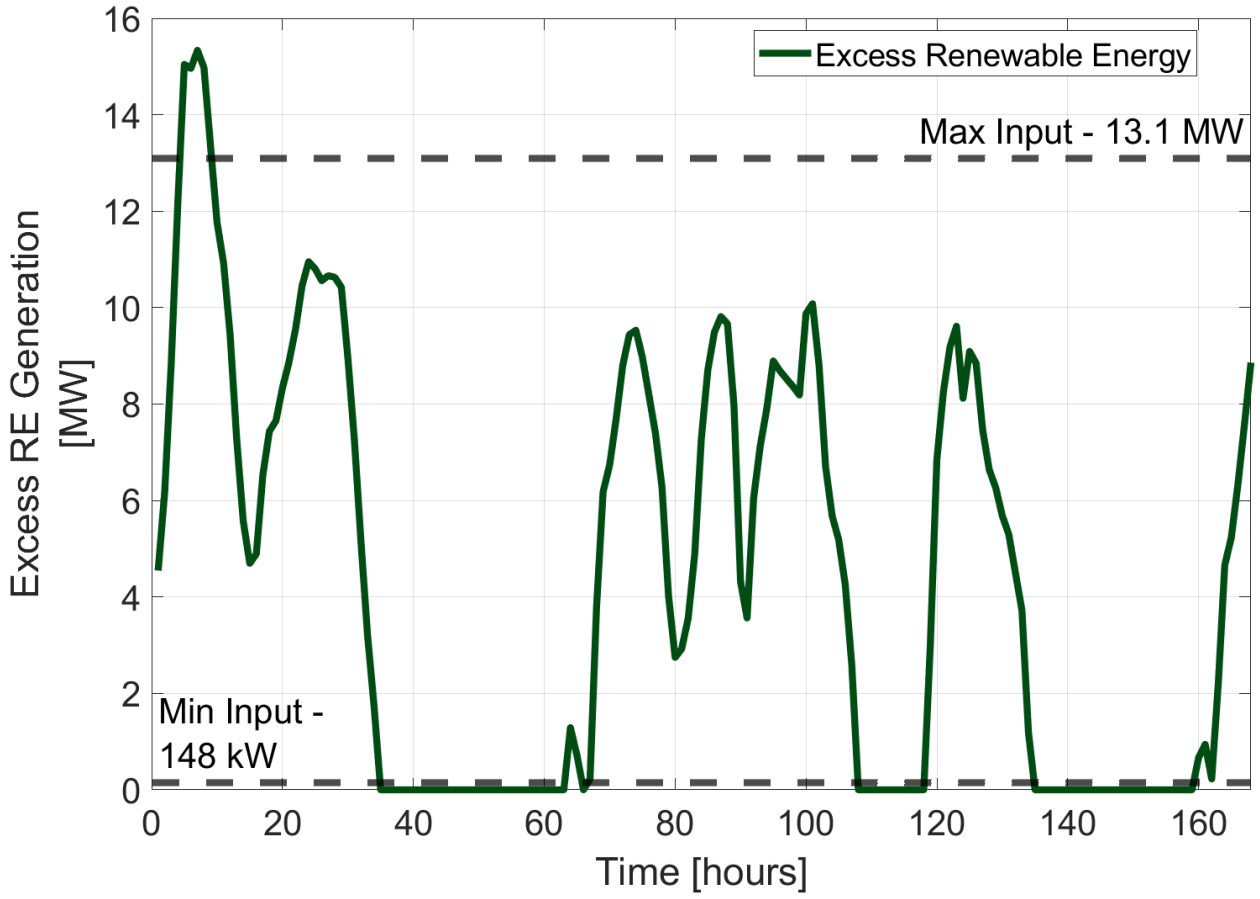

Figure 19: Snapshot from Jan 1st to Jan 7th, 2022 of excess RE generation from the scaled ERCOT data used as the model input [36].

The results presented for this model analysis are unique to the case study of ERCOT RE generation and will change somewhat depending on the profile of input AC power. For example, figure 19 shows that for the 7-day period, only once was the RE generation greater than what could be used by the multi-electrolyzer system. If the amount of incoming RE was much larger and resulted in a case where most of the time that excess RE is available, it is more than what the system can use, then performance of the system would change, and the same loading strategies may produce different results. The system model is a great tool to look at a specific RE generation site to determine the optimal method of operating the system with the site-specific generation profile.

3.3: MULTI-ELECTROLYZER SYSTEM RESULTS AND DISCUSSION

The excess RE generation shown in figure 19 can be imposed on the system model to observe how the system performs with a variable and intermittent input of power. Figure 20 shows the overall system energy conversion efficiency for the year 2022 with the SL scheme and the PL scheme using different minimum electrolyzer power setpoints. It is important to note that the energy conversion efficiency is based upon the total RE generation available to the green hydrogen generation system and therefore any amount of RE input that is curtailed because of the operating strategy will reduce the conversion efficiency. The amount of hydrogen produced for the ERCOT case study follows the same trend as the system energy conversion efficiency in figure 20 with the most amount of hydrogen being produced with the SL strategy and a minimum electrolyzer power of 10% of the rated electrolyzer power.

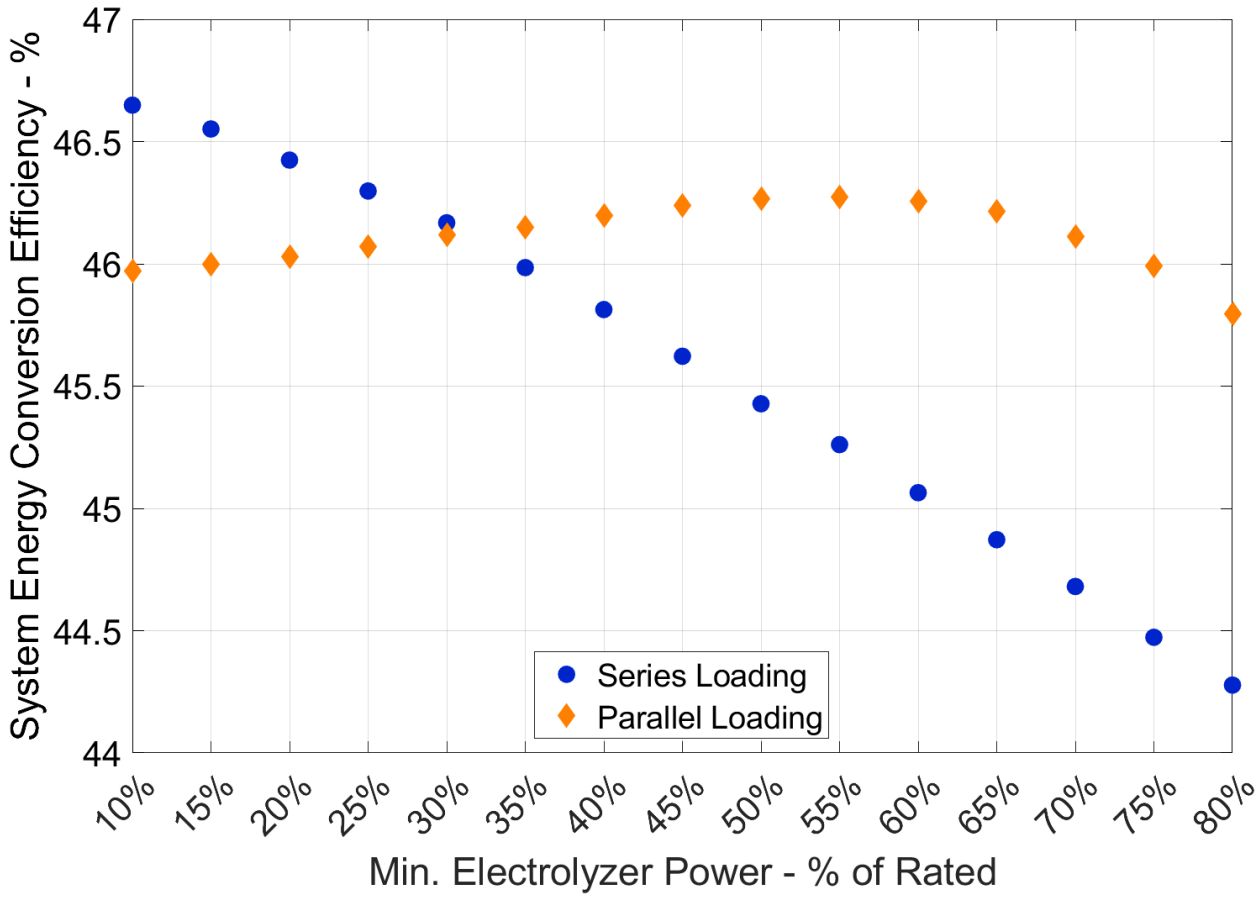

Figure 20: Multi-electrolyzer system energy conversion efficiency comparison between series and parallel loading strategies at 60 °C and 30 barg cathode pressure.

The SL scheme has a slightly higher energy conversion efficiency than the PL scheme when the selected minimum turndown range is between 10% and around 30% of the electrolyzer rating. Beyond around 30% of the electrolyzer rating as the minimum turndown range, the PL strategy results in a higher energy conversion efficiency. This increase is because the amount of curtailed RE increases as the minimum electrolyzer power limit increases for the SL scheme. Another factor impacting the switch of PL being more efficient than SL is that as the minimum electrolyzer power is increased for the PL scheme, the average electrolyzer power increases which causes a reduction in the operating specific energy consumption. Figure 21 shows the average electrolyzer power for each of the 10 electrolyzer stacks based on the loading strategy and minimum electrolyzer power setpoint.

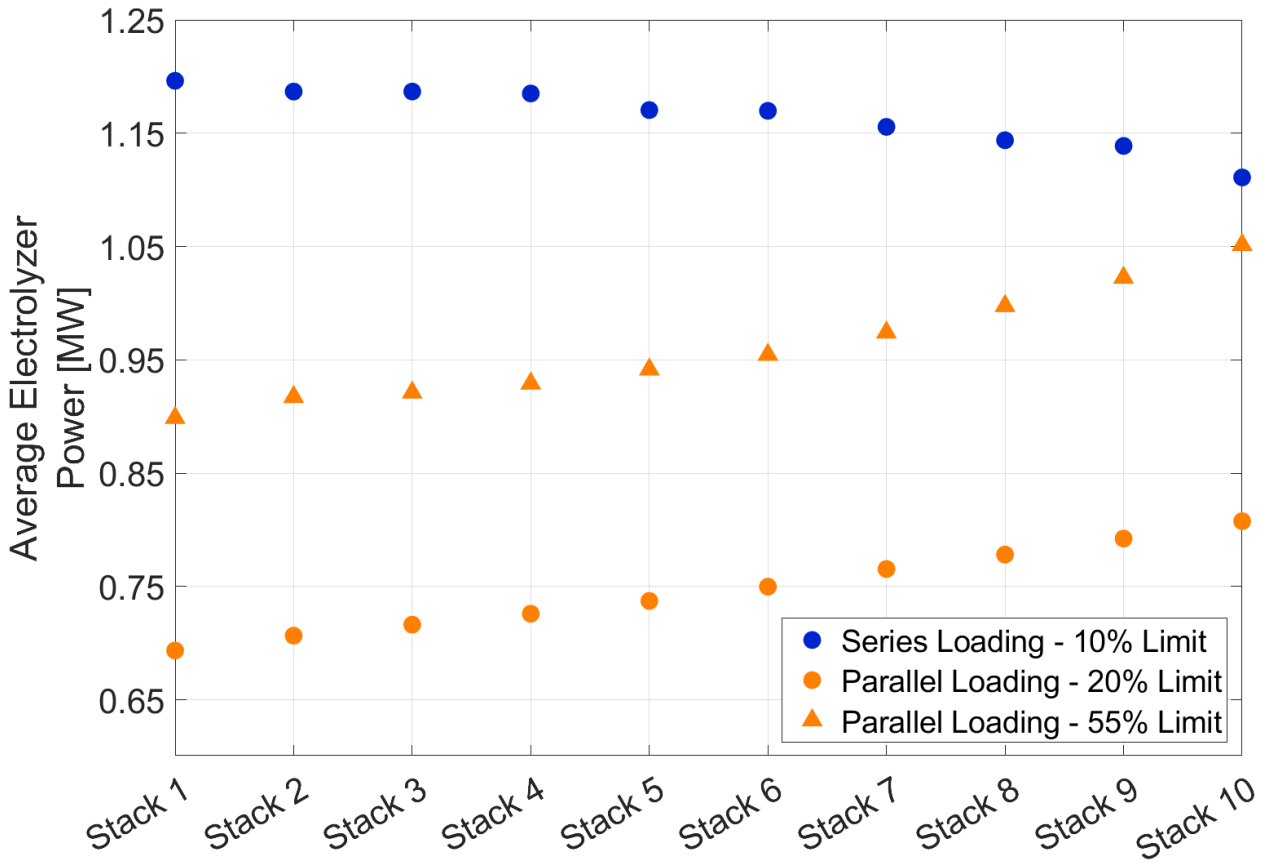

Figure 21: Average electrolyzer stack power comparison between series and parallel loading strategies at 60 °C and 30 barg cathode pressure.

Figure 22 shows the amount of incoming RE that is wasted with the SL and PL loading schemes. For the SL strategy the amount of curtailed input energy increases as the minimum electrolyzer power setpoint increases. This behavior is explained because as the minimum setpoint increases, the amount of input electricity needed to load the next electrolyzer stack in the series increases and causes more events where the total amount of input electricity is not sufficient to load the next stack beyond the minimum power setpoint. The curtailed input energy is less for the PL strategy because the system can split generation between any number of electrolyzer stacks whereas the SL strategy is limited in loading electrolyzer stacks one after another. The case where the SL scheme is unable to load the next stack is mitigated with the PL strategy because the load can be distributed between multiple stacks if each stack can be loaded past the minimum electrolyzer power setpoint and avoids curtailing the input power. As

the minimum electrolyzer power setpoint is increased, the PL scheme experiences an increase in the curtailed input energy because it becomes more difficult to load several stacks with an even amount of power above the minimum setpoint. The curtailed RE input within the system means that some of the electrolyzer stacks are not used as frequently as is technically possible and may lead to an undesirable economic situation where expensive equipment such as the electrolyzer system is unutilized.

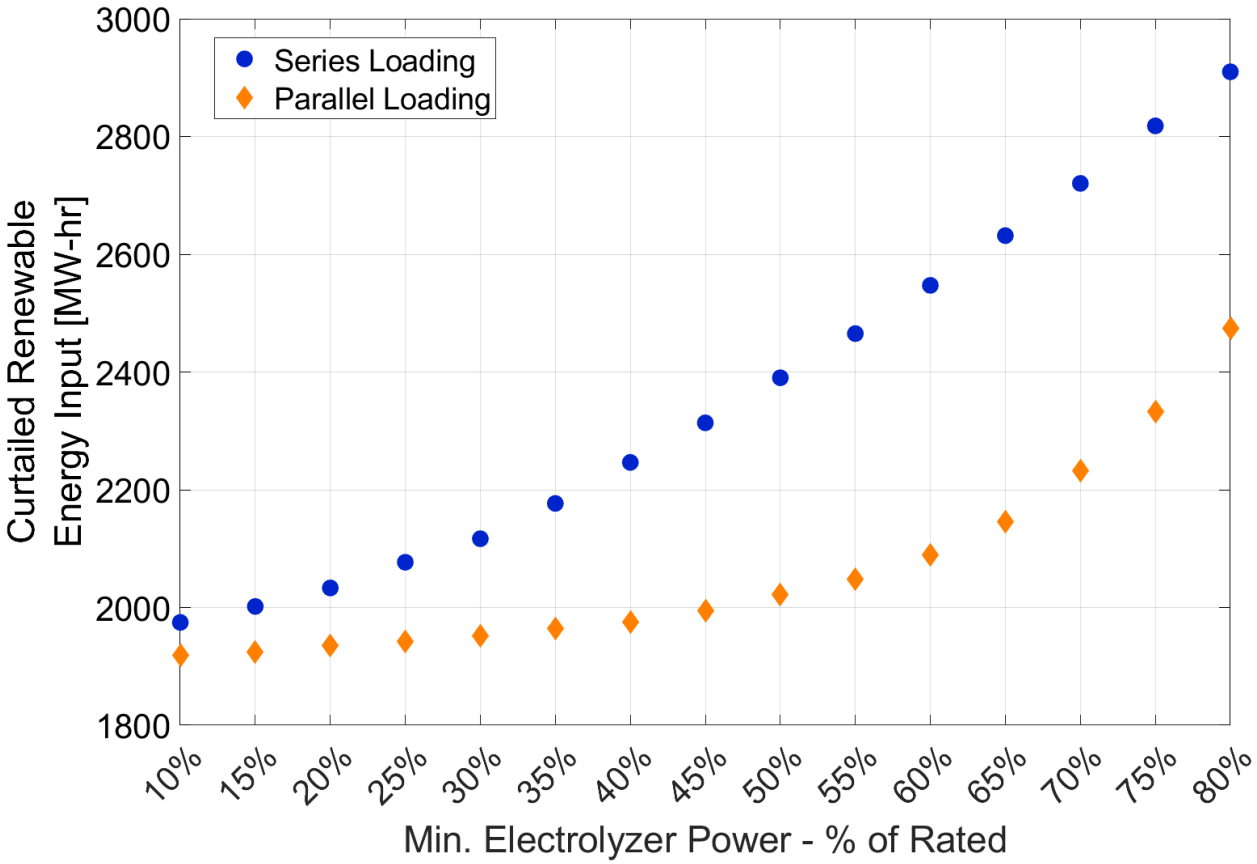

Figure 22: Curtailed power input comparison between series and parallel loading strategies at 60 °C and 30 barg cathode pressure.

Another important performance metric of the multi-electrolyzer system is how often each electrolyzer stack shuts down and starts up. Figure 23 shows the number of times that each electrolyzer stack was shut down using the SL loading strategy during the ERCOT case study. The electrolyzer with the highest number of shutdowns is stack 1. Each stack progressively decreases in the number of shutdowns with the SL strategy. The reason for the number of

shutdowns decreasing in the SL strategy is because the higher stack numbers are only loaded if all the lower stack numbers are loaded up to 100%. Because of the series loading nature, the higher number electrolyzer stacks in general have a lower amount of time of which they are receiving power. There is a high amount of noise for some electrolyzer stacks with the number of shutdowns using the SL scheme as the minimum electrolyzer setpoint is increased. The specific input power profile for the ERCOT case study causes some noise in the number of shutdowns experienced with the SL strategy. The non-standard reaction of each electrolyzer stack with the SL strategy is due to the sequential nature of how power is distributed to the electrolyzers. The SL scheme results in each stack being powered with uneven amounts of power compared to the PL strategy where all the electrolyzer stacks that are currently active are powered evenly. If a different case study was analyzed, the number of shutdowns would change depending on how often the input power exceeds the bounds of what the system can accept.

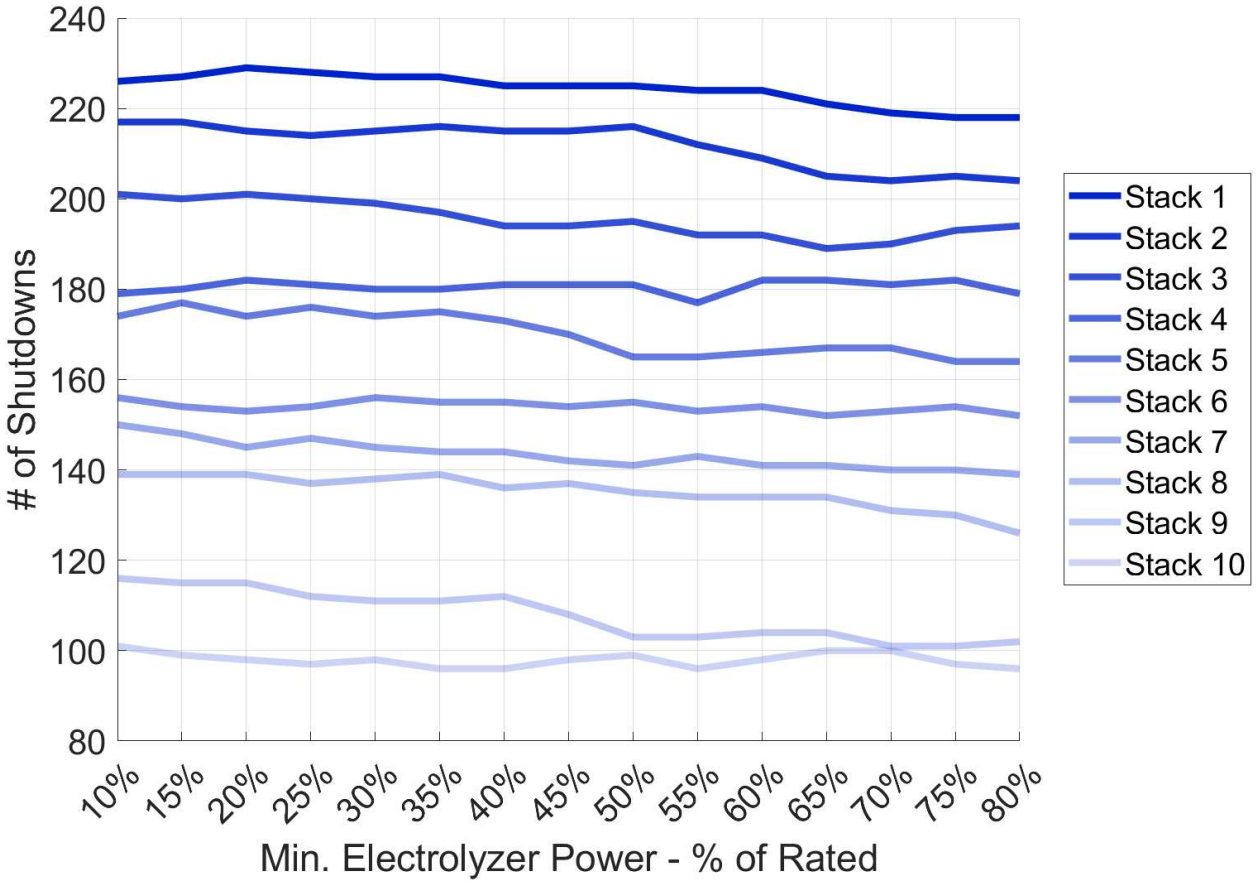

Figure 23: Number of shutdowns for each electrolyzer stack using the SL loading strategy during the ERCOT case study.

Figure 24 shows the number of times that each electrolyzer stack was shut down with the PL strategy during the ERCOT case study. As the stack number increases, the number of shutdowns decreases slightly with the PL strategy but not as much as with the SL strategy. Each electrolyzer stack shows a trend of decreasing numbers of shutdowns with the increasing minimum electrolyzer power setpoint. The decreasing trend is caused by the increasing difficulty of loading the electrolyzer stacks evenly with the required minimum electrolyzer power. This same challenge is what causes the increased amount of curtailed input power with increasing minimum electrolyzer power setpoints. Other than the first electrolyzer stack, the number of shutdowns for each stack is higher with the PL strategy compared to the SL strategy.

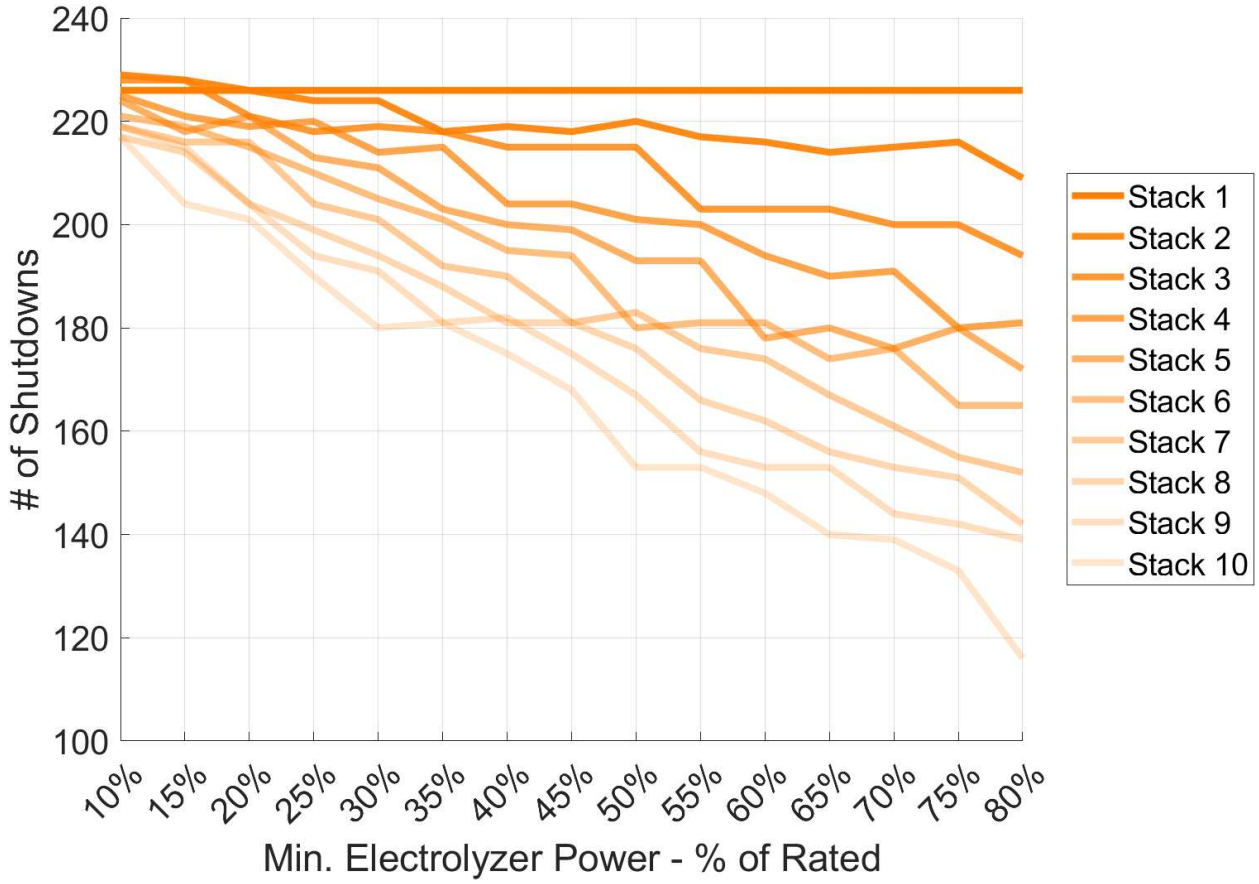

Figure 24: Number of shutdowns for each electrolyzer stack using the PL loading strategy during the ERCOT case study.

The two loading strategies can be compared at a high level by comparing the total number of shutdowns for all 10 electrolyzer stacks using each strategy. Figure 25 shows the total number of electrolyzer shutdowns between the SL and PL strategy. Overall, the SL strategy results in the lowest amount of electrolyzer shutdown events within the green hydrogen generation system across the range of minimum electrolyzer power setpoints evaluated. If the goal is to minimize the number of times an electrolyzer stack must shut down, then the SL strategy is the most effective.

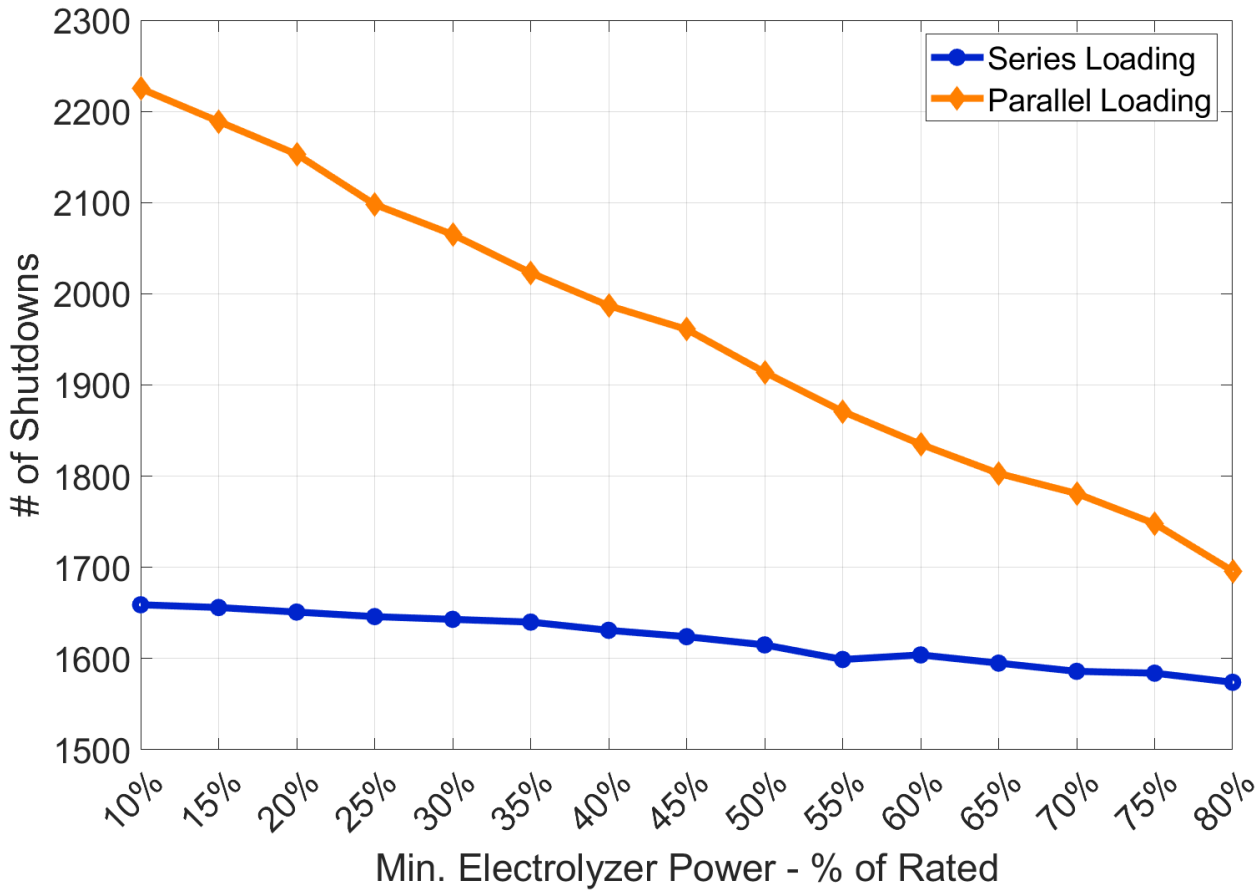

Figure 25: Total number of electrolyzer shutdown events for all 10 stacks using the SL and PL strategies.

From figure 20, the most efficient operation of the system for the ERCOT case study is sing the SL strategy with a minimum electrolyzer power of 10% of the rated power. The number of stacks was chosen arbitrarily and may not be the most effective scaling of the green hydrogen generation system to accept the scaled ERCOT generation. To study this, the most efficient operating strategy of using the SL scheme with 10% minimum electrolyzer power can be applied to a system with varying numbers of electrolyzers per system to observe the change in energy conversion efficiency. Figure 26 shows the energy conversion efficiency of the green hydrogen generation system as the number of electrolyzers per system is reduced. With the original scaling of the ERCOT data, the 10 electrolyzer system is the most efficient in producing hydrogen. It is important to remember that the energy conversion efficiency considers all the RE generation that is available to the system and therefore lowering the amount of electrolyzers per

system results in a higher amount of the available excess RE that is wasted, causing a lower efficiency.

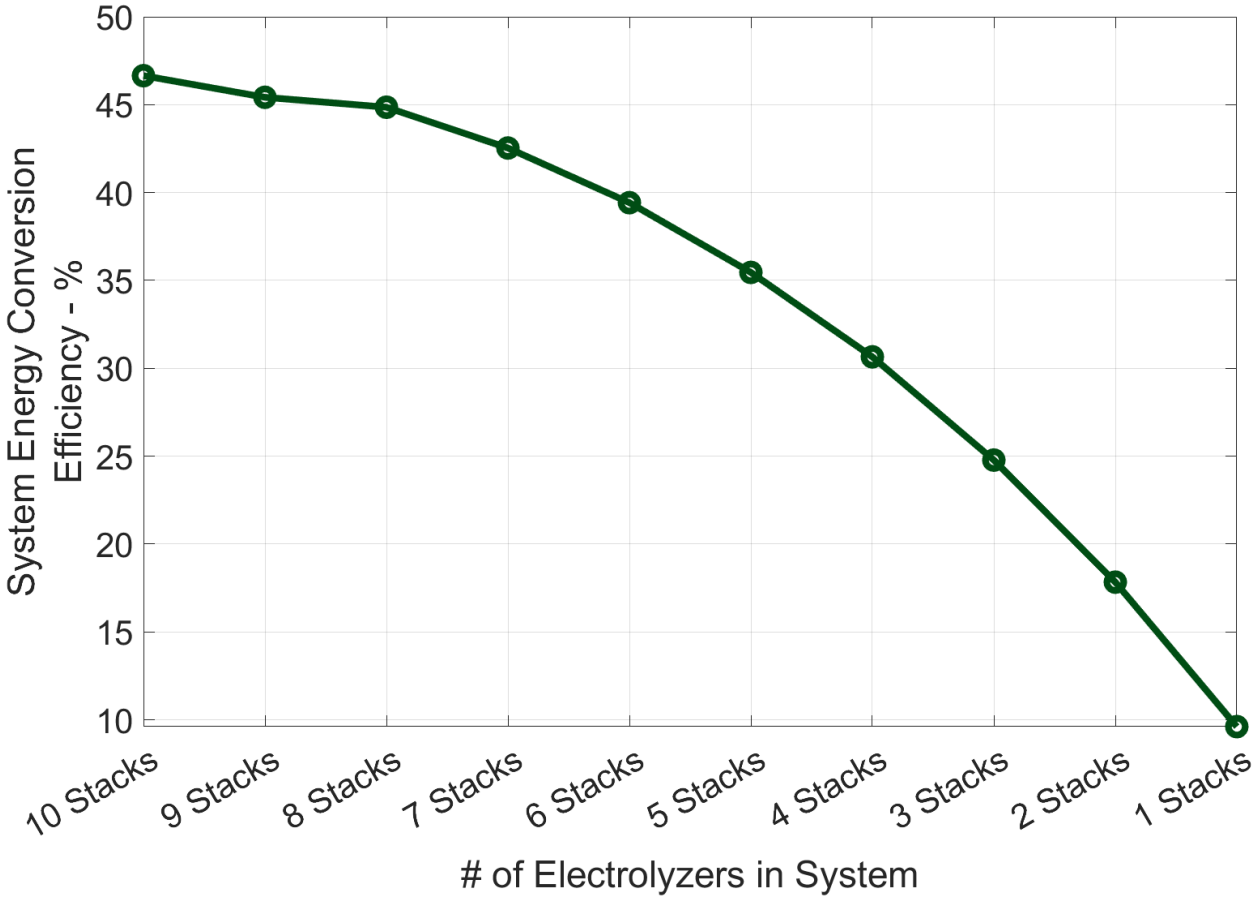

Figure 26: Multi-electrolyzer stack system energy conversion efficiency for ERCOT case study with varying number of electrolyzers per system.

With the original scaling of the ERCOT data, a maximum range of 10 electrolyzers does not result in an optimal sizing of system. To find the optimal number of electrolyzers per system, more than 10 stacks would likely be required to fully utilize the excess generation. Reducing the generation profile will show how the number of electrolyzers or installed electrolyzer capacity can be optimized for a specific case where the generation is known. Instead of scaling the RE capacity so that the amount of excess generation equals the amount of insufficient generation, the capacity can be scaled so that the excess generation is only 30% of the insufficient

generation. Figure 27 shows the reduced model input of excess RE generation with the lower scaling of the ERCOT case study.

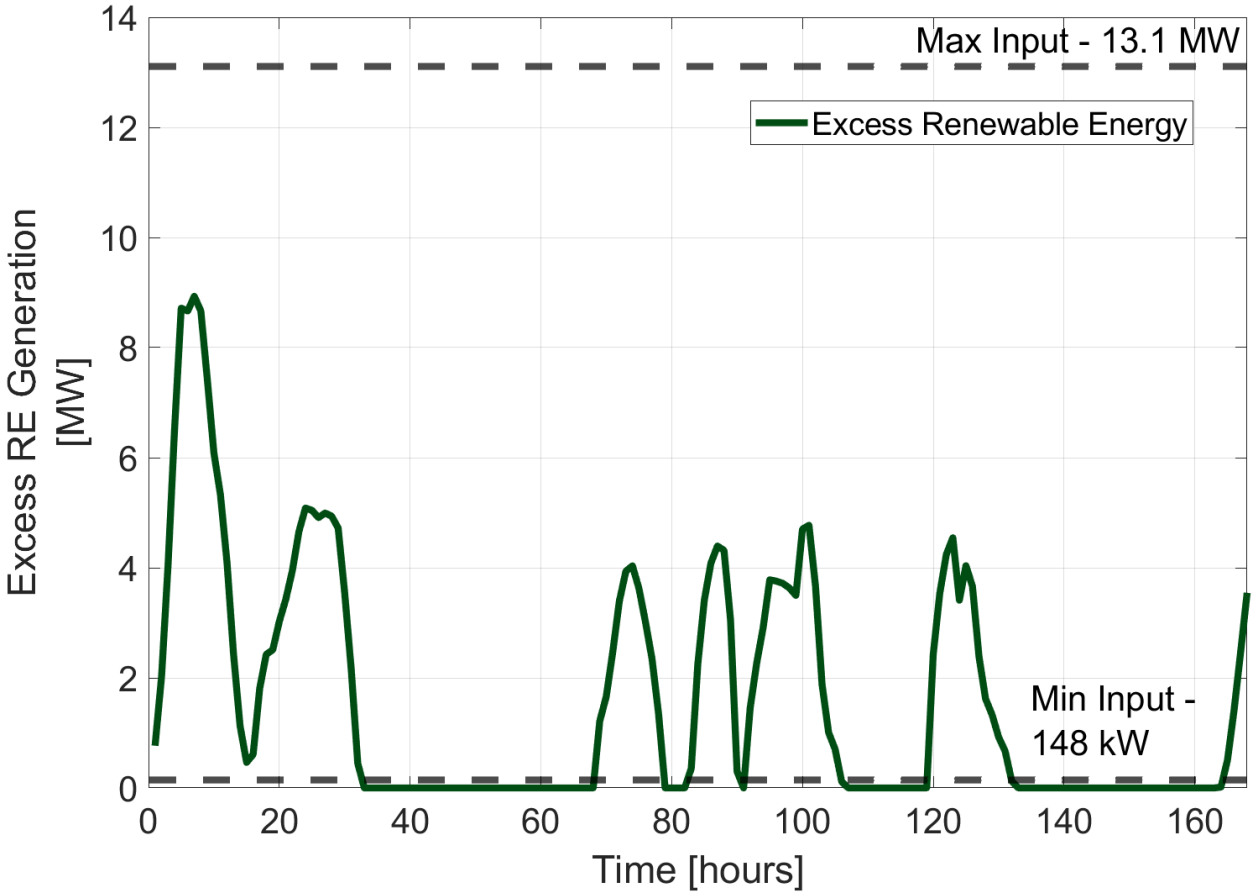

Figure 27: Snapshot from Jan 1st to Jan 7th, 2022 of excess RE generation used as the model input with reduced scaling of the ERCOT data [36].

This causes an overall reduction in the amount of excess RE generation that can be routed to the green hydrogen generation system. Figure 28 shows the energy conversion efficiency with the further scaled down generation input compared to the number of 1.25-MW electrolyzers the system contains. With the reduced excess generation input, the most efficient scaling of the green hydrogen generation system would be to include 8 electrolyzers using the SL strategy and minimum electrolyzer power of 10% of the rated power. Beyond 8 electrolyzers per system, there is too much installed electrolyzer capacity to effectively utilize the excess RE generation because of increased difficulty in distributing power to the electrolyzers and slightly

lower average electrolyzer power. Below 8 electrolyzers per system, there is not enough electrolyzer capacity to fully utilize the excess RE generation available.

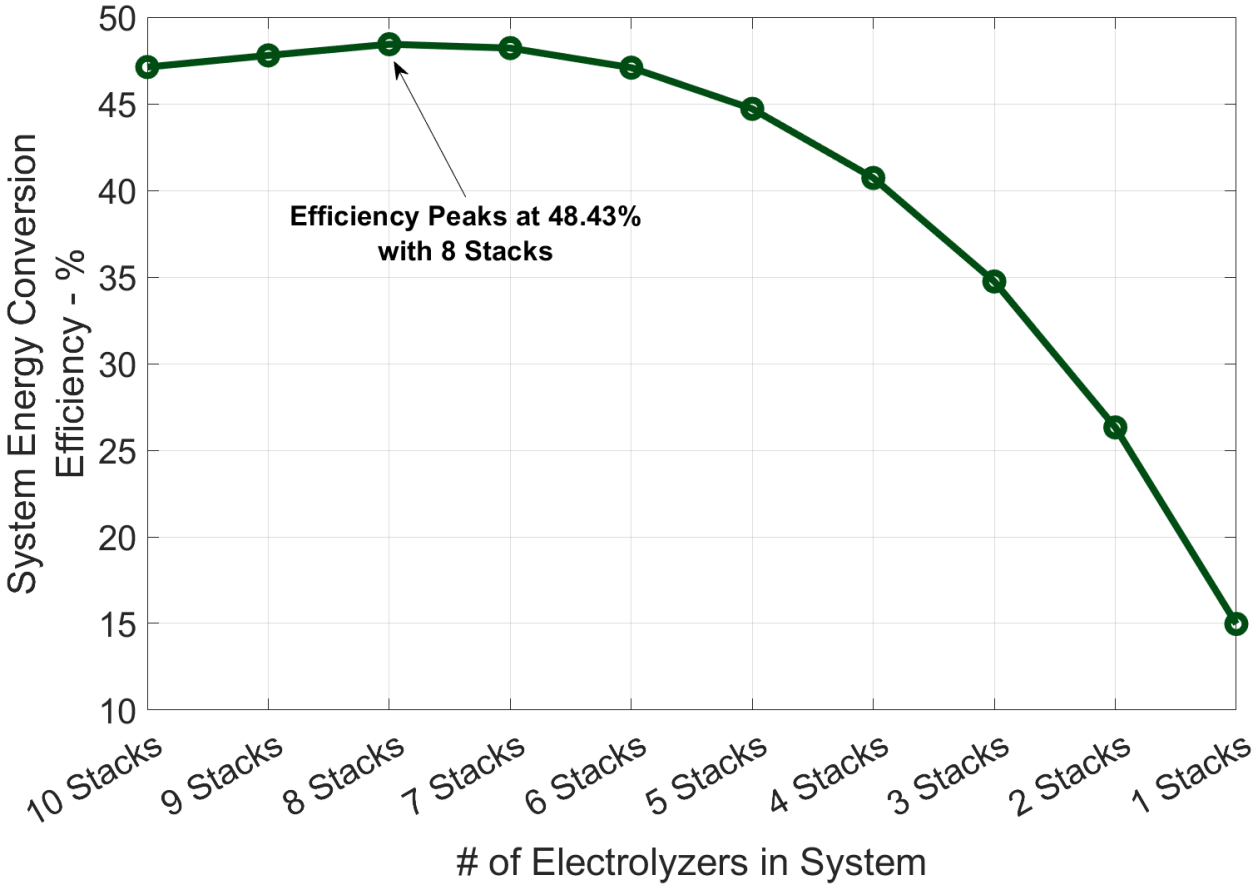

Figure 28: Multi-electrolyzer stack system energy conversion efficiency with reduced ERCOT generation and varying number of electrolyzers per system.

For the reduced scaling ERCOT case study, the model can be used to advise a site owner on how much electrolyzer capacity is needed to fully utilize the input power available. Figure 29 shows the optimal installed electrolyzer capacity to produce the most amount of hydrogen for the reduced scale ERCOT case study.

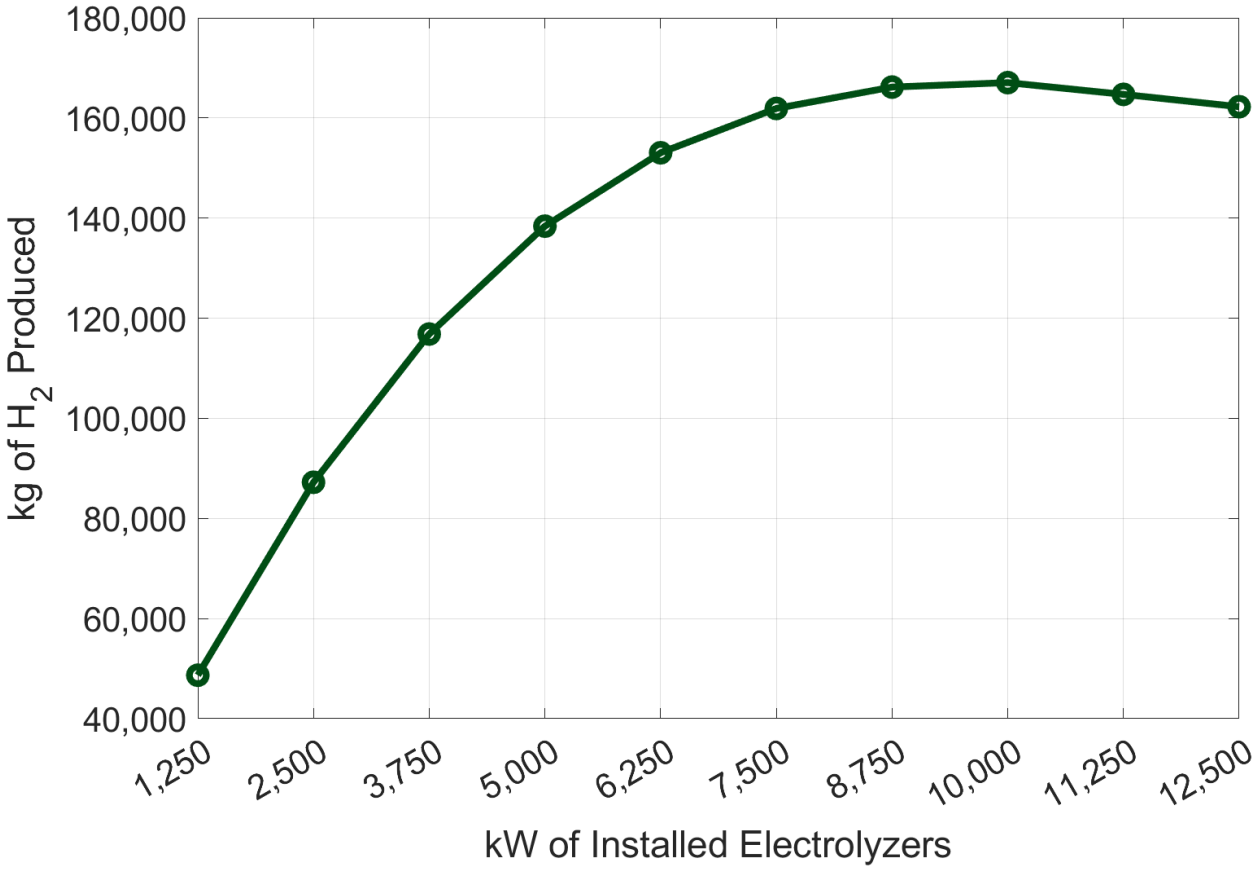

Figure 29: Hydrogen produced vs. kW of installed electrolyzer capacity for reduced ERCOT case study.

CHAPTER 4: CONCLUSION

The green hydrogen generation system model developed in this work expands beyond and improves upon electrolyzer modeling in previous literature by including simplified BOP subsystems such as power electronics, hydrogen purification, hydrogen compression, and system cooling. A useful case study of deploying a green hydrogen generation system at a utility scale is used to demonstrate the model's capability in optimization and controls studies of a multi-electrolyzer system. The model includes only the necessary calculations of recently published BOP models to maintain functionality in optimization and control development studies. The system model is verified and validated with experimental data available in literature.

By analyzing the part load operation of a single 120-kW electrolyzer stack system it is evident that the system's energy conversion efficiency decreases significantly at low electrolyzer power. This is due almost exclusively to the hydrogen loss from hydrogen crossover and the purge gas used in hydrogen purification. At lower electrolyzer power, the current flowing through the stack is low and therefore the production rate of hydrogen is low. Because the cathode pressure is held constant and the orifice used in the PSA dryer has a fixed diameter, the purge hydrogen flowrate remains constant entirely independent on the electrolyzer power which leads to a larger percentage loss of the produced hydrogen in the purification step. The hydrogen loss in the BOP supports the conclusion that BOP modeling is crucial for accurately modeling a green hydrogen generation system's performance. This model can be used to evaluate alternative methods of hydrogen purification such as using a controlled variable flow orifice for the PSA dryer which may allow for maintaining a fixed percentage of hydrogen flowrate lost in the purification step. As hydrogen flowrate decreases, so does the amount of impurities such as water entering the PSA dryer. The amount of purge gas needed to remove impurities should also decrease with a lower incoming flowrate. With a variable flow orifice in the PSA dryer, a controller can adjust the amount of hydrogen used to remove impurities based on the flowrate of

hydrogen coming from the electrolyzer which should in turn reduce the efficiency loss of these systems at low hydrogen production conditions. Another method that may be available depending upon the site is temperature swing adsorption which mitigates the amount of purge gas used and instead uses thermal swings to remove the impurities. The model is designed to evolve with different system configurations by editing/removing/adding modules as needed. For example, in the case of a temperature swing adsorber, the PSA module can be deleted or edited to instead account for the electricity required to drive the temperature swings needed to remove all the impurities present in the hydrogen stream. Some green hydrogen applications may not even need PSA dryers if the hydrogen purity coming out of the phase separators is acceptable for the end use, in this case the model can be run without the PSA module and the changes in system energy conversion efficiencies can be analyzed.

In some cases, it may be desirable to operate the electrolyzer at a higher cathode pressure to reduce or eliminate the need for expensive hydrogen compressors. One application that would be well suited for higher cathode pressure is a system which stores produced hydrogen in a metal hydride storage system. These storage systems operate at around 40 barg and use heat to store and release hydrogen. A metal hydride storage system would not need an expensive hydrogen compressor and instead would need a source of cooling/heating to store and release hydrogen. The model can be adapted by removing the hydrogen compressor module entirely and instead modeling the heat requirements of the metal hydride storage system. The system model can be used to predict the efficiency decrease of operating at a higher cathode pressure as well as to predict the reduced operating range of the green hydrogen generation system. When the system model is integrated with economic modeling the tradeoff of the system's capital expense can be evaluated on a performance basis. With low-pressure storage technology such as metal hydride storage, the expensive hydrogen compressor can be eliminated along with the expensive high pressure composite hydrogen storage tanks.

Even at the highest electrolyzer power, when the system is most efficient in converting electricity to usable hydrogen, the energy conversion efficiency is around 50%. This is an important aspect to consider when determining what applications make the most sense to adopt hydrogen. For example, light-duty passenger vehicles have been increasingly adopting battery technology to reduce emissions. Some manufacturers are developing hydrogen powered light-duty passenger vehicles. When you consider the overall efficiencies of using grid electricity or RE to charge batteries vs create hydrogen, it makes much more sense to charge the light-duty battery electric vehicles rather than create hydrogen because creating hydrogen would require more electricity to power the same number of vehicles due to the lower efficiency. However, battery range becomes an issue with medium- and heavy-duty transportation, and battery electric powertrains become exponentially more complex and costly. In these applications where range and charging time is limited with battery systems, hydrogen can play a role in extending that range if on-board storage systems for large amounts of hydrogen become available. The lower round trip efficiency of creating hydrogen may become economic because the cost of having a battery and charging system capable for extended heavy-duty range becomes more expensive than the added cost of creating hydrogen. Solid oxide electrolyzers generally have a higher efficiency compared to PEM electrolyzers and could help with the energy conversion efficiency of the green hydrogen generation system. The operation of green hydrogen generation systems using solid oxide electrolyzers would have to change dramatically due to the inability of solid oxide electrolyzers to accept rapid changes in power. This system model can be adapted in the future by expanding the model's capability in calculating the thermal response of a solid oxide electrolyzer. This would require the system to shift from optimizing the system at part load conditions to optimizing the system so that the solid oxide electrolyzer is run in a continuous fashion. This may entail adding an energy reserve module to power the solid oxide electrolyzer when the RE generation is unable to run the electrolyzer at sufficient power to maintain the required high temperatures.

The model developed in this work can utilize RE generation and grid load profiles to participate in site specific control studies as demonstrated with the comparison between two simple operating strategies and the scaled ERCOT generation data. If the goal is to minimize the amount of ERCOT RE generation that is wasted within the system while keeping the energy conversion efficiency as high as possible, it is recommended to use a sequential loading strategy with a minimum electrolyzer load point of between 10-30% of its rated power. If it is determined that the electrolyzers should only operate above 30% of its rated power, the PL strategy results in the highest energy conversion efficiency for the ERCOT case study. If the total amount of electrolyzer shutdown events is to be minimized, the SL strategy is much more effective than the PL strategy. At the highest minimum electrolyzer power setpoint studied (80% of rated electrolyzer power) the PL strategy can result in the production of 14,195 more kg of hydrogen produced for the sample ERCOT generation profile. This system model can also be used to model the expansion of a utility RE generation site if the utility is planning to expand on the RE capacity. The loading strategies will result in different system efficiencies based on how oversized the RE capacity is. The system model can also be used as a scaling tool to determine the ideal amount of installed electrolyzer capacity. Optimizing energy conversion efficiency allows the maximum generation of hydrogen for any given energy input. The added revenue of the increased hydrogen produced may be small in comparison to the costs associated with a utility scale green hydrogen generation system but, over the system's lifetime, can have a measurable impact on the rate of return and payback periods of green hydrogen production systems. The model developed and demonstrated in this paper is a powerful tool in optimizing the efficiency of PEM green hydrogen generation systems which aids in the deployment of practically carbon free hydrogen by improving the business case for large scale systems.

5.1.1: Hydrogen Refueling Station at Colorado State University

The model developed in this work expands upon modeling efforts that have been published in literature and is successful at predicting the performance of a multi-PEM electrolyzer stack green hydrogen generation system. The model has many possibilities for future expansion and integration but lacks an extensive dataset of experimental data that can be used to further validate and tune the model. Colorado State University (CSU) is currently installing a 120-kW PEM electrolyzer hydrogen refueling station which is shown in figure 30.

Figure 30: Nel Hydrogen vehicle refueling station being installed at the Colorado State University Powerhouse Campus [37].

The CSU refueling station is a containerized hydrogen production system composed of two 60-kW PEM electrolyzer stacks as well as all the BOP components modeled in this work.

The refueling station operates with a 3-phase 480V AC power input and contains two IGBT rectifiers to convert AC into DC. The electrolyzer system contains a hydrogen/water phase separator as well as a PSA dryer to create 99.9998% pure hydrogen. The system is designed to deliver hydrogen from the electrolyzer at 30 barg and maintains a temperature of around 60 °C. The refueling station takes hydrogen from the electrolyzer and compresses it to refueling pressures (maximum of 950 barg) using a two-stage compressor with intercooling. The refueling station uses an R407C chiller to provide cooling to the rectifiers, electrolyzers, and hydrogen compressor intercooling. The refueling station also contains the necessary equipment to store hydrogen in high pressure composite tanks and dispense hydrogen at 700 barg.

The next step to progress this model is to instrument the hydrogen refueling station at CSU with numerous sensors to measure parameters such as electrolyzer stack voltage/current, temperature, hydrogen pressures, coolant flowrate, and hydrogen flowrate. The system should be operated with a range of operating parameters that might be seen in a scaled PEM green hydrogen production facility. The power of the system can be controlled using the current control mode of the rectifiers. The refueling station is not directly connected to a RE generation facility and will be operating with grid electricity. A RE generation profile will have to be converted into a signal profile which will control the amount of current the rectifiers output to the electrolyzer and simulate what the electrolyzer system will experience in the field. Parameters such as cathode pressure can be changed within the system by replacing the back pressure regulator in the hydrogen gas piping system. The electrolyzer temperature can be altered by changing the targeted temperature in the control system. The control system will then actuate the cooling circuit within the electrolyzer system to maintain the set electrolyzer temperature. An example of ranges for operating parameters would be to sweep the electrolyzer current from around 10% electrolyzer power up to the rated maximum as well as sweep the electrolyzer temperature setpoint between values that would typically be seen in the field such as temperatures experienced during start-up conditions. The system already contains various

sensors within the system which feed information to the control system such as thermocouples, pressure sensors, dewpoint monitors, and water resistivity sensors. The existing sensors can be used to create an experimental dataset and any gaps can be filled by adding the necessary sensors. Factorial and fractional factorial experiment designs can be used to economically produce a useful dataset covering multiple different operating factors.

Once the experimental refueling station dataset is made, the Simulink model can be tuned to reduce the model to experiment error. New empirical models for AC-DC rectifier efficiency can be fitted to a larger set of data to better represent the actual conversion efficiency. Empirical constants such as the PSA discharge coefficient or exchange current density that are used in the model can be optimized to reduce model to experiment error. One of the most important sections of the model to tune is the ionic resistance of the electrolyzer. The mismatch between the general slope of the experimental voltage data and the model prediction in figure 8 is likely due to a mismatch in the empirical equation that is used to predict the membrane conductivity. A Matlab script can be used to iterate and tune the empirical portions of the model to reduce the model to experiment error. Appendix A contains a table of model parameters that can easily be tuned and their general effect on the model.

5.1.2: Future System Model Applications

After the model has been fully validated towards an exhaustive experimental dataset it can be used in several different ways to optimize a green hydrogen generation system. The ERCOT case study presented in this work spanned the year of 2022 and was broken up into 1-hour snapshots. The model can simulate the ERCOT load profile in a little over 1 minute and is economical to run. Increasing the recording frequency of input generation data to the second/minute timescale will dramatically increase the number of datapoints produced from the model as well as increase the simulation run time. The physical reaction of the system could be assumed as instantaneous with the ERCOT case study because of the long 1-hour duration between data points. The model should be expanded to include some highly transient reactions

of the system such as the electrolyzer stack temperature and cathode pressure accumulation during start-up conditions if the input data is on the second/minute timescale. For example, the startup time for the 60-kW PEM electrolyzer in [21] was around 4 minutes, during that time the electrolyzer temperature and pressure would have some change over time and could not be considered an instantaneous change.

A green hydrogen generation system will likely operate for 10-20 years and thus it will be important to be able to predict a system's performance over the entire estimated life of the system. If a load/generation dataset is available for the system's lifetime, it can be input to the model which will in turn calculate how the system responds and how much hydrogen is ultimately produced over the entire lifespan. For this model to be used in a lifecycle analysis it will first need some way to model the degradation of the system components. PEM electrolyzers experience a decrease in performance over time which is measured as an increasing cell voltage with the same amount of current. Several studies have shown that highly transient and start/stop operations of PEM electrolyzers contribute to accelerated degradation [38], [39]. The electrolyzer module will require a method of predicting degraded performance based upon the operating condition of the electrolyzer. One way to add degradation capability is to create an empirical model with the measured voltage data from the electrolyzer stack. The change in cell voltage for a certain current over time can be fit to parameters such as the number of shutdowns or how much time the electrolyzer spends in a highly transient condition.

One important conclusion drawn from analyzing the model is that the purge hydrogen lost in the PSA process is detrimental to the system efficiency at low electrolyzer load conditions. This is driven because of the fixed orifice used to provide the purge hydrogen. One way to mitigate this hydrogen loss is by designing a PSA system that can control the orifice flow based on the current production rate and impurity concentration of the hydrogen coming out of the electrolyzer. Alternatively, a temperature swing adsorber may be designed to practically eliminate the purge hydrogen and instead remove impurities using an external heat source. The

green hydrogen must be compressed to very high pressure to be used in the transportation sector, but other applications may not need as high of pressure. This introduces the opportunity to examine alternative methods of storing hydrogen such as salt cavern storage or storage with a metal hydride or liquid hydrogen carrier. These different storage technologies all require different forms of energy input and would require the system model to be updated to calculate the energy consumption of each storage technology. For example, a metal hydride module would calculate the energy consumption of a heat pump or electrical heater based on the modeled energy requirement to absorb the hydrogen produced instead of the hydrogen compressor module that solves for AC motor consumption to drive the compressor. An important thing to consider when expanding the model to include alternative technologies is that the new portions of the model will need to be validated with experimental data before they can be used.

The system model assumes high purity water is available to the green hydrogen generation system and does not account for any energy consumed in on-site water purification. Depending on the location of the green hydrogen generation system, obtaining purified water may be a challenge and require on-site purification. The electrical consumption of an on-site water purification system can be added to the system model by including an empirical equation for AC motor electricity consumption based on the required flowrate of purified water. The model would have to solve for water that would be consumed with the electrolyzer power and back calculate what the water purification system would need to provide. The added electrical consumption for even seawater reverse osmosis is very small in comparison to the electrical consumption of the electrolyzer stack at only 0.1% of the total energy consumed in a PEM electrolyzer system evaluated in [40]. Because the electrical consumption for seawater reverse osmosis is so low in comparison, it is not one of the main balance of plant subsystems that must be modeled within the system.

This model may be used as a tool to evaluate the economics of a proposed green hydrogen generation system. If a utility company wanted to install a PEM electrolyzer system at one of their RE generation facilities, they can use this model to input their actual generation profile and get a good sense of how that green hydrogen generation system will perform. This in-depth model that includes the BOP will better predict the actual energy consumption and hydrogen production of a green hydrogen generation system and therefore will better predict the different value and cost streams of the system. The utility can perform cost effective optimizations of the virtual system during the development stage of the project using this system model. The two loading strategies resulted in different efficiencies, amounts of wasted input energy, and number of electrolyzer shutdowns based on the selected minimum electrolyzer power. Another layer of optimization could include switching between the two loading strategies based on a set of constraints for the system. The constraints used to switch the loading strategies could be performance metrics such as the maximum amount of curtailed energy per year or the maximum amount of electrolyzer shutdowns per year. In future model analysis, the model could be expanded to include logic to switch what loading strategy is used based on the set of constraints. For example, the model could switch from the PL strategy to the SL strategy if the total amount of electrolyzer shutdowns was rapidly approaching the constraint on the system. The PL strategy would reduce the amount of shutdowns with a tradeoff of increased curtailed input. The added level of control would allow the energy conversion efficiency, curtailed input, and number of shutdowns to be optimized all at once.

Alternative business strategies can be evaluated using the system model such as the strategy of prioritizing powering the green hydrogen system above providing energy to the grid. In a RE storage scenario such as the ERCOT case study, it is common that the green hydrogen generation system experiences intermittent periods of multiple hours where no power is input to the system. If the priority of powering the grid first and green hydrogen generation system second is switched, the frequency of intermittent periods of zero input power can be reduced

and the electrolyzer utilization factors can be increased. This business case may also result in relatively higher average electrolyzer power and increase the system efficiency with the tradeoff of less electricity provided to the grid. With expensive equipment such as green hydrogen generation systems and PEM electrolyzers, it is generally a priority to avoid times when the equipment goes unutilized. Higher electrolyzer utilization factors may lead to the alternative business strategy becoming more economic.

One objective of the system model is to provide a clear understanding on how each part of the green hydrogen production system contributes to the overall energy conversion efficiency and identify areas of the system that can be optimized. The reason for optimizing the efficiency of the green hydrogen generation system is to increase the economic feasibility of deploying these systems at a large scale. The model can be integrated into larger technoeconomic analysis which may look at different system sizing and component configurations to reduce the capital expense of the system while also increasing the energy conversion efficiency. The owners of these systems will want to see the best return on investment. One way of getting a better return on investment is by increasing the system's energy conversion efficiency while maintaining or even lowering the capital expense. Lowering the capital expense can be achieved in several ways, one of which would be increasing the electrolyzer cathode pressure and eliminating the need for an expensive hydrogen compressor by using an alternative method of storing hydrogen. Different system configurations and alternative technologies will change the cost of the system but will also change the performance. This model can be applied to predict the system's performance with any configuration. As shown in the analysis of the ERCOT case study, different loading schemes can produce different energy conversion efficiencies for the same RE input. Even slight increases in efficiency can have large economic impacts over the life of the system and models such as the one developed in this work are powerful tools to be used in scaling the generation of green hydrogen.

REFERENCES

[1] A. Badgett, M. Ruth, and B. Pivovar, “Chapter 10 - Economic considerations for hydrogen production with a focus on polymer electrolyte membrane electrolysis,” in *Electrochemical Power Sources: Fundamentals, Systems, and Applications*, Elsevier, 2022, pp. 327–364. [Online]. Available: https://www.sciencedirect.com/science/article/pii/B9780128194249000057

[2] IEA, “Towards hydrogen definitions based on their emissions intensity,” IEA, Paris, 2023. [Online]. Available: https://www.iea.org/reports/towards-hydrogen-definitions-based-on-their-emissions-intensity

[3] IRENA, “Green Hydrogen for Industry: A Guide to Policy Making,” IRENA, Abu Dhabi United Arab Emirates, 2022. [Online]. Available: https://www.irena.org/publications/2022/Mar/Green-Hydrogen-for-Industry

[4] J. A. Dowling *et al.*, “Role of Long-Duration Energy Storage in Variable Renewable Electricity Systems,” *Joule*, vol. 4, no. 9, pp. 1907–1928, Sep. 2020, doi: 10.1016/j.joule.2020.07.007.

[5] T. C. Allison, N. R. Smith, A. M. Rimpel, and K. Brun, “Overview of Machinery-Based Grid-Scale Energy Storage Technologies,” in *Proceedings of Turbomachinery and Pump Symposium, Texas A&M University, Virtual*, 2020.

[6] M. Mohanpurkar *et al.*, “Electrolyzers Enhancing Flexibility in Electric Grids,” *Energies*, vol. 10, no. 11, Art. no. 11, Nov. 2017, doi: 10.3390/en10111836.

[7] R. E. Clarke, S. Giddey, F. T. Ciacchi, S. P. S. Badwal, B. Paul, and J. Andrews, “Direct coupling of an electrolyser to a solar PV system for generating hydrogen,” *Int. J. Hydrog. Energy*, vol. 34, no. 6, pp. 2531–2542, Mar. 2009, doi: 10.1016/j.ijhydene.2009.01.053.

[8] T. Maeda, H. Ito, Y. Hasegawa, Z. Zhou, and M. Ishida, “Study on control method of the stand-alone direct-coupling photovoltaic – Water electrolyzer,” *Int. J. Hydrog. Energy*, vol. 37, no. 6, pp. 4819–4828, Mar. 2012, doi: 10.1016/j.ijhydene.2011.12.013.

[9] T. L. Gibson and N. A. Kelly, “Predicting efficiency of solar powered hydrogen generation using photovoltaic-electrolysis devices,” *Int. J. Hydrog. Energy*, vol. 35, no. 3, pp. 900–911, Feb. 2010, doi: 10.1016/j.ijhydene.2009.11.074.

[10] D. S. Falcão and A. M. F. R. Pinto, “A review on PEM electrolyzer modelling: Guidelines for beginners,” *J. Clean. Prod.*, vol. 261, p. 121184, Jul. 2020, doi: 10.1016/j.jclepro.2020.121184.

[11] Ø. Ulleberg, “Modeling of advanced alkaline electrolyzers: a system simulation approach,” *Int. J. Hydrog. Energy*, vol. 28, no. 1, pp. 21–33, Jan. 2003, doi: 10.1016/S0360-3199(02)00033-2.

[12] F. Marangio, M. Santarelli, and M. Calì, “Theoretical model and experimental analysis of a high pressure PEM water electrolyser for hydrogen production,” *Int. J. Hydrog. Energy*, vol. 34, no. 3, pp. 1143–1158, Feb. 2009, doi: 10.1016/j.ijhydene.2008.11.083.

[13] L. Valverde, F. Rosa, A. J. del Real, A. Arce, and C. Bordons, “Modeling, simulation and experimental set-up of a renewable hydrogen-based domestic microgrid,” *Int. J. Hydrog. Energy*, vol. 38, no. 27, pp. 11672–11684, Sep. 2013, doi: 10.1016/j.ijhydene.2013.06.113.

[14] T. Yigit and O. F. Selamet, “Mathematical modeling and dynamic Simulink simulation of high-pressure PEM electrolyzer system,” *Int. J. Hydrog. Energy*, vol. 41, no. 32, pp. 13901–13914, Aug. 2016, doi: 10.1016/j.ijhydene.2016.06.022.

[15] S. Sood *et al.*, “Generic Dynamical Model of PEM Electrolyser under Intermittent Sources,” *Energies*, vol. 13, no. 24, Art. no. 24, Jan. 2020, doi: 10.3390/en13246556.

[16] P. Olivier, C. Bourasseau, and B. Bouamama, “Dynamic and multiphysic PEM electrolysis system modelling: A bond graph approach,” *Int. J. Hydrog. Energy*, vol. 42, no. 22, pp. 14872–14904, Jun. 2017, doi: 10.1016/j.ijhydene.2017.03.002.
[17] D. Ipsakis, S. Voutetakis, P. Seferlis, F. Stergiopoulos, and C. Elmasides, “Power management strategies for a stand-alone power system using renewable energy sources and hydrogen storage,” *Int. J. Hydrog. Energy*, vol. 34, no. 16, pp. 7081–7095, Aug. 2009, doi: 10.1016/j.ijhydene.2008.06.051.
[18] Dynapower Corporation, “Switch Mode DC Power Supply for Hydrogen Generation: First Article Test Procedure/Results,” Dynapower/Rapid Power Corporation, South Burlington, VT, Nov. 2009.
[19] G. Pan, W. Gu, H. Qiu, Y. Lu, S. Zhou, and Z. Wu, “Bi-level mixed-integer planning for electricity-hydrogen integrated energy system considering levelized cost of hydrogen,” *Appl. Energy*, vol. 270, p. 115176, Jul. 2020, doi: 10.1016/j.apenergy.2020.115176.
[20] Z. Li, H. Dong, S. Hou, L. Cheng, and H. Sun, “Coordinated control scheme of a hybrid renewable power system based on hydrogen energy storage,” *ENERGY Rep.*, vol. 7, pp. 5597–5611, Nov. 2021, doi: 10.1016/j.egyr.2021.08.176.
[21] J. Stansberry, “Dynamic Analysis of a Proton Exchange Membrane Electrolyzer Integrated with a Natural Gas Combined Cycle Power Plant for Power-to-Gas Applications,” M.S. Thesis, Mech. and Aerosp. Eng., UC Irvine, Irvine, CA, 2018. [Online]. Available: https://escholarship.org/uc/item/9ww7g5nf
[22] M. Schalenbach, T. Hoefner, P. Paciok, M. Carmo, W. Lueke, and D. Stolten, “Gas Permeation through Nafion. Part 1: Measurements,” *J. Phys. Chem. C*, vol. 119, no. 45, pp. 25145–25155, Nov. 2015, doi: 10.1021/acs.jpcc.5b04155.
[23] P. Medina and M. Santarelli, “Analysis of water transport in a high pressure PEM electrolyzer,” *Int. J. Hydrog. Energy*, vol. 35, no. 11, pp. 5173–5186, Jun. 2010, doi: 10.1016/j.ijhydene.2010.02.130.
[24] M. G. Santarelli, M. F. Torchio, and P. Cochis, “Parameters estimation of a PEM fuel cell polarization curve and analysis of their behavior with temperature,” *J. Power Sources*, vol. 159, no. 2, pp. 824–835, Sep. 2006, doi: 10.1016/j.jpowsour.2005.11.099.
[25] J. C. Amphlett, R. M. Baumert, R. F. Mann, B. A. Peppley, P. R. Roberge, and T. J. Harris, “Performance Modeling of the Ballard Mark IV Solid Polymer Electrolyte Fuel Cell: I . Mechanistic Model Development,” *J. Electrochem. Soc.*, vol. 142, no. 1, p. 1, Jan. 1995, doi: 10.1149/1.2043866.
[26] Q. Duan, H. Wang, and J. Benziger, “Transport of liquid water through Nafion membranes,” *J. Membr. Sci.*, vol. 392–393, pp. 88–94, Mar. 2012, doi: 10.1016/j.memsci.2011.12.004.
[27] M. Ise, K. D. Kreuer, and J. Maier, “Electroosmotic drag in polymer electrolyte membranes: an electrophoretic NMR study,” *Solid State Ion.*, vol. 125, no. 1, pp. 213–223, Oct. 1999, doi: 10.1016/S0167-2738(99)00178-2.
[28] M. Shen, N. Bennett, Y. Ding, and K. Scott, “A concise model for evaluating water electrolysis,” *Int. J. Hydrog. Energy*, vol. 36, no. 22, pp. 14335–14341, Nov. 2011, doi: 10.1016/j.ijhydene.2010.12.029.
[29] T. E. Springer, T. A. Zawodzinski, and S. Gottesfeld, “Polymer Electrolyte Fuel Cell Model,” *J. Electrochem. Soc.*, vol. 138, no. 8, pp. 2334–2342, Aug. 1991, doi: 10.1149/1.2085971.
[30] The Linde Group, “Hydrogen Recovery by Pressure Swing Adsorption,” Linde, Surrey, United Kingdom, 2023. [Online]. Available: https://www.linde-engineering.com/en/images/HA_H_1_1_e_09_150dpi_NB_tcm19-6130.pdf
[31] M. Gardiner, “Energy requirements for hydrogen gas compression and liquefaction as related to vehicle storage needs,” DOE Hydrogen and Fuel Cells Program, Rec. 9013, Jul. 2009. [Online]. Available: https://www.hydrogen.energy.gov/pdfs/9013_energy_requirements_for_hydrogen_gas_compression.pdf

[32] V. Siva Reddy, N. L. Panwar, and S. C. Kaushik, “Exergetic analysis of a vapour compression refrigeration system with R134a, R143a, R152a, R404A, R407C, R410A, R502 and R507A,” *Clean Technol. Environ. Policy*, vol. 14, no. 1, pp. 47–53, Feb. 2012, doi: 10.1007/s10098-011-0374-0.
[33] H.-S. Kim, M.-H. Ryu, J.-W. Baek, and J.-H. Jung, “High-Efficiency Isolated Bidirectional AC–DC Converter for a DC Distribution System,” *IEEE Trans. Power Electron.*, vol. 28, no. 4, pp. 1642–1654, Apr. 2013, doi: 10.1109/TPEL.2012.2213347.
[34] “C Series PEM Electrolyser,” *Nel Hydrogen*, May 28, 2018. https://nelhydrogen.com/product/c10-c20-c30/ (accessed Jun. 09, 2023).
[35] J. Koponen, A. Kosonen, V. Ruuskanen, K. Huoman, M. Niemelä, and J. Ahola, “Control and energy efficiency of PEM water electrolyzers in renewable energy systems,” *Int. J. Hydrog. Energy*, vol. 42, no. 50, pp. 29648–29660, Dec. 2017, doi: 10.1016/j.ijhydene.2017.10.056.
[36] ERCOT, Jan. 2023, “Hourly Aggregated Wind and Solar Output (2022).” [Online]. Available: https://www.ercot.com/mp/data-products/data-product-details?id=PG7-126-M
[37] A. Vitt, “CSU acquires public hydrogen fuel station, a first for the state of Colorado,” *Walter Scott, Jr. College of Engineering News*, Oct. 06, 2020. Accessed: Jun. 06, 2023. [Online]. Available: https://engr.source.colostate.edu/csu-acquires-public-hydrogen-fuel-station-a-first-for-the-state-of-colorado/
[38] M. Chandesris, V. Medeau, N. Guillet, S. Chelghoum, D. Thoby, and F. Fouda-Onana, “Membrane degradation in PEM water electrolyzer: Numerical modeling and experimental evidence of the influence of temperature and current density,” *Int. J. Hydrog. ENERGY*, vol. 40, no. 3, pp. 1353–1366, Jan. 2015, doi: 10.1016/j.ijhydene.2014.11.111.
[39] C. Spöri, J. T. H. Kwan, A. Bonakdarpour, D. P. Wilkinson, and P. Strasser, “The Stability Challenges of Oxygen Evolving Catalysts: Towards a Common Fundamental Understanding and Mitigation of Catalyst Degradation,” *Angew. Chem. Int. Ed.*, vol. 56, no. 22, pp. 5994–6021, 2017, doi: 10.1002/anie.201608601.
[40] M. A. Khan *et al.*, “Seawater electrolysis for hydrogen production: a solution looking for a problem?,” *Energy Environ. Sci.*, vol. 14, no. 9, pp. 4831–4839, 2021, doi: 10.1039/D1EE00870F.

APPENDICES

Appendix A: Tunable Model Parameters.

Table 3: Tunable model parameters and their general effect on the system model.

Parameter:	Effect on Model:
Power electronics curve fit	Changes power electronics efficiency
Membrane conductivity	Changes slope of electrolyzer voltage-current relationship via ohmic overpotential
Charge transfer coefficient	Changes activation overpotential
Exchange current density	Changes activation overpotential
Faradaic efficiency	Changes hydrogen generation rate
PSA Orifice coefficient of discharge	Changes PSA purge gas flowrate
PSA Uptime	Changes PSA purge gas flowrate
Chiller COP	Changes chiller power consumption

Appendix B: Matlab script used for single electrolyzer system.

The Matlab script in this appendix was used to set the necessary Simulink model parameters and iterate through different cathode pressures with a single electrolyzer system. The Simulink model outputs are sent to Matlab via a MAT file. Once the Simulink output is imported, the variables can be manipulated to perform any unit conversions. The figures used in this work are generated in the final section of the code.

```
%% Hydrogen Pressure Study
clc
clear
close all
tic
% Open the simulink model
GHGS_v7
% Load supporting files and 2D lookup tables
load('Rectifier_eff_AC.mat')
load('Rectifier_eff_DC.mat')
load('SingleSystemCurt_P.mat')
load('SingleSystemCurt_t.mat')
load('UCI_Electrolyzer_Setpoint_I.mat')
load('UCI_Electrolyzer_Setpoint_P.mat')
load('UCI_Electrolyzer_Setpoint_T.mat')

% Set model parameters
set_param('GHGS_v7/Power Electronics/kW to W','Gain','1') %Set gain because
curtailment profile is in kW and constant load is in W
set_param('GHGS_v7/Manual Switch1','sw','0') %1 = follow load profile, 0 = constant
AC power input
set_param('GHGS_v7/Power Electronics/Stack 1 Operating Factor','value','1'); %Set
operating factors so that only one stack is operating (single stack system)
set_param('GHGS_v7/Power Electronics/Stack 2 Operating Factor','value','0');
set_param('GHGS_v7/Power Electronics/Stack 3 Operating Factor','value','0');
set_param('GHGS_v7/Power Electronics/Stack 4 Operating Factor','value','0');
set_param('GHGS_v7/PSA Dryer/D_o [m]','value','0.00013') %Set PSA orifice diameter,
results in 6.3% loss

%% Run Simulink Model at 60 deg C
AC_in = [127411.6856 114010.9613 101039.1894 88095.15169 75305.02199 62729.62063
50298.96633 37960.11724 31839.292 25760.10107 19703.0849 13586.60722]; % Array with
all of the part load AC power values (10-100%)
T_stack = 60; %Electrolyzer temperature [C]
P_cath = 100000.*[30 60 90]; %Cathode pressure [Pa]
P_an = 1.6*100000; %Anode pressure [Pa]
set_param('GHGS_v7/Stack Temp Setpoint [C]','Value',num2str(T_stack))
SimTime = 100;
% Pre allocation of variables
n = length(P_cath);
p = length(AC_in);
Time = zeros(n,p);
```

```
Stack1PowerConsumption = zeros(n,p);
Stack2PowerConsumption = zeros(n,p);
Stack3PowerConsumption = zeros(n,p);
Stack4PowerConsumption = zeros(n,p);
ACPowerConsumption = zeros(n,p);
CompressorPowerConsumption = zeros(n,p);
CoolingPowerConsumption = zeros(n,p);
HydrogenProduced = zeros(n,p);
H2_gen = zeros(n,p);
H2_gen_kg = zeros(n,p);
H2_gen_th = zeros(n,p);
H2_gen_th_kg = zeros(n,p);
HydrogenLost = zeros(n,p);
HydrogenLost_kWh = zeros(n,p);
PE_loss = zeros(n,p);
tot_eng_cons = zeros(n,p);
perc_PowerElectronics = zeros(n,p);
perc_PowerElectronics_f = zeros(n,p);
BOPPowerCons = zeros(n,p);
BOPPowerCons_f = zeros(n,p);
SpecStackPowerCons_Prod = zeros(n,p);
SpecStackPowerConsProd_f = zeros(n,p);
SpecStackPowerCons = zeros(n,p);
SpecStackPowerCons_f = zeros(n,p);
perc_Stack1Power = zeros(n,p);
perc_Stack1Power_f = zeros(n,p);
perc_Stack2Power = zeros(n,p);
perc_Stack2Power_f = zeros(n,p);
perc_Stack3Power = zeros(n,p);
perc_Stack3Power_f = zeros(n,p);
perc_Stack4Power = zeros(n,p);
perc_Stack4Power_f = zeros(n,p);
perc_CompPower = zeros(n,p);
perc_CompPower_f = zeros(n,p);
perc_CoolPower = zeros(n,p);
perc_CoolPower_f = zeros(n,p);
perc_H2Loss = zeros(n,p);
perc_H2Loss_f = zeros(n,p);
check = zeros(n,p);
eta_total = zeros(n,p);
eta_total_f = zeros(n,p);
AC_in_cons = zeros(n,p);
SEC = zeros(n,p);
SEC_f = zeros(n,p);
HydrogenLost_kg = zeros(n,p);
Spec_H2Loss = zeros(n,p);
Spec_H2Loss_kg = zeros(n,p);
Spec_H2Loss_kg_f = zeros(n,p);
Spec_H2Loss_kWh = zeros(n,p);
Spec_H2Loss_kWh_f = zeros(n,p);
eta_cell_1 = zeros(n,p);
eta_cell_2 = zeros(n,p);
eta_cell_3 = zeros(n,p);
eta_cell_4 = zeros(n,p);
eta_PE_1 = zeros(n,p);
```

```
BOP_sec = zeros(n,p);
BOP_sec_f = zeros(n,p);
Comp_sec = zeros(n,p);
Comp_sec_f = zeros(n,p);
Cool_sec = zeros(n,p);
Cool_sec_f = zeros(n,p);
for j=1:length(P_cath)
    set_param('GHGS_v7/Cathode Pressure [Pa]','Value',num2str(P_cath(j))) % Set
cathode pressure
    for i=1:length(AC_in)
        set_param('GHGS_v7/ConstantACPower','Value',num2str(AC_in(i))) %Iterate
through part load conditions
        sim('GHGS_v7.slx',SimTime);
        load('SimOutput.mat');
        Time(j,i) = SimOutput(1,end)./3600; %Time in hours
        Stack1PowerConsumption(j,i) = SimOutput(2,end);
        Stack2PowerConsumption(j,i) = SimOutput(3,end);
        Stack3PowerConsumption(j,i) = SimOutput(4,end);
        Stack4PowerConsumption(j,i) = SimOutput(5,end);
        CompressorPowerConsumption(j,i) = SimOutput(6,end);
        CoolingPowerConsumption(j,i) = SimOutput(7,end);
        HydrogenProduced(j,i) = SimOutput(8,end);
        HydrogenLost(j,i) = SimOutput(9,end);
        ACPowerConsumption(j,i) = SimOutput(17,end);
        PE_loss(j,i) = SimOutput(18,end);
        eta_cell_1(j,i) = SimOutput(19,end);
        eta_cell_2(j,i) = SimOutput(20,end);
        eta_cell_3(j,i) = SimOutput(21,end);
        eta_cell_4(j,i) = SimOutput(22,end);
        eta_cell_1_f(j,:) = flip(eta_cell_1(j,:));
        eta_cell_2_f(j,:) = flip(eta_cell_2(j,:));
        eta_cell_3_f(j,:) = flip(eta_cell_3(j,:));
        eta_cell_4_f(j,:) = flip(eta_cell_4(j,:));
        H2_gen(j,i) = SimOutput(23,end);
        H2_gen_th(j,i) = SimOutput(24,end);
        eta_PE_1(j,i) = SimOutput(25,end);
        eta_PE_1_f(j,:) = flip(eta_PE_1(j,:));
        %Convert Joules to kWh
        ACPowerConsumption(j,i) = ACPowerConsumption(j,i)*(1/(3600*1000));
        Stack1PowerConsumption(j,i) = Stack1PowerConsumption(j,i).*(1/(3600*1000));
        Stack2PowerConsumption(j,i) = Stack2PowerConsumption(j,i).*(1/(3600*1000));
        Stack3PowerConsumption(j,i) = Stack3PowerConsumption(j,i).*(1/(3600*1000));
        Stack4PowerConsumption(j,i) = Stack4PowerConsumption(j,i).*(1/(3600*1000));
        CompressorPowerConsumption(j,i) =
CompressorPowerConsumption(j,i).*(1/(3600*1000));
        CoolingPowerConsumption(j,i) = CoolingPowerConsumption(j,i).*(1/(3600*1000));
        PE_loss(j,i) = PE_loss(j,i)*(1/(3600*1000));
        %Convert mol H2 to kWh
        HydrogenLost_kWh(j,i) =
HydrogenLost(j,i).*((2.016/1000)*(141.88*(10^6))/(3600*1000));
        %Convert mol to kg
        HydrogenProduced(j,i) = HydrogenProduced(j,i).*(2.016/1000);
        HydrogenLost_kg(j,i) = HydrogenLost(j,i).*(2.016/1000);
        H2_gen_kg(j,i) = H2_gen(j,i).*(2.016/1000);
        H2_gen_th_kg(j,i) = H2_gen_th(j,i).*(2.016/1000);
```

```
        %System Specific Power Consumption Method 1
        AC_in_cons(j,i) = AC_in(i)*Time(j,i)/1000; %kWh of AC going to PEMEC
        SEC(j,i) =
(AC_in_cons(j,i)+CompressorPowerConsumption(j,i)+CoolingPowerConsumption(j,i))/Hydrog
enProduced(j,i);
        SEC_f(j,:) = flip(SEC(j,:));
        Spec_H2Loss_kg(j,i) = HydrogenLost_kg(j,i)/H2_gen_th_kg(j,i);
        Spec_H2Loss_kg_f(j,:) = flip(Spec_H2Loss_kg(j,:));
        Spec_H2Loss_kWh(j,i) = HydrogenLost_kWh(j,i)/H2_gen_kg(j,i);
        Spec_H2Loss_kWh_f(j,:) = flip(Spec_H2Loss_kWh(j,:));
        perc_Stack1Power(j,i) =
(Stack1PowerConsumption(j,i)/HydrogenProduced(j,i))/SEC(j,i);
        perc_Stack2Power(j,i) =
(Stack2PowerConsumption(j,i)/HydrogenProduced(j,i))/SEC(j,i);
        perc_Stack3Power(j,i) =
(Stack3PowerConsumption(j,i)/HydrogenProduced(j,i))/SEC(j,i);
        perc_Stack4Power(j,i) =
(Stack4PowerConsumption(j,i)/HydrogenProduced(j,i))/SEC(j,i);
        perc_PowerElectronics(j,i) = (PE_loss(j,i)/HydrogenProduced(j,i))/SEC(j,i);
        perc_CompPower(j,i) =
(CompressorPowerConsumption(j,i)/HydrogenProduced(j,i))/SEC(j,i);
        perc_CoolPower(j,i) =
(CoolingPowerConsumption(j,i)/HydrogenProduced(j,i))/SEC(j,i);
        eta_total(j,i) = (1/SEC(j,i))*141.88/3.6;
        %System Specific Power Consumption Method 2
        tot_eng_cons(j,i) =
PE_loss(j,i)+Stack1PowerConsumption(j,i)+Stack2PowerConsumption(j,i)+Stack3PowerConsu
mption(j,i)+Stack4PowerConsumption(j,i)+CompressorPowerConsumption(j,i)+CoolingPowerC
onsumption(j,i)+HydrogenLost(j,i);
        BOPPowerCons(j,i) = (tot_eng_cons(j,i)-
(Stack1PowerConsumption(j,i)+Stack2PowerConsumption(j,i)+Stack3PowerConsumption(j,i)+
Stack4PowerConsumption(j,i)))./HydrogenProduced(j,i);
        BOPPowerCons_f(j,:) = flip(BOPPowerCons(j,:));
        SpecStackPowerCons_Prod(j,i) =
(Stack1PowerConsumption(j,i)+Stack2PowerConsumption(j,i)+Stack3PowerConsumption(j,i)+
Stack4PowerConsumption(j,i))./(H2_gen_th_kg(j,i));
        SpecStackPowerConsProd_f(j,:) = flip(SpecStackPowerCons_Prod(j,:));
        BOP_sec(j,i) =
(CompressorPowerConsumption(j,i)+CoolingPowerConsumption(j,i))/(H2_gen_th_kg(j,i));
        BOP_sec_f(j,:) = flip(BOP_sec(j,:));
        Comp_sec(j,i) = (CompressorPowerConsumption(j,i))/(H2_gen_th_kg(j,i));
        Comp_sec_f(j,:) = flip(Comp_sec(j,:));
        Cool_sec(j,i) = (CoolingPowerConsumption(j,i))/(H2_gen_th_kg(j,i));
        Cool_sec_f(j,:) = flip(Cool_sec(j,:));
        SpecStackPowerCons(j,i) =
(Stack1PowerConsumption(j,i)+Stack2PowerConsumption(j,i)+Stack3PowerConsumption(j,i)+
Stack4PowerConsumption(j,i))./(HydrogenProduced(j,i)+HydrogenLost(j,i)); %Not right
        SpecStackPowerCons_f(j,:) = flip(SpecStackPowerCons(j,:));
        % Flip arrays to read as increasing electrolyzer power
        perc_Stack1Power_f(j,:) = flip(perc_Stack1Power(j,:));
        perc_Stack2Power_f(j,:) = flip(perc_Stack2Power(j,:));
        perc_Stack3Power_f(j,:) = flip(perc_Stack3Power(j,:));
        perc_Stack4Power_f(j,:) = flip(perc_Stack4Power(j,:));
        perc_PowerElectronics_f(j,:) = flip(perc_PowerElectronics(j,:));
        perc_CompPower_f(j,:) = flip(perc_CompPower(j,:));
```

```
        perc_CoolPower_f(j,:) = flip(perc_CoolPower(j,:));
        eta_total_f(j,:) = flip(eta_total(j,:));
        % Make sure percentages add up to 100%
        check(j,i) =
perc_PowerElectronics(j,i)+perc_Stack1Power(j,i)+perc_Stack2Power(j,i)+perc_Stack3Pow
er(j,i)+perc_Stack4Power(j,i)+perc_CompPower(j,i)+perc_CoolPower(j,i);%+perc_H2Loss(j
,i);
    end
end

% Save simulink model
save_system("GHGS_v7")
toc
%% Create Plots
%Remove zeros
eta_total_f(eta_total_f==0) = nan;
%Add in fake nan to fix plotting scale
eta_total_f_new = zeros(length(P_cath),length(10:5:100));
perc_Stack1Power_f_new = zeros(length(P_cath),length(10:5:100));
perc_PowerElectronics_f_new = zeros(length(P_cath),length(10:5:100));
perc_CompPower_f_new = zeros(length(P_cath),length(10:5:100));
perc_CoolPower_f_new = zeros(length(P_cath),length(10:5:100));
SEC_f_new = zeros(length(P_cath),length(10:5:100));
BOPPowerCons_f_new = zeros(length(P_cath),length(10:5:100));
SpecStackPowerCons_f_new = zeros(length(P_cath),length(10:5:100));
Spec_H2Loss_kg_f_new = zeros(length(P_cath),length(10:5:100));
Spec_H2Loss_kWh_f_new = zeros(length(P_cath),length(10:5:100));
eta_cell_1_f_new = zeros(length(P_cath),length(10:5:100));
eta_cell_2_f_new = zeros(length(P_cath),length(10:5:100));
eta_cell_3_f_new = zeros(length(P_cath),length(10:5:100));
eta_cell_4_f_new = zeros(length(P_cath),length(10:5:100));
eta_PE_1_f_new = zeros(length(P_cath),length(10:5:100));
SpecStackPowerConsProd_f_new = zeros(length(P_cath),length(10:5:100));
BOP_sec_f_new = zeros(length(P_cath),length(10:5:100));
Comp_sec_f_new = zeros(length(P_cath),length(10:5:100));
Cool_sec_f_new = zeros(length(P_cath),length(10:5:100));
p = 6;
for q=1:length(P_cath)
    for i=1:length(10:5:100)
        if i<=5
            eta_total_f_new(q,i) = eta_total_f(q,i);
            SEC_f_new(q,i) = SEC_f(q,i);
            perc_Stack1Power_f_new(q,i) = perc_Stack1Power_f(q,i);
            perc_PowerElectronics_f_new(q,i) = perc_PowerElectronics_f(q,i);
            perc_CompPower_f_new(q,i) = perc_CompPower_f(q,i);
            perc_CoolPower_f_new(q,i) = perc_CoolPower_f(q,i);
            BOPPowerCons_f_new(q,i) = BOPPowerCons_f(q,i);
            SpecStackPowerCons_f_new(q,i) = SpecStackPowerCons_f(q,i);
            Spec_H2Loss_kg_f_new(q,i) = Spec_H2Loss_kg_f(q,i);
            Spec_H2Loss_kWh_f_new(q,i) = Spec_H2Loss_kWh_f(q,i);
            eta_cell_1_f_new(q,i) = eta_cell_1_f(q,i);
            eta_cell_2_f_new(q,i) = eta_cell_2_f(q,i);
            eta_cell_3_f_new(q,i) = eta_cell_3_f(q,i);
            eta_cell_4_f_new(q,i) = eta_cell_4_f(q,i);
            eta_PE_1_f_new(q,i) = eta_PE_1_f(q,i);
```

```
            SpecStackPowerConsProd_f_new(q,i) = SpecStackPowerConsProd_f(q,i);
            BOP_sec_f_new(q,i) = BOP_sec_f(q,i);
            Comp_sec_f_new(q,i) = Comp_sec_f(q,i);
            Cool_sec_f_new(q,i) = Cool_sec_f(q,i);
        elseif (i>=5) && (rem(i,2)==0) %even i
            eta_total_f_new(q,i) = nan;
            SEC_f_new(q,i) = nan;
            perc_Stack1Power_f_new(q,i) = nan;
            perc_PowerElectronics_f_new(q,i) = nan;
            perc_CompPower_f_new(q,i) = nan;
            perc_CoolPower_f_new(q,i) = nan;
            BOPPowerCons_f_new(q,i) = nan;
            SpecStackPowerCons_f_new(q,i) = nan;
            Spec_H2Loss_kg_f_new(q,i) = nan;
            Spec_H2Loss_kWh_f_new(q,i) = nan;
            eta_cell_1_f_new(q,i) = nan;
            eta_cell_2_f_new(q,i) = nan;
            eta_cell_3_f_new(q,i) = nan;
            eta_cell_4_f_new(q,i) = nan;
            eta_PE_1_f_new(q,i) = nan;
            SpecStackPowerConsProd_f_new(q,i) = nan;
            BOP_sec_f_new(q,i) = nan;
            Comp_sec_f_new(q,i) = nan;
            Cool_sec_f_new(q,i) = nan;
        else %odd i
            eta_total_f_new(q,i) = eta_total_f(q,p);
            SEC_f_new(q,i) = SEC_f(q,p);
            perc_Stack1Power_f_new(q,i) = perc_Stack1Power_f(q,p);
            perc_PowerElectronics_f_new(q,i) = perc_PowerElectronics_f(q,p);
            perc_CompPower_f_new(q,i) = perc_CompPower_f(q,p);
            perc_CoolPower_f_new(q,i) = perc_CoolPower_f(q,p);
            BOPPowerCons_f_new(q,i) = BOPPowerCons_f(q,p);
            SpecStackPowerCons_f_new(q,i) = SpecStackPowerCons_f(q,p);
            Spec_H2Loss_kg_f_new(q,i) = Spec_H2Loss_kg_f(q,p);
            Spec_H2Loss_kWh_f_new(q,i) = Spec_H2Loss_kWh_f(q,p);
            eta_cell_1_f_new(q,i) = eta_cell_1_f(q,p);
            eta_cell_2_f_new(q,i) = eta_cell_2_f(q,p);
            eta_cell_3_f_new(q,i) = eta_cell_3_f(q,p);
            eta_cell_4_f_new(q,i) = eta_cell_4_f(q,p);
            eta_PE_1_f_new(q,i) = eta_PE_1_f(q,p);
            SpecStackPowerConsProd_f_new(q,i) = SpecStackPowerConsProd_f(q,p);
            BOP_sec_f_new(q,i) = BOP_sec_f(q,p);
            Comp_sec_f_new(q,i) = Comp_sec_f(q,p);
            Cool_sec_f_new(q,i) = Cool_sec_f(q,p);
            p=p+1;
        end
    end
    p=6;
end
r = length(eta_total_f_new);
xax = [1:r];
id1 = ~isnan(eta_total_f_new(1,:));
close all
figure('name','System Efficiency','position',[0 0 1200 800])
    yyaxis left
```

```
    p1 = plot(xax(id1),eta_total_f_new(1,id1),'-o',xax(id1),eta_total_f_new(2,id1),'-
square',xax(id1),eta_total_f_new(3,id1),'-^');
    xlabel('Electrolyzer Power - % of Rated')
    xlim ([1 r])
    ylim([0 1])
    yticks([0.1:0.1:1])
    yticklabels({'10%' '20%' '30%' '40%' '50%' '60%' '70%' '80%' '90%' '100%'})
    xticklabels({'10%' '15%' '20%' '25%' '30%' '' '40%' '' '50%' '' '60%' '' '70%' ''
'80%' '' '90%' '' '100%'})
    ylabel('System Efficiency - HHV Basis')

    yyaxis right
    p2 = plot(xax(id1),SEC_f_new(1,id1),'-o',xax(id1),SEC_f_new(2,id1),'-
square',xax(id1),SEC_f_new(3,id1),'-^');
    ylabel('System Specific Energy Consumption - kWh/kg')
    ylim([70 150])
    yticks([70:10:150])
    yticklabels([70:10:150])

    legend({'System Efficiency - 30 Bar H2','System Efficiency - 60 Bar H2','System
Efficiency - 90 Bar H2','System Specific Energy Consumption - 30 Bar H2','System
Specific Energy Consumption - 60 Bar H2','System Specific Energy Consumption - 90 Bar
H2'})
    p1(1).LineWidth = 4;
    p1(1).MarkerSize = 10;
    p1(1).Color = [0 .3 .08];
    p1(2).LineWidth = 4;
    p1(2).MarkerSize = 10;
    p1(2).Color = [0 .3 .08];
    p1(3).LineWidth = 4;
    p1(3).MarkerSize = 10;
    p1(3).Color = [0 .3 .08];
    p2(1).LineWidth = 4;
    p2(1).MarkerSize = 10;
    p2(1).Color = [1 .49804 0];
    p2(2).LineWidth = 4;
    p2(2).MarkerSize = 10;
    p2(2).Color = [1 .49804 0];
    p2(3).LineWidth = 4;
    p2(3).MarkerSize = 10;
    p2(3).Color = [1 .49804 0];
    grid('on')
    ax = gca;
    set(ax,'Fontsize',20)
    set(ax,'Xtick',[1:r])
    ax.YAxis(1).Color = [0 .3 .08];
    ax.YAxis(2).Color = [1 .49804 0];
figure('name','Specific Power Consumption Breakdown','position',[0 0 1200 800])
    t = tiledlayout(2,2);
    ax1 = nexttile;
    p3 = plot(xax(id1),perc_Stack1Power_f_new(1,id1),'-
o',xax(id1),perc_PowerElectronics_f_new(1,id1),'-
square',xax(id1),perc_CompPower_f_new(1,id1),'-
diamond',xax(id1),perc_CoolPower_f_new(1,id1),'-
*');%xax(id1),perc_H2Loss_f_new(1,id1),'-^');
```

```
    xlim ([1 r])
    ylim([0 1])
    yticks([0.1:0.1:1])
    yticklabels([0.1:0.1:1])
    xticks([1:r])
    xticklabels({'10%' '15%' '20%' '25%' '30%' '' '40%' '' '50%' '' '60%' '' '70%' ''
'80%' '' '90%' '' '100%'})
    grid('on')
    %Electrolyzer Color
    p3(1).LineWidth = 4;
    p3(1).MarkerSize = 10;
    p3(1).Color = [0 .3 .08];
    %PE Color
    p3(2).LineWidth = 4;
    p3(2).MarkerSize = 10;
    p3(2).Color = [1 .7 0];
    %Comp Color
    p3(3).LineWidth = 4;
    p3(3).MarkerSize = 10;
    p3(3).Color = [0 0.2 0.50196];
    %Cool Color
    p3(4).LineWidth = 4;
    p3(4).MarkerSize = 12;
    p3(4).Color = [0 0.74902 1];

    ax = gca;
    set(ax,'Fontsize',18)

    ax2 = nexttile;
    p4 = plot(xax(id1),perc_Stack1Power_f_new(2,id1),'-
o',xax(id1),perc_PowerElectronics_f_new(2,id1),'-
square',xax(id1),perc_CompPower_f_new(2,id1),'-
diamond',xax(id1),perc_CoolPower_f_new(2,id1),'-
*');%xax(id1),perc_H2Loss_f_new(2,id1),'-^');
    xlim ([1 r])
    ylim([0 1])
    yticks([0.1:0.1:1])
    yticklabels([0.1:0.1:1])
    xticks([1:r])
    xticklabels({'10%' '15%' '20%' '25%' '30%' '' '40%' '' '50%' '' '60%' '' '70%' ''
'80%' '' '90%' '' '100%'})
    grid('on')
    %Electrolyzer Color
    p4(1).LineWidth = 4;
    p4(1).MarkerSize = 10;
    p4(1).Color = [0 .3 .08];
    %PE Color
    p4(2).LineWidth = 4;
    p4(2).MarkerSize = 10;
    p4(2).Color = [1 .7 0];
    %Comp Color
    p4(3).LineWidth = 4;
    p4(3).MarkerSize = 10;
    p4(3).Color = [0 0.2 0.50196];
    %Cool Color
```

```
    p4(4).LineWidth = 4;
    p4(4).MarkerSize = 12;
    p4(4).Color = [0 0.74902 1];

    ax = gca;
    set(ax,'Fontsize',18)

    ax3 = nexttile;
    p5 = plot(xax(id1),perc_Stack1Power_f_new(3,id1),'-
o',xax(id1),perc_PowerElectronics_f_new(3,id1),'-
square',xax(id1),perc_CompPower_f_new(3,id1),'-
diamond',xax(id1),perc_CoolPower_f_new(3,id1),'-
*');%xax(id1),perc_H2Loss_f_new(3,id1),'-^');
    xlim ([1 r])
    ylim([0 1])
    yticks([0.1:0.1:1])
    yticklabels([0.1:0.1:1])
    xticks([1:r])
    xticklabels(ax3,{'10%' '15%' '20%' '25%' '30%' '' '40%' '' '50%' '' '60%' ''
'70%' '' '80%' '' '90%' '' '100%'})
    grid('on')
    %Electrolyzer Color
    p5(1).LineWidth = 4;
    p5(1).MarkerSize = 10;
    p5(1).Color = [0 .3 .08];
    %PE Color
    p5(2).LineWidth = 4;
    p5(2).MarkerSize = 10;
    p5(2).Color = [1 .7 0];
    %Comp Color
    p5(3).LineWidth = 4;
    p5(3).MarkerSize = 10;
    p5(3).Color = [0 0.2 0.50196];
    %Cool Color
    p5(4).LineWidth = 4;
    p5(4).MarkerSize = 12;
    p5(4).Color = [0 0.74902 1];

    ax = gca;
    set(ax,'Fontsize',18)

    lgd = legend({'Stack Power Consumption','PE Conversion Losses','Compressor Power
Consumption','Cooling System Power Consumption'});%,'H2 Loss'});
    lgd.Layout.Tile = 4;

    linkaxes([ax1,ax2,ax3],'x');
    xlabel(t,'Electrolyzer Power - % of Rated','Fontsize',18)
    ylabel(t,'Fraction of Total Specific Energy Consumption','Fontsize',18)
figure('name','H2 Loss and System Efficiency','position',[0 0 1200 800])
    yyaxis left
    p6 = plot(xax(id1),eta_total_f_new(1,id1),'-
o',xax(id1),eta_cell_1_f_new(1,id1),'-^');
    ylabel('Efficiency')
    ylim([0 1])
    yticks([0.1:0.1:1])
```

```
    yticklabels({'10%' '20%' '30%' '40%' '50%' '60%' '70%' '80%' '90%' '100%'})
    p6(1).LineWidth = 4;
    p6(1).MarkerSize = 10;
    p6(1).Color = [0 .3 .08];
    p6(2).LineWidth = 4;
    p6(2).MarkerSize = 10;
    p6(2).Color = [0 0 0];

    yyaxis right
    p7 = plot(xax(id1),Spec_H2Loss_kg_f_new(1,id1),'-diamond');
    ylabel({'Hydrogen Lost per', 'kg of H_2 Generated [kg/kg]'},'Color','k')
    xlabel('Electrolyzer Power - % of Rated')
    xlim ([1 r])
    xticklabels({'10%' '15%' '20%' '25%' '30%' '' '40%' '' '50%' '' '60%' '' '70%' ''
'80%' '' '90%' '' '100%'})
    p7(1).LineWidth = 4;
    p7(1).MarkerSize = 10;
    p7(1).Color = [1 0 0];
    grid('on')
    ax = gca;
    set(ax,'Fontsize',20)
    set(ax,'Xtick',[1:r])
    ax.YAxis(1).Color = [0 0 0];
    ax.YAxis(2).Color = [1 0 0];
    lgd = legend({'System Efficiency HHV Basis','Electrolyzer Voltage
Efficiency','Specific Hydrogen Loss'});
figure('name','System Efficiency','position',[0 0 1200 800])
    yyaxis left
    p8 = plot(xax(id1),eta_total_f_new(1,id1),'-o','color',[0 .3 .08]);
    xlabel('Electrolyzer Power - % of Rated')
    xlim ([1 r])
    ylim([0 1])
    yticks([0.1:0.1:1])
    yticklabels({'10%' '20%' '30%' '40%' '50%' '60%' '70%' '80%' '90%' '100%'})
    xticklabels({'10%' '15%' '20%' '25%' '30%' '' '40%' '' '50%' '' '60%' '' '70%' ''
'80%' '' '90%' '' '100%'})
    ylabel('System Efficiency - HHV Basis')

    yyaxis right
    p9 = plot(xax(id1),SEC_f_new(1,id1),'-o','Color',[1 .49804 0]);
    ylabel('System Specific Energy Consumption - kWh/kg')

    p8(1).LineWidth = 4;
    p8(1).MarkerSize = 10;
    p9(1).LineWidth = 4;
    p9(1).MarkerSize = 10;
    grid('on')
    legend({'Energy Conversion Efficiency','Specific Energy Consumption'})
    ax = gca;
    set(ax,'Fontsize',20)
    set(ax,'Xtick',[1:r])
    ax.YAxis(1).Color = [0 .3 .08];
    ax.YAxis(2).Color = [1 .49804 0];
figure('name','H2 Loss and Specific Energy Cons','position',[0 0 1200 800])
```

```
    p6 = plot(xax(id1),SpecStackPowerConsProd_f_new(1,id1),'-
^',xax(id1),Comp_sec_f_new(1,id1),'-square',xax(id1),Cool_sec_f_new(1,id1),'-*');
    ylabel({'Energy Consumption per','kg of H_2 Generated [kWh/kg H_2]'})
    p6(1).LineWidth = 4;
    p6(1).MarkerSize = 10;
    p6(1).Color = [0 0 0];
    p6(2).LineWidth = 4;
    p6(2).MarkerSize = 10;
    p6(2).Color = [0 0.2 0.50196];
    p6(3).LineWidth = 4;
    p6(3).MarkerSize = 10;
    p6(3).Color = [0 0.74902 1];
    xlabel('Electrolyzer Power - % of Rated')
    xlim ([1 r])
    xticklabels({'10%' '15%' '20%' '25%' '30%' '' '40%' '' '50%' '' '60%' '' '70%' ''
'80%' '' '90%' '' '100%'})
    grid('on')
    ax = gca;
    set(ax,'Fontsize',20)
    set(ax,'Xtick',[1:r])
    ax.YAxis(1).Color = [0 0 0];
    lgd = legend({'Electrolyzer Energy Consumption','Compressor Energy
Consumption','Cooling System Energy Consumption'},'location','east');
figure('name','PE and Electrolyzer Eff','position',[0 0 1200 800])
    p = plot(xax(id1),eta_PE_1_f_new(1,id1),'-
diamond',xax(id1),eta_cell_1_f_new(1,id1),'-^');
    p(1).LineWidth = 4;
    p(1).MarkerSize = 10;
    p(1).Color = [1 .49804 0];
    p(2).LineWidth = 4;
    p(2).MarkerSize = 10;
    p(2).Color = [0 .3 .08];
    ylabel('Efficiency')
    ylim([0.6 1])
    yticks([0.6:0.05:1])
    yticklabels({'60%' '65%' '70%' '75%' '80%' '85%' '90%' '95%' '100%'})
    xlabel('Electrolyzer Power - % of Rated')
    xlim ([1 r])
    xticklabels({'10%' '15%' '20%' '25%' '30%' '' '40%' '' '50%' '' '60%' '' '70%' ''
'80%' '' '90%' '' '100%'})
    grid('on')
    ax = gca;
    set(ax,'Fontsize',20)
    set(ax,'Xtick',[1:r])
    lgd = legend({'AC-DC Conversion Efficiency','Electrolyzer Voltage
Efficiency'},'location','east');
```

Appendix C: Matlab script used for scaled multi-electrolyzer system.

The Matlab script in this appendix was used to evaluate the multi-electrolyzer system with the ERCOT case study. The code sets the relevant Simulink parameters and prompts the user to select the loading strategy within the Simulink model. The Matlab script imports the outputs of the Simulink model and performs some unit conversions and verification calculations. The figures and values used in this work are created in the last section of the script.

```
%% ERCOT Case Study
clc
clear
format long
tic
%% Read ERCOT Data
ERCOT_time = [1:1:365*24]';
ERCOT_load =
table2array(readtable('rpt.00013424.0000000000000000.20230118.170454825.ERCOT_2022_Ho
urly_WindSolar_Output.xlsx','Sheet','Wind Data','Range','C2:C8761'));
ERCOT_wind_gen =
table2array(readtable('rpt.00013424.0000000000000000.20230118.170454825.ERCOT_2022_Ho
urly_WindSolar_Output.xlsx','Sheet','Wind Data','Range','D2:D8761'));
ERCOT_wind_cap =
table2array(readtable('rpt.00013424.0000000000000000.20230118.170454825.ERCOT_2022_Ho
urly_WindSolar_Output.xlsx','Sheet','Wind Data','Range','E2:E8761'));
ERCOT_wind_cf =
table2array(readtable('rpt.00013424.0000000000000000.20230118.170454825.ERCOT_2022_Ho
urly_WindSolar_Output.xlsx','Sheet','Wind Data','Range','F2:F8761'))/100;
ERCOT_pv_gen =
table2array(readtable('rpt.00013424.0000000000000000.20230118.170454825.ERCOT_2022_Ho
urly_WindSolar_Output.xlsx','Sheet','Solar Data','Range','D2:D8761'));
ERCOT_pv_cap =
table2array(readtable('rpt.00013424.0000000000000000.20230118.170454825.ERCOT_2022_Ho
urly_WindSolar_Output.xlsx','Sheet','Solar Data','Range','E2:E8761'));
ERCOT_pv_cf =
table2array(readtable('rpt.00013424.0000000000000000.20230118.170454825.ERCOT_2022_Ho
urly_WindSolar_Output.xlsx','Sheet','Solar Data','Range','F2:F8761'))/100;
Total_RE_cap = ERCOT_wind_cap+ERCOT_pv_cap;
perc_wind = mean(ERCOT_wind_cap./Total_RE_cap);
perc_pv = mean(ERCOT_pv_cap./Total_RE_cap);
%Scale Data to 100% RE
SF = mean(ERCOT_load)/mean(ERCOT_wind_gen+ERCOT_pv_gen); %average total RE generation
= average grid load
ERCOT_wind_cap_s = max(ERCOT_wind_cap)*SF;
ERCOT_pv_cap_s = max(ERCOT_pv_cap)*SF;
ERCOT_wind_gen_s = ERCOT_wind_cf*ERCOT_wind_cap_s;
ERCOT_pv_gen_s = ERCOT_pv_cf*ERCOT_pv_cap_s;
Total_RE_gen_s = ERCOT_wind_gen_s+ERCOT_pv_gen_s;
%Scale to single system
HGS_cap = 12.5; %Total electrolyzer MW rating, 10 x 1.25 MW electrolyzers
```

```
sys_load = ERCOT_load*(HGS_cap/mean(ERCOT_load)); %Scale load down so that mean load
= mean RE gen = hgs cap
sys_RE_cap = HGS_cap; %start with RE capacity = HGS capacity
sys_wind_gen = sys_RE_cap*perc_wind.*ERCOT_wind_cf;
sys_pv_gen = sys_RE_cap*perc_pv.*ERCOT_pv_cf;
sys_RE_gen = sys_wind_gen+sys_pv_gen;
sys_net = (sys_wind_gen+sys_pv_gen)-sys_load;
for i=1:length(sys_net)
    if sys_net(i)>=0
        ex_RE(i) = (sys_wind_gen(i)+sys_pv_gen(i))-sys_load(i); % Excess RE
        short_RE(i) = 0;
    else
        ex_RE(i) = 0;
        short_RE(i) = (sys_wind_gen(i)+sys_pv_gen(i))-sys_load(i); %Short RE
    end
end
kWh_extra = cumtrapz(ERCOT_time,ex_RE);
kWh_short = cumtrapz(ERCOT_time,short_RE);
extra_RE_ratio = abs(kWh_extra(end)/kWh_short(end));
save('ERCOT_time.mat','ERCOT_time')

%Scale RE capacity until the ratio of excess RE to short RE is 1:1
while extra_RE_ratio < 1
    sys_RE_cap = sys_RE_cap*1.01; %increase capacity by 1%
    sys_wind_gen = sys_RE_cap*perc_wind.*ERCOT_wind_cf;
    sys_pv_gen = sys_RE_cap*perc_pv.*ERCOT_pv_cf;
    sys_RE_gen = sys_wind_gen+sys_pv_gen;
    sys_net = (sys_wind_gen+sys_pv_gen)-sys_load;
    for i=1:length(sys_net)
        if sys_net(i)>=0
            ex_RE(i) = (sys_wind_gen(i)+sys_pv_gen(i))-sys_load(i); % Excess RE
            short_RE(i) = 0;
        else
            ex_RE(i) = 0;
            short_RE(i) = (sys_wind_gen(i)+sys_pv_gen(i))-sys_load(i); %Short RE
        end
    end
    kWh_extra = cumtrapz(ERCOT_time,ex_RE);
    kWh_short = cumtrapz(ERCOT_time,short_RE);
    extra_RE_ratio = abs(kWh_extra(end)/kWh_short(end));
end
% Create load profile for HGS model
save('ex_RE.mat','ex_RE')

% Open the simulink model and load input data
GHGS_MSA_v5
set_param('GHGS_MSA_v5/AC Power Input','Table','ex_RE');
set_param('GHGS_MSA_v5/AC Power Input','BreakpointsForDimension1','ERCOT_time');

% Set model parameters
DC_Rating = 1.25*1e6;
set_param('GHGS_MSA_v5/Power Electronics/Stack Rating
[W]','Value',num2str(DC_Rating))
set_param('GHGS_MSA_v5/Power Electronics/kW to W','Gain','1e6') %Set gain because
curtailment profile is in kW and constant load is in W
```

```
set_param('GHGS_MSA_v5/Manual Switch1','sw','1') %1 = follow load profile, 0 =
constant AC power input
set_param('GHGS_MSA_v5/Model Outputs/kW to W','Gain','1e6') %Input to integrator must
be in W
A_cell = 0.594966311636225; %Cell Active area with lower faraday eff
n_cells = 65; %Numbers of Cells per Stack
set_param('GHGS_MSA_v5/PSA Dryer/D_o [m]','Value','0.001477574149664'); %Fitted
scaling method with lower faraday eff
set_param('GHGS_MSA_v5/Cell Area [m^2]','Value',num2str(A_cell)); %Fitted scaling
method
set_param('GHGS_MSA_v5/Power Electronics/Rated Input
[W]','value','(73/60)*1250*1000'); %Set rated AC in to match electrolyzer rating
set_param('GHGS_MSA_v5/PSA Dryer/molpers to molperhr','Gain','3600')
set_param('GHGS_MSA_v5/PSA Dryer/Manual Switch','sw','1') %1 for fixed vent flow and
0 for variable vent flow
set_param('GHGS_MSA_v5/Power Electronics/Manual Switch','sw',num2str(1));
set_param('GHGS_MSA_v5/Power Electronics/Manual Switch1','sw',num2str(1));
set_param('GHGS_MSA_v5/Power Electronics/Manual Switch2','sw',num2str(1));
set_param('GHGS_MSA_v5/Power Electronics/Manual Switch3','sw',num2str(1));
set_param('GHGS_MSA_v5/Power Electronics/Manual Switch4','sw',num2str(1));
set_param('GHGS_MSA_v5/Power Electronics/Manual Switch5','sw',num2str(1));
set_param('GHGS_MSA_v5/Power Electronics/Manual Switch6','sw',num2str(1));
set_param('GHGS_MSA_v5/Power Electronics/Manual Switch7','sw',num2str(1));
set_param('GHGS_MSA_v5/Power Electronics/Manual Switch8','sw',num2str(1));
set_param('GHGS_MSA_v5/Power Electronics/Manual Switch9','sw',num2str(1));
%% Pause code and tell user to change the loading scheme in the simulink model
warning('Please verify that the Simulink model is set to use the sequential loading
scheme, then press any key to continue.')
pause
%% Run Simulink model with the sequential loading scheme (SL)
MinStackSetpoint = [0.1:0.05:0.8]; % Sweep Selected Minumum stack operating fraction
for i=1:length(MinStackSetpoint)
    set_param('GHGS_MSA_v5/Power Electronics/Min Perc
Load','value',num2str(MinStackSetpoint(i))) %Set the minimum turndown range of the
electrolyzer stacks

sim('GHGS_MSA_v5.slx','StartTime',num2str(ERCOT_time(1)),'StopTime',num2str(ERCOT_tim
e(end)),'FixedStep','1');
    load('SimOutput.mat');
    Time_SL(i,:) = SimOutput(1,:); %Time in hours
    Stack1PowerConsumption_SL(i) = SimOutput(2,end);
    Stack2PowerConsumption_SL(i) = SimOutput(3,end);
    Stack3PowerConsumption_SL(i) = SimOutput(4,end);
    Stack4PowerConsumption_SL(i) = SimOutput(5,end);
    Stack5PowerConsumption_SL(i) = SimOutput(6,end);
    Stack6PowerConsumption_SL(i) = SimOutput(7,end);
    Stack7PowerConsumption_SL(i) = SimOutput(8,end);
    Stack8PowerConsumption_SL(i) = SimOutput(9,end);
    Stack9PowerConsumption_SL(i) = SimOutput(10,end);
    Stack10PowerConsumption_SL(i) = SimOutput(11,end);
    CompressorPowerConsumption_SL(i) = SimOutput(12,end);
    CoolingPowerConsumption_SL(i) = SimOutput(13,end);
    HydrogenProduced_SL(i,:) = SimOutput(14,:);
    HydrogenLost_SL(i,:) = SimOutput(15,:);
    Stack1Power_SL(i,:) = SimOutput(16,:);
```

```
Stack2Power_SL(i,:) = SimOutput(17,:);
Stack3Power_SL(i,:) = SimOutput(18,:);
Stack4Power_SL(i,:) = SimOutput(19,:);
Stack5Power_SL(i,:)= SimOutput(20,:);
Stack6Power_SL(i,:) = SimOutput(21,:);
Stack7Power_SL(i,:) = SimOutput(22,:);
Stack8Power_SL(i,:) = SimOutput(23,:);
Stack9Power_SL(i,:) = SimOutput(24,:);
Stack10Power_SL(i,:) = SimOutput(25,:);
CompPower_SL(i,:) = SimOutput(26,:);
CoolPower_SL(i,:) = SimOutput(27,:);
H2Flowrate_SL(i,:) = SimOutput(28,:);
ACPowerConsumption_SL(i) = SimOutput(29,end);
PE_loss_SL(i) = SimOutput(30,end);
eta_cell_1_SL(i,:) = SimOutput(31,:);
eta_cell_2_SL(i,:) = SimOutput(32,:);
eta_cell_3_SL(i,:) = SimOutput(33,:);
eta_cell_4_SL(i,:) = SimOutput(34,:);
eta_cell_5_SL(i,:) = SimOutput(35,:);
eta_cell_6_SL(i,:) = SimOutput(36,:);
eta_cell_7_SL(i,:) = SimOutput(37,:);
eta_cell_8_SL(i,:) = SimOutput(38,:);
eta_cell_9_SL(i,:) = SimOutput(39,:);
eta_cell_10_SL(i,:) = SimOutput(40,:);
H2_gen_SL(i,:) = SimOutput(41,:);
i_1_SL(i,:) = SimOutput(42,:);
i_2_SL(i,:) = SimOutput(43,:);
i_3_SL(i,:) = SimOutput(44,:);
i_4_SL(i,:) = SimOutput(45,:);
i_5_SL(i,:) = SimOutput(46,:);
i_6_SL(i,:) = SimOutput(47,:);
i_7_SL(i,:) = SimOutput(48,:);
i_8_SL(i,:) = SimOutput(49,:);
i_9_SL(i,:) = SimOutput(50,:);
i_10_SL(i,:) = SimOutput(51,:);
OF1_SL(i,:) = SimOutput(52,:);
OF2_SL(i,:) = SimOutput(53,:);
OF3_SL(i,:) = SimOutput(54,:);
OF4_SL(i,:) = SimOutput(55,:);
OF5_SL(i,:) = SimOutput(56,:);
OF6_SL(i,:) = SimOutput(57,:);
OF7_SL(i,:) = SimOutput(58,:);
OF8_SL(i,:) = SimOutput(59,:);
OF9_SL(i,:) = SimOutput(60,:);
OF10_SL(i,:) = SimOutput(61,:);
Vcell_1_SL(i,:) = SimOutput(62,:);
Vcell_2_SL(i,:) = SimOutput(63,:);
Vcell_3_SL(i,:) = SimOutput(64,:);
Vcell_4_SL(i,:) = SimOutput(65,:);
Vcell_5_SL(i,:) = SimOutput(66,:);
Vcell_6_SL(i,:) = SimOutput(67,:);
Vcell_7_SL(i,:) = SimOutput(68,:);
Vcell_8_SL(i,:) = SimOutput(69,:);
Vcell_9_SL(i,:) = SimOutput(70,:);
Vcell_10_SL(i,:) = SimOutput(71,:);
```

```
PE_in_SL(i,:) = SimOutput(72,:);
H2_gen_1_SL(i,:) = SimOutput(73,:);
H2_gen_2_SL(i,:) = SimOutput(74,:);
H2_gen_3_SL(i,:) = SimOutput(75,:);
H2_gen_4_SL(i,:) = SimOutput(76,:);
H2_gen_5_SL(i,:) = SimOutput(77,:);
H2_gen_6_SL(i,:) = SimOutput(78,:);
H2_gen_7_SL(i,:) = SimOutput(79,:);
H2_gen_8_SL(i,:) = SimOutput(80,:);
H2_gen_9_SL(i,:) = SimOutput(81,:);
H2_gen_10_SL(i,:) = SimOutput(82,:);
H2_diff_1_SL(i,:) = SimOutput(83,:);
H2_diff_2_SL(i,:) = SimOutput(84,:);
H2_diff_3_SL(i,:) = SimOutput(85,:);
H2_diff_4_SL(i,:) = SimOutput(86,:);
H2_diff_5_SL(i,:) = SimOutput(87,:);
H2_diff_6_SL(i,:) = SimOutput(88,:);
H2_diff_7_SL(i,:) = SimOutput(89,:);
H2_diff_8_SL(i,:) = SimOutput(90,:);
H2_diff_9_SL(i,:) = SimOutput(91,:);
H2_diff_10_SL(i,:) = SimOutput(92,:);
O2_gen_1_SL(i,:) = SimOutput(93,:);
O2_gen_2_SL(i,:) = SimOutput(94,:);
O2_gen_3_SL(i,:) = SimOutput(95,:);
O2_gen_4_SL(i,:) = SimOutput(96,:);
O2_gen_5_SL(i,:) = SimOutput(97,:);
O2_gen_6_SL(i,:) = SimOutput(98,:);
O2_gen_7_SL(i,:) = SimOutput(99,:);
O2_gen_8_SL(i,:) = SimOutput(100,:);
O2_gen_9_SL(i,:) = SimOutput(101,:);
O2_gen_10_SL(i,:) = SimOutput(102,:);
P_H2O_sat_SL(i,:) = SimOutput(103,:);
AC_curt_SL(i) = SimOutput(104,end);
%Convert mol/s to kg/sec
H2Flowrate_SL(i,:) = H2Flowrate_SL(i,:).*(2.016/1000);
%Convert W-hr to kW-hr
ACPowerConsumption_SL(i) = ACPowerConsumption_SL(i)*(1/(1000));
AC_curt_SL(i) = AC_curt_SL(i)*(1/(1000000)); %To MW-hr
Stack1PowerConsumption_SL(i) = Stack1PowerConsumption_SL(i).*(1/(1000));
Stack2PowerConsumption_SL(i) = Stack2PowerConsumption_SL(i).*(1/(1000));
Stack3PowerConsumption_SL(i) = Stack3PowerConsumption_SL(i).*(1/(1000));
Stack4PowerConsumption_SL(i) = Stack4PowerConsumption_SL(i).*(1/(1000));
Stack5PowerConsumption_SL(i) = Stack5PowerConsumption_SL(i).*(1/(1000));
Stack6PowerConsumption_SL(i) = Stack6PowerConsumption_SL(i).*(1/(1000));
Stack7PowerConsumption_SL(i) = Stack7PowerConsumption_SL(i).*(1/(1000));
Stack8PowerConsumption_SL(i) = Stack8PowerConsumption_SL(i).*(1/(1000));
Stack9PowerConsumption_SL(i) = Stack9PowerConsumption_SL(i).*(1/(1000));
Stack10PowerConsumption_SL(i) = Stack10PowerConsumption_SL(i).*(1/(1000));
CompressorPowerConsumption_SL(i) = CompressorPowerConsumption_SL(i).*(1/(1000));
CoolingPowerConsumption_SL(i) = CoolingPowerConsumption_SL(i).*(1/(1000));
PE_loss_SL(i) = PE_loss_SL(i)*(1/(1000));
%Convert mol to kg
HydrogenProduced_SL(i,:) = HydrogenProduced_SL(i,:).*(2.016/1000);
HydrogenLost_kg_SL(i,:) = HydrogenLost_SL(i,:).*(2.016/1000);
H2_gen_kg_SL(i,:) = H2_gen_SL(i,:).*(2.016/1000);
```

```
    %System Specific Power Consumption Method 1
    SEC_SL(i) =
(ACPowerConsumption_SL(i)+CompressorPowerConsumption_SL(i)+CoolingPowerConsumption_SL
(i))/HydrogenProduced_SL(i,end);
    Spec_H2Loss_kg_SL(i) = HydrogenLost_kg_SL(i,end)/H2_gen_kg_SL(i,end);
    perc_Stack1Power_SL(i) =
(Stack1PowerConsumption_SL(i)/HydrogenProduced_SL(i,end))/SEC_SL(i);
    perc_Stack2Power_SL(i) =
(Stack2PowerConsumption_SL(i)/HydrogenProduced_SL(i,end))/SEC_SL(i);
    perc_Stack3Power_SL(i) =
(Stack3PowerConsumption_SL(i)/HydrogenProduced_SL(i,end))/SEC_SL(i);
    perc_Stack4Power_SL(i) =
(Stack4PowerConsumption_SL(i)/HydrogenProduced_SL(i,end))/SEC_SL(i);
    perc_PowerElectronics_SL(i) =
(PE_loss_SL(i)/HydrogenProduced_SL(i,end))/SEC_SL(i);
    perc_CompPower_SL(i) =
(CompressorPowerConsumption_SL(i)/HydrogenProduced_SL(i,end))/SEC_SL(i);
    perc_CoolPower_SL(i) =
(CoolingPowerConsumption_SL(i)/HydrogenProduced_SL(i,end))/SEC_SL(i);
    eta_total_SL(i) = (1/SEC_SL(i))*141.88/3.6;
    % Calculate the hydrogen molefraction in the anode (volume fraction)
    O2_gen_1_SL(i,O2_gen_1_SL(i,:)<600) = 0;
    O2_gen_2_SL(i,O2_gen_2_SL(i,:)<600) = 0;
    O2_gen_3_SL(i,O2_gen_3_SL(i,:)<600) = 0;
    O2_gen_4_SL(i,O2_gen_4_SL(i,:)<600) = 0;
    O2_gen_5_SL(i,O2_gen_5_SL(i,:)<600) = 0;
    O2_gen_6_SL(i,O2_gen_6_SL(i,:)<600) = 0;
    O2_gen_7_SL(i,O2_gen_7_SL(i,:)<600) = 0;
    O2_gen_8_SL(i,O2_gen_8_SL(i,:)<600) = 0;
    O2_gen_9_SL(i,O2_gen_9_SL(i,:)<600) = 0;
    O2_gen_10_SL(i,O2_gen_10_SL(i,:)<600) = 0;
    V_H2_1_SL(i,O2_gen_1_SL(i,:)>0) =
(abs(H2_diff_1_SL(i,O2_gen_1_SL(i,:)>0))./(abs(H2_diff_1_SL(i,O2_gen_1_SL(i,:)>0))+O2
_gen_1_SL(i,O2_gen_1_SL(i,:)>0)))*(1-P_H2O_sat_SL(i,end)/101325);
    V_H2_2_SL(i,O2_gen_2_SL(i,:)>0) =
(abs(H2_diff_2_SL(i,O2_gen_2_SL(i,:)>0))./(abs(H2_diff_2_SL(i,O2_gen_2_SL(i,:)>0))+O2
_gen_2_SL(i,O2_gen_2_SL(i,:)>0)))*(1-P_H2O_sat_SL(i,end)/101325);
    V_H2_3_SL(i,O2_gen_3_SL(i,:)>0) =
(abs(H2_diff_3_SL(i,O2_gen_3_SL(i,:)>0))./(abs(H2_diff_3_SL(i,O2_gen_3_SL(i,:)>0))+O2
_gen_3_SL(i,O2_gen_3_SL(i,:)>0)))*(1-P_H2O_sat_SL(i,end)/101325);
    V_H2_4_SL(i,O2_gen_4_SL(i,:)>0) =
(abs(H2_diff_4_SL(i,O2_gen_4_SL(i,:)>0))./(abs(H2_diff_4_SL(i,O2_gen_4_SL(i,:)>0))+O2
_gen_4_SL(i,O2_gen_4_SL(i,:)>0)))*(1-P_H2O_sat_SL(i,end)/101325);
    V_H2_5_SL(i,O2_gen_5_SL(i,:)>0) =
(abs(H2_diff_5_SL(i,O2_gen_5_SL(i,:)>0))./(abs(H2_diff_5_SL(i,O2_gen_5_SL(i,:)>0))+O2
_gen_5_SL(i,O2_gen_5_SL(i,:)>0)))*(1-P_H2O_sat_SL(i,end)/101325);
    V_H2_6_SL(i,O2_gen_6_SL(i,:)>0) =
(abs(H2_diff_6_SL(i,O2_gen_6_SL(i,:)>0))./(abs(H2_diff_6_SL(i,O2_gen_6_SL(i,:)>0))+O2
_gen_6_SL(i,O2_gen_6_SL(i,:)>0)))*(1-P_H2O_sat_SL(i,end)/101325);
    V_H2_7_SL(i,O2_gen_7_SL(i,:)>0) =
(abs(H2_diff_7_SL(i,O2_gen_7_SL(i,:)>0))./(abs(H2_diff_7_SL(i,O2_gen_7_SL(i,:)>0))+O2
_gen_7_SL(i,O2_gen_7_SL(i,:)>0)))*(1-P_H2O_sat_SL(i,end)/101325);
    V_H2_8_SL(i,O2_gen_8_SL(i,:)>0) =
(abs(H2_diff_8_SL(i,O2_gen_8_SL(i,:)>0))./(abs(H2_diff_8_SL(i,O2_gen_8_SL(i,:)>0))+O2
_gen_8_SL(i,O2_gen_8_SL(i,:)>0)))*(1-P_H2O_sat_SL(i,end)/101325);
```

```
    V_H2_9_SL(i,O2_gen_9_SL(i,:)>0) =
(abs(H2_diff_9_SL(i,O2_gen_9_SL(i,:)>0))./(abs(H2_diff_9_SL(i,O2_gen_9_SL(i,:)>0))+O2
_gen_9_SL(i,O2_gen_9_SL(i,:)>0)))*(1-P_H2O_sat_SL(i,end)/101325);
    V_H2_10_SL(i,O2_gen_10_SL(i,:)>0) =
(abs(H2_diff_10_SL(i,O2_gen_10_SL(i,:)>0))./(abs(H2_diff_10_SL(i,O2_gen_10_SL(i,:)>0)
)+O2_gen_10_SL(i,O2_gen_10_SL(i,:)>0)))*(1-P_H2O_sat_SL(i,end)/101325);
    V_H2_1_SL(i,O2_gen_1_SL(i,:)==0) = 0;
    V_H2_2_SL(i,O2_gen_2_SL(i,:)==0) = 0;
    V_H2_3_SL(i,O2_gen_3_SL(i,:)==0) = 0;
    V_H2_4_SL(i,O2_gen_4_SL(i,:)==0) = 0;
    V_H2_5_SL(i,O2_gen_5_SL(i,:)==0) = 0;
    V_H2_6_SL(i,O2_gen_6_SL(i,:)==0) = 0;
    V_H2_7_SL(i,O2_gen_7_SL(i,:)==0) = 0;
    V_H2_8_SL(i,O2_gen_8_SL(i,:)==0) = 0;
    V_H2_9_SL(i,O2_gen_9_SL(i,:)==0) = 0;
    V_H2_10_SL(i,O2_gen_10_SL(i,:)==0) = 0;
end
save_system("GHGS_MSA_v5")
%% Pause code and tell user to change the loading scheme in the simulink model
warning('Please switch loading scheme in Simulink model, then press any key to
continue.')
pause
%% Run Simulink model with the even loading strategy (EL)
MinStackSetpoint = [0.1:0.05:0.8]; % Sweep Selected Minumum stack operating fraction
for i=1:length(MinStackSetpoint)
    set_param('GHGS_MSA_v5/Power Electronics/Min Perc
Load','value',num2str(MinStackSetpoint(i))) %Set the minimum turndown range of the
electrolyzer stacks

sim('GHGS_MSA_v5.slx','StartTime',num2str(ERCOT_time(1)),'StopTime',num2str(ERCOT_tim
e(end)),'FixedStep','1');
    load('SimOutput.mat');
    Time_EL(i,:) = SimOutput(1,:); %Time in hours
    Stack1PowerConsumption_EL(i) = SimOutput(2,end);
    Stack2PowerConsumption_EL(i) = SimOutput(3,end);
    Stack3PowerConsumption_EL(i) = SimOutput(4,end);
    Stack4PowerConsumption_EL(i) = SimOutput(5,end);
    Stack5PowerConsumption_EL(i) = SimOutput(6,end);
    Stack6PowerConsumption_EL(i) = SimOutput(7,end);
    Stack7PowerConsumption_EL(i) = SimOutput(8,end);
    Stack8PowerConsumption_EL(i) = SimOutput(9,end);
    Stack9PowerConsumption_EL(i) = SimOutput(10,end);
    Stack10PowerConsumption_EL(i) = SimOutput(11,end);
    CompressorPowerConsumption_EL(i) = SimOutput(12,end);
    CoolingPowerConsumption_EL(i) = SimOutput(13,end);
    HydrogenProduced_EL(i,:) = SimOutput(14,:);
    HydrogenLost_EL(i,:) = SimOutput(15,:);
    Stack1Power_EL(i,:) = SimOutput(16,:);
    Stack2Power_EL(i,:) = SimOutput(17,:);
    Stack3Power_EL(i,:) = SimOutput(18,:);
    Stack4Power_EL(i,:) = SimOutput(19,:);
    Stack5Power_EL(i,:)= SimOutput(20,:);
    Stack6Power_EL(i,:) = SimOutput(21,:);
    Stack7Power_EL(i,:) = SimOutput(22,:);
    Stack8Power_EL(i,:) = SimOutput(23,:);
```

```
Stack9Power_EL(i,:) = SimOutput(24,:);
Stack10Power_EL(i,:) = SimOutput(25,:);
CompPower_EL(i,:) = SimOutput(26,:);
CoolPower_EL(i,:) = SimOutput(27,:);
H2Flowrate_EL(i,:) = SimOutput(28,:);
ACPowerConsumption_EL(i) = SimOutput(29,end);
PE_loss_EL(i) = SimOutput(30,end);
eta_cell_1_EL(i,:) = SimOutput(31,:);
eta_cell_2_EL(i,:) = SimOutput(32,:);
eta_cell_3_EL(i,:) = SimOutput(33,:);
eta_cell_4_EL(i,:) = SimOutput(34,:);
eta_cell_5_EL(i,:) = SimOutput(35,:);
eta_cell_6_EL(i,:) = SimOutput(36,:);
eta_cell_7_EL(i,:) = SimOutput(37,:);
eta_cell_8_EL(i,:) = SimOutput(38,:);
eta_cell_9_EL(i,:) = SimOutput(39,:);
eta_cell_10_EL(i,:) = SimOutput(40,:);
H2_gen_EL(i,:) = SimOutput(41,:);
i_1_EL(i,:) = SimOutput(42,:);
i_2_EL(i,:) = SimOutput(43,:);
i_3_EL(i,:) = SimOutput(44,:);
i_4_EL(i,:) = SimOutput(45,:);
i_5_EL(i,:) = SimOutput(46,:);
i_6_EL(i,:) = SimOutput(47,:);
i_7_EL(i,:) = SimOutput(48,:);
i_8_EL(i,:) = SimOutput(49,:);
i_9_EL(i,:) = SimOutput(50,:);
i_10_EL(i,:) = SimOutput(51,:);
OF1_EL(i,:) = SimOutput(52,:);
OF2_EL(i,:) = SimOutput(53,:);
OF3_EL(i,:) = SimOutput(54,:);
OF4_EL(i,:) = SimOutput(55,:);
OF5_EL(i,:) = SimOutput(56,:);
OF6_EL(i,:) = SimOutput(57,:);
OF7_EL(i,:) = SimOutput(58,:);
OF8_EL(i,:) = SimOutput(59,:);
OF9_EL(i,:) = SimOutput(60,:);
OF10_EL(i,:) = SimOutput(61,:);
Vcell_1_EL(i,:) = SimOutput(62,:);
Vcell_2_EL(i,:) = SimOutput(63,:);
Vcell_3_EL(i,:) = SimOutput(64,:);
Vcell_4_EL(i,:) = SimOutput(65,:);
Vcell_5_EL(i,:) = SimOutput(66,:);
Vcell_6_EL(i,:) = SimOutput(67,:);
Vcell_7_EL(i,:) = SimOutput(68,:);
Vcell_8_EL(i,:) = SimOutput(69,:);
Vcell_9_EL(i,:) = SimOutput(70,:);
Vcell_10_EL(i,:) = SimOutput(71,:);
PE_in_EL(i,:) = SimOutput(72,:);
H2_gen_1_EL(i,:) = SimOutput(73,:);
H2_gen_2_EL(i,:) = SimOutput(74,:);
H2_gen_3_EL(i,:) = SimOutput(75,:);
H2_gen_4_EL(i,:) = SimOutput(76,:);
H2_gen_5_EL(i,:) = SimOutput(77,:);
H2_gen_6_EL(i,:) = SimOutput(78,:);
```

```
    H2_gen_7_EL(i,:) = SimOutput(79,:);
    H2_gen_8_EL(i,:) = SimOutput(80,:);
    H2_gen_9_EL(i,:) = SimOutput(81,:);
    H2_gen_10_EL(i,:) = SimOutput(82,:);
    H2_diff_1_EL(i,:) = SimOutput(83,:);
    H2_diff_2_EL(i,:) = SimOutput(84,:);
    H2_diff_3_EL(i,:) = SimOutput(85,:);
    H2_diff_4_EL(i,:) = SimOutput(86,:);
    H2_diff_5_EL(i,:) = SimOutput(87,:);
    H2_diff_6_EL(i,:) = SimOutput(88,:);
    H2_diff_7_EL(i,:) = SimOutput(89,:);
    H2_diff_8_EL(i,:) = SimOutput(90,:);
    H2_diff_9_EL(i,:) = SimOutput(91,:);
    H2_diff_10_EL(i,:) = SimOutput(92,:);
    O2_gen_1_EL(i,:) = SimOutput(93,:);
    O2_gen_2_EL(i,:) = SimOutput(94,:);
    O2_gen_3_EL(i,:) = SimOutput(95,:);
    O2_gen_4_EL(i,:) = SimOutput(96,:);
    O2_gen_5_EL(i,:) = SimOutput(97,:);
    O2_gen_6_EL(i,:) = SimOutput(98,:);
    O2_gen_7_EL(i,:) = SimOutput(99,:);
    O2_gen_8_EL(i,:) = SimOutput(100,:);
    O2_gen_9_EL(i,:) = SimOutput(101,:);
    O2_gen_10_EL(i,:) = SimOutput(102,:);
    P_H2O_sat_EL(i,:) = SimOutput(103,:);
    AC_curt_EL(i) = SimOutput(104,end);
    %Convert mol/s to kg/sec
    H2Flowrate_EL(i,:) = H2Flowrate_EL(i,:).*(2.016/1000);
    %Convert W-hr to kW-hr
    ACPowerConsumption_EL(i) = ACPowerConsumption_EL(i)*(1/(1000));
    AC_curt_EL(i) = AC_curt_EL(i)*(1/(1000000)); %to MW-hr
    Stack1PowerConsumption_EL(i) = Stack1PowerConsumption_EL(i).*(1/(1000));
    Stack2PowerConsumption_EL(i) = Stack2PowerConsumption_EL(i).*(1/(1000));
    Stack3PowerConsumption_EL(i) = Stack3PowerConsumption_EL(i).*(1/(1000));
    Stack4PowerConsumption_EL(i) = Stack4PowerConsumption_EL(i).*(1/(1000));
    Stack5PowerConsumption_EL(i) = Stack5PowerConsumption_EL(i).*(1/(1000));
    Stack6PowerConsumption_EL(i) = Stack6PowerConsumption_EL(i).*(1/(1000));
    Stack7PowerConsumption_EL(i) = Stack7PowerConsumption_EL(i).*(1/(1000));
    Stack8PowerConsumption_EL(i) = Stack8PowerConsumption_EL(i).*(1/(1000));
    Stack9PowerConsumption_EL(i) = Stack9PowerConsumption_EL(i).*(1/(1000));
    Stack10PowerConsumption_EL(i) = Stack10PowerConsumption_EL(i).*(1/(1000));
    CompressorPowerConsumption_EL(i) = CompressorPowerConsumption_EL(i).*(1/(1000));
    CoolingPowerConsumption_EL(i) = CoolingPowerConsumption_EL(i).*(1/(1000));
    PE_loss_EL(i) = PE_loss_EL(i)*(1/(1000));
    %Convert mol to kg
    HydrogenProduced_EL(i,:) = HydrogenProduced_EL(i,:).*(2.016/1000);
    HydrogenLost_kg_EL(i,:) = HydrogenLost_EL(i,:).*(2.016/1000);
    H2_gen_kg_EL(i,:) = H2_gen_EL(i,:).*(2.016/1000);
    %System Specific Power Consumption Method 1
    SEC_EL(i) =
(ACPowerConsumption_EL(i)+CompressorPowerConsumption_EL(i)+CoolingPowerConsumption_EL
(i))/HydrogenProduced_EL(i,end);
    Spec_H2Loss_kg_EL(i) = HydrogenLost_kg_EL(i,end)/H2_gen_kg_EL(i,end);
    perc_Stack1Power_EL(i) =
(Stack1PowerConsumption_EL(i)/HydrogenProduced_EL(i,end))/SEC_EL(i);
```

```
    perc_Stack2Power_EL(i) =
(Stack2PowerConsumption_EL(i)/HydrogenProduced_EL(i,end))/SEC_EL(i);
    perc_Stack3Power_EL(i) =
(Stack3PowerConsumption_EL(i)/HydrogenProduced_EL(i,end))/SEC_EL(i);
    perc_Stack4Power_EL(i) =
(Stack4PowerConsumption_EL(i)/HydrogenProduced_EL(i,end))/SEC_EL(i);
    perc_PowerElectronics_EL(i) =
(PE_loss_EL(i)/HydrogenProduced_EL(i,end))/SEC_EL(i);
    perc_CompPower_EL(i) =
(CompressorPowerConsumption_EL(i)/HydrogenProduced_EL(i,end))/SEC_EL(i);
    perc_CoolPower_EL(i) =
(CoolingPowerConsumption_EL(i)/HydrogenProduced_EL(i,end))/SEC_EL(i);
    eta_total_EL(i) = (1/SEC_EL(i))*141.88/3.6;
    % Calculate the hydrogen molefraction in the anode (volume fraction)
    O2_gen_1_EL(i,O2_gen_1_EL(i,:)<600) = 0;
    O2_gen_2_EL(i,O2_gen_2_EL(i,:)<600) = 0;
    O2_gen_3_EL(i,O2_gen_3_EL(i,:)<600) = 0;
    O2_gen_4_EL(i,O2_gen_4_EL(i,:)<600) = 0;
    O2_gen_5_EL(i,O2_gen_5_EL(i,:)<600) = 0;
    O2_gen_6_EL(i,O2_gen_6_EL(i,:)<600) = 0;
    O2_gen_7_EL(i,O2_gen_7_EL(i,:)<600) = 0;
    O2_gen_8_EL(i,O2_gen_8_EL(i,:)<600) = 0;
    O2_gen_9_EL(i,O2_gen_9_EL(i,:)<600) = 0;
    O2_gen_10_EL(i,O2_gen_10_EL(i,:)<600) = 0;
    V_H2_1_EL(i,O2_gen_1_EL(i,:)>0) =
(abs(H2_diff_1_EL(i,O2_gen_1_EL(i,:)>0))./(abs(H2_diff_1_EL(i,O2_gen_1_EL(i,:)>0))+O2
_gen_1_EL(i,O2_gen_1_EL(i,:)>0)))*(1-P_H2O_sat_EL(i,end)/101325);
    V_H2_2_EL(i,O2_gen_2_EL(i,:)>0) =
(abs(H2_diff_2_EL(i,O2_gen_2_EL(i,:)>0))./(abs(H2_diff_2_EL(i,O2_gen_2_EL(i,:)>0))+O2
_gen_2_EL(i,O2_gen_2_EL(i,:)>0)))*(1-P_H2O_sat_EL(i,end)/101325);
    V_H2_3_EL(i,O2_gen_3_EL(i,:)>0) =
(abs(H2_diff_3_EL(i,O2_gen_3_EL(i,:)>0))./(abs(H2_diff_3_EL(i,O2_gen_3_EL(i,:)>0))+O2
_gen_3_EL(i,O2_gen_3_EL(i,:)>0)))*(1-P_H2O_sat_EL(i,end)/101325);
    V_H2_4_EL(i,O2_gen_4_EL(i,:)>0) =
(abs(H2_diff_4_EL(i,O2_gen_4_EL(i,:)>0))./(abs(H2_diff_4_EL(i,O2_gen_4_EL(i,:)>0))+O2
_gen_4_EL(i,O2_gen_4_EL(i,:)>0)))*(1-P_H2O_sat_EL(i,end)/101325);
    V_H2_5_EL(i,O2_gen_5_EL(i,:)>0) =
(abs(H2_diff_5_EL(i,O2_gen_5_EL(i,:)>0))./(abs(H2_diff_5_EL(i,O2_gen_5_EL(i,:)>0))+O2
_gen_5_EL(i,O2_gen_5_EL(i,:)>0)))*(1-P_H2O_sat_EL(i,end)/101325);
    V_H2_6_EL(i,O2_gen_6_EL(i,:)>0) =
(abs(H2_diff_6_EL(i,O2_gen_6_EL(i,:)>0))./(abs(H2_diff_6_EL(i,O2_gen_6_EL(i,:)>0))+O2
_gen_6_EL(i,O2_gen_6_EL(i,:)>0)))*(1-P_H2O_sat_EL(i,end)/101325);
    V_H2_7_EL(i,O2_gen_7_EL(i,:)>0) =
(abs(H2_diff_7_EL(i,O2_gen_7_EL(i,:)>0))./(abs(H2_diff_7_EL(i,O2_gen_7_EL(i,:)>0))+O2
_gen_7_EL(i,O2_gen_7_EL(i,:)>0)))*(1-P_H2O_sat_EL(i,end)/101325);
    V_H2_8_EL(i,O2_gen_8_EL(i,:)>0) =
(abs(H2_diff_8_EL(i,O2_gen_8_EL(i,:)>0))./(abs(H2_diff_8_EL(i,O2_gen_8_EL(i,:)>0))+O2
_gen_8_EL(i,O2_gen_8_EL(i,:)>0)))*(1-P_H2O_sat_EL(i,end)/101325);
    V_H2_9_EL(i,O2_gen_9_EL(i,:)>0) =
(abs(H2_diff_9_EL(i,O2_gen_9_EL(i,:)>0))./(abs(H2_diff_9_EL(i,O2_gen_9_EL(i,:)>0))+O2
_gen_9_EL(i,O2_gen_9_EL(i,:)>0)))*(1-P_H2O_sat_EL(i,end)/101325);
    V_H2_10_EL(i,O2_gen_10_EL(i,:)>0) =
(abs(H2_diff_10_EL(i,O2_gen_10_EL(i,:)>0))./(abs(H2_diff_10_EL(i,O2_gen_10_EL(i,:)>0)
)+O2_gen_10_EL(i,O2_gen_10_EL(i,:)>0)))*(1-P_H2O_sat_EL(i,end)/101325);
    V_H2_1_EL(i,O2_gen_1_EL(i,:)==0) = 0;
```

```
    V_H2_2_EL(i,O2_gen_2_EL(i,:)==0) = 0;
    V_H2_3_EL(i,O2_gen_3_EL(i,:)==0) = 0;
    V_H2_4_EL(i,O2_gen_4_EL(i,:)==0) = 0;
    V_H2_5_EL(i,O2_gen_5_EL(i,:)==0) = 0;
    V_H2_6_EL(i,O2_gen_6_EL(i,:)==0) = 0;
    V_H2_7_EL(i,O2_gen_7_EL(i,:)==0) = 0;
    V_H2_8_EL(i,O2_gen_8_EL(i,:)==0) = 0;
    V_H2_9_EL(i,O2_gen_9_EL(i,:)==0) = 0;
    V_H2_10_EL(i,O2_gen_10_EL(i,:)==0) = 0;
end
save_system("GHGS_MSA_v5")
toc
%% Clean up variables
% removing false efficiencies
eta_cell_1_SL(eta_cell_1_SL==1) = 0;
eta_cell_2_SL(eta_cell_2_SL==1) = 0;
eta_cell_3_SL(eta_cell_3_SL==1) = 0;
eta_cell_4_SL(eta_cell_4_SL==1) = 0;
eta_cell_5_SL(eta_cell_5_SL==1) = 0;
eta_cell_6_SL(eta_cell_6_SL==1) = 0;
eta_cell_7_SL(eta_cell_7_SL==1) = 0;
eta_cell_8_SL(eta_cell_8_SL==1) = 0;
eta_cell_9_SL(eta_cell_9_SL==1) = 0;
eta_cell_10_SL(eta_cell_10_SL==1) = 0;
eta_cell_1_EL(eta_cell_1_EL==1) = 0;
eta_cell_2_EL(eta_cell_2_EL==1) = 0;
eta_cell_3_EL(eta_cell_3_EL==1) = 0;
eta_cell_4_EL(eta_cell_4_EL==1) = 0;
eta_cell_5_EL(eta_cell_5_EL==1) = 0;
eta_cell_6_EL(eta_cell_6_EL==1) = 0;
eta_cell_7_EL(eta_cell_7_EL==1) = 0;
eta_cell_8_EL(eta_cell_8_EL==1) = 0;
eta_cell_9_EL(eta_cell_9_EL==1) = 0;
eta_cell_10_EL(eta_cell_10_EL==1) = 0;
for j=1:length(MinStackSetpoint)
    avg_eta_cell_EL(1,j) = [mean(eta_cell_1_EL(j,eta_cell_1_EL(j,:)>0))];
    avg_eta_cell_EL(2,j) = [mean(eta_cell_2_EL(j,eta_cell_2_EL(j,:)>0))];
    avg_eta_cell_EL(3,j) = [mean(eta_cell_3_EL(j,eta_cell_3_EL(j,:)>0))];
    avg_eta_cell_EL(4,j) = [mean(eta_cell_4_EL(j,eta_cell_4_EL(j,:)>0))];
    avg_eta_cell_EL(5,j) = [mean(eta_cell_5_EL(j,eta_cell_5_EL(j,:)>0))];
    avg_eta_cell_EL(6,j) = [mean(eta_cell_6_EL(j,eta_cell_6_EL(j,:)>0))];
    avg_eta_cell_EL(7,j) = [mean(eta_cell_7_EL(j,eta_cell_7_EL(j,:)>0))];
    avg_eta_cell_EL(8,j) = [mean(eta_cell_8_EL(j,eta_cell_8_EL(j,:)>0))];
    avg_eta_cell_EL(9,j) = [mean(eta_cell_9_EL(j,eta_cell_9_EL(j,:)>0))];
    avg_eta_cell_EL(10,j) = [mean(eta_cell_10_EL(j,eta_cell_10_EL(j,:)>0))];
    avg_eta_cell_SL(1,j) = [mean(eta_cell_1_SL(j,eta_cell_1_SL(j,:)>0))];
    avg_eta_cell_SL(2,j) = [mean(eta_cell_2_SL(j,eta_cell_2_SL(j,:)>0))];
    avg_eta_cell_SL(3,j) = [mean(eta_cell_3_SL(j,eta_cell_3_SL(j,:)>0))];
    avg_eta_cell_SL(4,j) = [mean(eta_cell_4_SL(j,eta_cell_4_SL(j,:)>0))];
    avg_eta_cell_SL(5,j) = [mean(eta_cell_5_SL(j,eta_cell_5_SL(j,:)>0))];
    avg_eta_cell_SL(6,j) = [mean(eta_cell_6_SL(j,eta_cell_6_SL(j,:)>0))];
    avg_eta_cell_SL(7,j) = [mean(eta_cell_7_SL(j,eta_cell_7_SL(j,:)>0))];
    avg_eta_cell_SL(8,j) = [mean(eta_cell_8_SL(j,eta_cell_8_SL(j,:)>0))];
    avg_eta_cell_SL(9,j) = [mean(eta_cell_9_SL(j,eta_cell_9_SL(j,:)>0))];
    avg_eta_cell_SL(10,j) = [mean(eta_cell_10_SL(j,eta_cell_10_SL(j,:)>0))];
```

```
end
%% Verify Model Results
for j=1:length(MinStackSetpoint)
    avg_stack_load_EL(1,j) = [mean(Stack1Power_EL(j,Stack1Power_EL(j,:)>0))]/(1e6);
    avg_stack_load_EL(2,j) = [mean(Stack2Power_EL(j,Stack2Power_EL(j,:)>0))]/(1e6);
    avg_stack_load_EL(3,j) = [mean(Stack3Power_EL(j,Stack3Power_EL(j,:)>0))]/(1e6);
    avg_stack_load_EL(4,j) = [mean(Stack4Power_EL(j,Stack4Power_EL(j,:)>0))]/(1e6);
    avg_stack_load_EL(5,j) = [mean(Stack5Power_EL(j,Stack5Power_EL(j,:)>0))]/(1e6);
    avg_stack_load_EL(6,j) = [mean(Stack6Power_EL(j,Stack6Power_EL(j,:)>0))]/(1e6);
    avg_stack_load_EL(7,j) = [mean(Stack7Power_EL(j,Stack7Power_EL(j,:)>0))]/(1e6);
    avg_stack_load_EL(8,j) = [mean(Stack8Power_EL(j,Stack8Power_EL(j,:)>0))]/(1e6);
    avg_stack_load_EL(9,j) = [mean(Stack9Power_EL(j,Stack9Power_EL(j,:)>0))]/(1e6);
    avg_stack_load_EL(10,j) =
[mean(Stack10Power_EL(j,Stack10Power_EL(j,:)>0))]/(1e6);
    avg_overall_stack_load_EL(j) = mean([Stack1Power_EL(j,:) Stack2Power_EL(j,:)
Stack3Power_EL(j,:) Stack4Power_EL(j,:) Stack5Power_EL(j,:) Stack6Power_EL(j,:)
Stack7Power_EL(j,:) Stack8Power_EL(j,:) Stack9Power_EL(j,:)
Stack10Power_EL(j,:)])/(1e6);
    maximum_stack_load_EL(1,j) = [max(Stack1Power_EL(j,:))]/(1e6);
    maximum_stack_load_EL(2,j) = [max(Stack2Power_EL(j,:))]/(1e6);
    maximum_stack_load_EL(3,j) = [max(Stack3Power_EL(j,:))]/(1e6);
    maximum_stack_load_EL(4,j) = [max(Stack4Power_EL(j,:))]/(1e6);
    maximum_stack_load_EL(5,j) = [max(Stack5Power_EL(j,:))]/(1e6);
    maximum_stack_load_EL(6,j) = [max(Stack6Power_EL(j,:))]/(1e6);
    maximum_stack_load_EL(7,j) = [max(Stack7Power_EL(j,:))]/(1e6);
    maximum_stack_load_EL(8,j) = [max(Stack8Power_EL(j,:))]/(1e6);
    maximum_stack_load_EL(9,j) = [max(Stack9Power_EL(j,:))]/(1e6);
    maximum_stack_load_EL(10,j) = [max(Stack10Power_EL(j,:))]/(1e6);
    minimum_stack_load_EL(1,j) =
[min(Stack1Power_EL(j,Stack1Power_EL(j,:)>0))]/(1e6);
    minimum_stack_load_EL(2,j) =
[min(Stack2Power_EL(j,Stack2Power_EL(j,:)>0))]/(1e6);
    minimum_stack_load_EL(3,j) =
[min(Stack3Power_EL(j,Stack3Power_EL(j,:)>0))]/(1e6);
    minimum_stack_load_EL(4,j) =
[min(Stack4Power_EL(j,Stack4Power_EL(j,:)>0))]/(1e6);
    minimum_stack_load_EL(5,j) =
[min(Stack5Power_EL(j,Stack5Power_EL(j,:)>0))]/(1e6);
    minimum_stack_load_EL(6,j) =
[min(Stack6Power_EL(j,Stack6Power_EL(j,:)>0))]/(1e6);
    minimum_stack_load_EL(7,j) =
[min(Stack7Power_EL(j,Stack7Power_EL(j,:)>0))]/(1e6);
    minimum_stack_load_EL(8,j) =
[min(Stack8Power_EL(j,Stack8Power_EL(j,:)>0))]/(1e6);
    minimum_stack_load_EL(9,j) =
[min(Stack9Power_EL(j,Stack9Power_EL(j,:)>0))]/(1e6);
    minimum_stack_load_EL(10,j) =
[min(Stack10Power_EL(j,Stack10Power_EL(j,:)>0))]/(1e6);
    max_an_H2_EL(1,j) = [max(V_H2_1_EL(j,:))];
    max_an_H2_EL(2,j) = [max(V_H2_2_EL(j,:))];
    max_an_H2_EL(3,j) = [max(V_H2_3_EL(j,:))];
    max_an_H2_EL(4,j) = [max(V_H2_4_EL(j,:))];
    max_an_H2_EL(5,j) = [max(V_H2_5_EL(j,:))];
    max_an_H2_EL(6,j) = [max(V_H2_6_EL(j,:))];
    max_an_H2_EL(7,j) = [max(V_H2_7_EL(j,:))];
```

```
    max_an_H2_EL(8,j) = [max(V_H2_8_EL(j,:))];
    max_an_H2_EL(9,j) = [max(V_H2_9_EL(j,:))];
    max_an_H2_EL(10,j) = [max(V_H2_10_EL(j,:))];
    avg_stack_load_SL(1,j) = [mean(Stack1Power_SL(j,Stack1Power_SL(j,:)>0))]/(1e6);
    avg_stack_load_SL(2,j) = [mean(Stack2Power_SL(j,Stack2Power_SL(j,:)>0))]/(1e6);
    avg_stack_load_SL(3,j) = [mean(Stack3Power_SL(j,Stack3Power_SL(j,:)>0))]/(1e6);
    avg_stack_load_SL(4,j) = [mean(Stack4Power_SL(j,Stack4Power_SL(j,:)>0))]/(1e6);
    avg_stack_load_SL(5,j) = [mean(Stack5Power_SL(j,Stack5Power_SL(j,:)>0))]/(1e6);
    avg_stack_load_SL(6,j) = [mean(Stack6Power_SL(j,Stack6Power_SL(j,:)>0))]/(1e6);
    avg_stack_load_SL(7,j) = [mean(Stack7Power_SL(j,Stack7Power_SL(j,:)>0))]/(1e6);
    avg_stack_load_SL(8,j) = [mean(Stack8Power_SL(j,Stack8Power_SL(j,:)>0))]/(1e6);
    avg_stack_load_SL(9,j) = [mean(Stack9Power_SL(j,Stack9Power_SL(j,:)>0))]/(1e6);
    avg_stack_load_SL(10,j) =
[mean(Stack10Power_SL(j,Stack10Power_SL(j,:)>0))]/(1e6);
    avg_overall_stack_load_SL(j) = mean([Stack1Power_SL(j,:) Stack2Power_SL(j,:)
Stack3Power_SL(j,:) Stack4Power_SL(j,:) Stack5Power_SL(j,:) Stack6Power_SL(j,:)
Stack7Power_SL(j,:) Stack8Power_SL(j,:) Stack9Power_SL(j,:)
Stack10Power_SL(j,:)])/(1e6);
    maximum_stack_load_SL(1,j) = [max(Stack1Power_SL(j,:))]/(1e6);
    maximum_stack_load_SL(2,j) = [max(Stack2Power_SL(j,:))]/(1e6);
    maximum_stack_load_SL(3,j) = [max(Stack3Power_SL(j,:))]/(1e6);
    maximum_stack_load_SL(4,j) = [max(Stack4Power_SL(j,:))]/(1e6);
    maximum_stack_load_SL(5,j) = [max(Stack5Power_SL(j,:))]/(1e6);
    maximum_stack_load_SL(6,j) = [max(Stack6Power_SL(j,:))]/(1e6);
    maximum_stack_load_SL(7,j) = [max(Stack7Power_SL(j,:))]/(1e6);
    maximum_stack_load_SL(8,j) = [max(Stack8Power_SL(j,:))]/(1e6);
    maximum_stack_load_SL(9,j) = [max(Stack9Power_SL(j,:))]/(1e6);
    maximum_stack_load_SL(10,j) = [max(Stack10Power_SL(j,:))]/(1e6);
    minimum_stack_load_SL(1,j) =
[min(Stack1Power_SL(j,Stack1Power_SL(j,:)>0))]/(1e6);
    minimum_stack_load_SL(2,j) =
[min(Stack2Power_SL(j,Stack2Power_SL(j,:)>0))]/(1e6);
    minimum_stack_load_SL(3,j) =
[min(Stack3Power_SL(j,Stack3Power_SL(j,:)>0))]/(1e6);
    minimum_stack_load_SL(4,j) =
[min(Stack4Power_SL(j,Stack4Power_SL(j,:)>0))]/(1e6);
    minimum_stack_load_SL(5,j) =
[min(Stack5Power_SL(j,Stack5Power_SL(j,:)>0))]/(1e6);
    minimum_stack_load_SL(6,j) =
[min(Stack6Power_SL(j,Stack6Power_SL(j,:)>0))]/(1e6);
    minimum_stack_load_SL(7,j) =
[min(Stack7Power_SL(j,Stack7Power_SL(j,:)>0))]/(1e6);
    minimum_stack_load_SL(8,j) =
[min(Stack8Power_SL(j,Stack8Power_SL(j,:)>0))]/(1e6);
    minimum_stack_load_SL(9,j) =
[min(Stack9Power_SL(j,Stack9Power_SL(j,:)>0))]/(1e6);
    minimum_stack_load_SL(10,j) =
[min(Stack10Power_SL(j,Stack10Power_SL(j,:)>0))]/(1e6);
    max_an_H2_SL(1,j) = [max(V_H2_1_SL(j,:))];
    max_an_H2_SL(2,j) = [max(V_H2_2_SL(j,:))];
    max_an_H2_SL(3,j) = [max(V_H2_3_SL(j,:))];
    max_an_H2_SL(4,j) = [max(V_H2_4_SL(j,:))];
    max_an_H2_SL(5,j) = [max(V_H2_5_SL(j,:))];
    max_an_H2_SL(6,j) = [max(V_H2_6_SL(j,:))];
    max_an_H2_SL(7,j) = [max(V_H2_7_SL(j,:))];
```

```
    max_an_H2_SL(8,j) = [max(V_H2_8_SL(j,:))];
    max_an_H2_SL(9,j) = [max(V_H2_9_SL(j,:))];
    max_an_H2_SL(10,j) = [max(V_H2_10_SL(j,:))];
end
checkmin_SL = (minimum_stack_load_SL < 0.125);
checkmin_EL = (minimum_stack_load_EL < 0.125);
checkminset = minimum_stack_load_EL < (DC_Rating*MinStackSetpoint/(1e6));
checkmax_SL = (abs(maximum_stack_load_SL-1.25) > 0.0001);
checkmax_EL = (abs(maximum_stack_load_EL-1.25) > 0.0001);
checkmax_H2_an_SL = max_an_H2_SL > 0.01;
checkmax_H2_an_EL = max_an_H2_EL > 0.01;
if max(checkmin_SL) ==1
    warning("At least one electrolyzer stack in the SL scheme drops below 10% of it's
rated power")
end
if max(checkmin_EL) ==1
    warning("At least one electrolyzer stack in the EL scheme drops below 10% of it's
rated power")
end
if max(checkminset(2:10,:)) ==1
    warning("At least one electrolyzer stack in the EL scheme drops below the
selected minimum of it's rated power")
end
if max(max(checkmax_SL)) ==1
    warning("At least one electrolyzer stack in the SL scheme operates above 100.1%
of it's rated power")
end
if max(max(checkmax_EL)) ==1
    warning("At least one electrolyzer stack in the EL scheme operates above 100.1%
of it's rated power")
end
if max(max(checkmax_H2_an_SL)) ==1
    warning("At least one electrolyzer stack in the SL scheme has greater than 25%
LEL H2 in the anode")
end
if max(max(checkmax_H2_an_EL)) ==1
    warning("At least one electrolyzer stack in the SL scheme has greater than 25%
LEL H2 in the anode")
end
%% Curtailed RE with different schemes
for g=1:length(ex_RE)
curt_SL = ex_RE(g)-(OF1_SL(:,g));
end
%% Solve for number of shut down cylces
shutdowns1_SL = [];
shutdowns2_SL = [];
shutdowns3_SL = [];
shutdowns4_SL = [];
shutdowns5_SL = [];
shutdowns6_SL = [];
shutdowns7_SL = [];
shutdowns8_SL = [];
shutdowns9_SL = [];
shutdowns10_SL = [];
shutdowns1_EL = [];
```

```
shutdowns2_EL = [];
shutdowns3_EL = [];
shutdowns4_EL = [];
shutdowns5_EL = [];
shutdowns6_EL = [];
shutdowns7_EL = [];
shutdowns8_EL = [];
shutdowns9_EL = [];
shutdowns10_EL = [];
for j=1:length(MinStackSetpoint)
    for i=2:length(ex_RE)
        if (OF1_SL(j,i-1)>0) && (OF1_SL(j,i)==0)
            shutdowns1_SL(j,i) = 1;
        else
            shutdowns1_SL(j,i) = 0;
        end
        if (OF2_SL(j,i-1)>0) && (OF2_SL(j,i)==0)
            shutdowns2_SL(j,i) = 1;
        else
            shutdowns2_SL(j,i) = 0;
        end
        if (OF3_SL(j,i-1)>0) && (OF3_SL(j,i)==0)
            shutdowns3_SL(j,i) = 1;
        else
            shutdowns3_SL(j,i) = 0;
        end
        if (OF4_SL(j,i-1)>0) && (OF4_SL(j,i)==0)
            shutdowns4_SL(j,i) = 1;
        else
            shutdowns4_SL(j,i) = 0;
        end
        if (OF5_SL(j,i-1)>0) && (OF5_SL(j,i)==0)
            shutdowns5_SL(j,i) = 1;
        else
            shutdowns5_SL(j,i) = 0;
        end
        if (OF6_SL(j,i-1)>0) && (OF6_SL(j,i)==0)
            shutdowns6_SL(j,i) = 1;
        else
            shutdowns6_SL(j,i) = 0;
        end
        if (OF7_SL(j,i-1)>0) && (OF7_SL(j,i)==0)
            shutdowns7_SL(j,i) = 1;
        else
            shutdowns7_SL(j,i) = 0;
        end
        if (OF8_SL(j,i-1)>0) && (OF8_SL(j,i)==0)
            shutdowns8_SL(j,i) = 1;
        else
            shutdowns8_SL(j,i) = 0;
        end
        if (OF9_SL(j,i-1)>0) && (OF9_SL(j,i)==0)
            shutdowns9_SL(j,i) = 1;
        else
            shutdowns9_SL(j,i) = 0;
```

```
end
if (OF10_SL(j,i-1)>0) && (OF10_SL(j,i)==0)
    shutdowns10_SL(j,i) = 1;
else
    shutdowns10_SL(j,i) = 0;
end
if (OF1_EL(j,i-1)>0) && (OF1_EL(j,i)==0)
    shutdowns1_EL(j,i) = 1;
else
    shutdowns1_EL(j,i) = 0;
end
if (OF2_EL(j,i-1)>0) && (OF2_EL(j,i)==0)
    shutdowns2_EL(j,i) = 1;
else
    shutdowns2_EL(j,i) = 0;
end
if (OF3_EL(j,i-1)>0) && (OF3_EL(j,i)==0)
    shutdowns3_EL(j,i) = 1;
else
    shutdowns3_EL(j,i) = 0;
end
if (OF4_EL(j,i-1)>0) && (OF4_EL(j,i)==0)
    shutdowns4_EL(j,i) = 1;
else
    shutdowns4_EL(j,i) = 0;
end
if (OF5_EL(j,i-1)>0) && (OF5_EL(j,i)==0)
    shutdowns5_EL(j,i) = 1;
else
    shutdowns5_EL(j,i) = 0;
end
if (OF6_EL(j,i-1)>0) && (OF6_EL(j,i)==0)
    shutdowns6_EL(j,i) = 1;
else
    shutdowns6_EL(j,i) = 0;
end
if (OF7_EL(j,i-1)>0) && (OF7_EL(j,i)==0)
    shutdowns7_EL(j,i) = 1;
else
    shutdowns7_EL(j,i) = 0;
end
if (OF8_EL(j,i-1)>0) && (OF8_EL(j,i)==0)
    shutdowns8_EL(j,i) = 1;
else
    shutdowns8_EL(j,i) = 0;
end
if (OF9_EL(j,i-1)>0) && (OF9_EL(j,i)==0)
    shutdowns9_EL(j,i) = 1;
else
    shutdowns9_EL(j,i) = 0;
end
if (OF10_EL(j,i-1)>0) && (OF10_EL(j,i)==0)
    shutdowns10_EL(j,i) = 1;
else
    shutdowns10_EL(j,i) = 0;
```

```
        end
    end
end
for j=1:length(MinStackSetpoint)
    num_shutdowns1_SL(j) = sum(shutdowns1_SL(j,:)==1);
    num_shutdowns2_SL(j) = sum(shutdowns2_SL(j,:)==1);
    num_shutdowns3_SL(j) = sum(shutdowns3_SL(j,:)==1);
    num_shutdowns4_SL(j) = sum(shutdowns4_SL(j,:)==1);
    num_shutdowns5_SL(j) = sum(shutdowns5_SL(j,:)==1);
    num_shutdowns6_SL(j) = sum(shutdowns6_SL(j,:)==1);
    num_shutdowns7_SL(j) = sum(shutdowns7_SL(j,:)==1);
    num_shutdowns8_SL(j) = sum(shutdowns8_SL(j,:)==1);
    num_shutdowns9_SL(j) = sum(shutdowns9_SL(j,:)==1);
    num_shutdowns10_SL(j) = sum(shutdowns10_SL(j,:)==1);
    num_shutdowns1_EL(j) = sum(shutdowns1_EL(j,:)==1);
    num_shutdowns2_EL(j) = sum(shutdowns2_EL(j,:)==1);
    num_shutdowns3_EL(j) = sum(shutdowns3_EL(j,:)==1);
    num_shutdowns4_EL(j) = sum(shutdowns4_EL(j,:)==1);
    num_shutdowns5_EL(j) = sum(shutdowns5_EL(j,:)==1);
    num_shutdowns6_EL(j) = sum(shutdowns6_EL(j,:)==1);
    num_shutdowns7_EL(j) = sum(shutdowns7_EL(j,:)==1);
    num_shutdowns8_EL(j) = sum(shutdowns8_EL(j,:)==1);
    num_shutdowns9_EL(j) = sum(shutdowns9_EL(j,:)==1);
    num_shutdowns10_EL(j) = sum(shutdowns10_EL(j,:)==1);
end
tot_shutdowns_SL =
num_shutdowns1_SL+num_shutdowns2_SL+num_shutdowns3_SL+num_shutdowns4_SL+num_shutdowns
5_SL+num_shutdowns6_SL+num_shutdowns7_SL+num_shutdowns8_SL+num_shutdowns9_SL+num_shut
downs10_SL;
tot_shutdowns_EL =
num_shutdowns1_EL+num_shutdowns2_EL+num_shutdowns3_EL+num_shutdowns4_EL+num_shutdowns
5_EL+num_shutdowns6_EL+num_shutdowns7_EL+num_shutdowns8_EL+num_shutdowns9_EL+num_shut
downs10_EL;
%% Sweep Electrolyzer Rating
% Select Loading Strategy
warning('Please switch loading scheme in Simulink model for the scaling study, then
press any key to continue.')
pause
% Set how many electrolyzers will operate in the system
OF_scale = [1 1 1 1 1 1 1 1 1 1;1 1 1 1 1 1 1 1 1 0;1 1 1 1 1 1 1 1 0 0;1 1 1 1 1 1 1
0 0 0;1 1 1 1 1 1 0 0 0 0;1 1 1 1 1 0 0 0 0 0;1 1 1 1 0 0 0 0 0 0;1 1 1 0 0 0 0 0 0
0;1 1 0 0 0 0 0 0 0 0;1 0 0 0 0 0 0 0 0 0]; % Each Row is a different scaling, ie
different number of stacks
% Scale down orifice diameter with corresponding number of stacks per
% system
scaled_ori = [0.00147757414966412 0.00140811480855985 0.00132710500401793
0.00123743611719269 0.00114547616361213 0.00104882748193785 0.000936068416233954
0.000810701020495850 0.000661814667245629 0.000468632325629515];
set_param('GHGS_MSA_v5/Power Electronics/Min Perc Load','value',num2str(0.1)); %Set
the minimum turndown range of the electrolyzer stacks
for i=1:10
    set_param('GHGS_MSA_v5/Power Electronics/Manual
Switch','sw',num2str(OF_scale(i,1))); %Set OF to follow loading scheme or
artificially off
```

```
    set_param('GHGS_MSA_v5/Power Electronics/Manual
Switch1','sw',num2str(OF_scale(i,2))); %Set OF to follow loading scheme or
artificially off
    set_param('GHGS_MSA_v5/Power Electronics/Manual
Switch2','sw',num2str(OF_scale(i,3))); %Set OF to follow loading scheme or
artificially off
    set_param('GHGS_MSA_v5/Power Electronics/Manual
Switch3','sw',num2str(OF_scale(i,4))); %Set OF to follow loading scheme or
artificially off
    set_param('GHGS_MSA_v5/Power Electronics/Manual
Switch4','sw',num2str(OF_scale(i,5))); %Set OF to follow loading scheme or
artificially off
    set_param('GHGS_MSA_v5/Power Electronics/Manual
Switch5','sw',num2str(OF_scale(i,6))); %Set OF to follow loading scheme or
artificially off
    set_param('GHGS_MSA_v5/Power Electronics/Manual
Switch6','sw',num2str(OF_scale(i,7))); %Set OF to follow loading scheme or
artificially off
    set_param('GHGS_MSA_v5/Power Electronics/Manual
Switch7','sw',num2str(OF_scale(i,8))); %Set OF to follow loading scheme or
artificially off
    set_param('GHGS_MSA_v5/Power Electronics/Manual
Switch8','sw',num2str(OF_scale(i,9))); %Set OF to follow loading scheme or
artificially off
    set_param('GHGS_MSA_v5/Power Electronics/Manual
Switch9','sw',num2str(OF_scale(i,10))); %Set OF to follow loading scheme or
artificially off
    set_param('GHGS_MSA_v5/PSA Dryer/D_o [m]','Value',num2str(scaled_ori(i)));
%Fitted scaling method for each stack system with lower faraday eff


sim('GHGS_MSA_v5.slx','StartTime',num2str(ERCOT_time(1)),'StopTime',num2str(ERCOT_tim
e(end)),'FixedStep','1');
    load('SimOutput.mat');
    Time_SS(i,:) = SimOutput(1,:); %Time in hours
    Stack1PowerConsumption_SS(i) = SimOutput(2,end);
    Stack2PowerConsumption_SS(i) = SimOutput(3,end);
    Stack3PowerConsumption_SS(i) = SimOutput(4,end);
    Stack4PowerConsumption_SS(i) = SimOutput(5,end);
    Stack5PowerConsumption_SS(i) = SimOutput(6,end);
    Stack6PowerConsumption_SS(i) = SimOutput(7,end);
    Stack7PowerConsumption_SS(i) = SimOutput(8,end);
    Stack8PowerConsumption_SS(i) = SimOutput(9,end);
    Stack9PowerConsumption_SS(i) = SimOutput(10,end);
    Stack10PowerConsumption_SS(i) = SimOutput(11,end);
    CompressorPowerConsumption_SS(i) = SimOutput(12,end);
    CoolingPowerConsumption_SS(i) = SimOutput(13,end);
    HydrogenProduced_SS(i,:) = SimOutput(14,:);
    HydrogenLost_SS(i,:) = SimOutput(15,:);
    Stack1Power_SS(i,:) = SimOutput(16,:);
    Stack2Power_SS(i,:) = SimOutput(17,:);
    Stack3Power_SS(i,:) = SimOutput(18,:);
    Stack4Power_SS(i,:) = SimOutput(19,:);
    Stack5Power_SS(i,:)= SimOutput(20,:);
    Stack6Power_SS(i,:) = SimOutput(21,:);
```

```
Stack7Power_SS(i,:) = SimOutput(22,:);
Stack8Power_SS(i,:) = SimOutput(23,:);
Stack9Power_SS(i,:) = SimOutput(24,:);
Stack10Power_SS(i,:) = SimOutput(25,:);
CompPower_SS(i,:) = SimOutput(26,:);
CoolPower_SS(i,:) = SimOutput(27,:);
H2Flowrate_SS(i,:) = SimOutput(28,:);
ACPowerConsumption_SS(i) = SimOutput(29,end);
PE_loss_SS(i) = SimOutput(30,end);
eta_cell_1_SS(i,:) = SimOutput(31,:);
eta_cell_2_SS(i,:) = SimOutput(32,:);
eta_cell_3_SS(i,:) = SimOutput(33,:);
eta_cell_4_SS(i,:) = SimOutput(34,:);
eta_cell_5_SS(i,:) = SimOutput(35,:);
eta_cell_6_SS(i,:) = SimOutput(36,:);
eta_cell_7_SS(i,:) = SimOutput(37,:);
eta_cell_8_SS(i,:) = SimOutput(38,:);
eta_cell_9_SS(i,:) = SimOutput(39,:);
eta_cell_10_SS(i,:) = SimOutput(40,:);
H2_gen_SS(i,:) = SimOutput(41,:);
i_1_SS(i,:) = SimOutput(42,:);
i_2_SS(i,:) = SimOutput(43,:);
i_3_SS(i,:) = SimOutput(44,:);
i_4_SS(i,:) = SimOutput(45,:);
i_5_SS(i,:) = SimOutput(46,:);
i_6_SS(i,:) = SimOutput(47,:);
i_7_SS(i,:) = SimOutput(48,:);
i_8_SS(i,:) = SimOutput(49,:);
i_9_SS(i,:) = SimOutput(50,:);
i_10_SS(i,:) = SimOutput(51,:);
OF1_SS(i,:) = SimOutput(52,:);
OF2_SS(i,:) = SimOutput(53,:);
OF3_SS(i,:) = SimOutput(54,:);
OF4_SS(i,:) = SimOutput(55,:);
OF5_SS(i,:) = SimOutput(56,:);
OF6_SS(i,:) = SimOutput(57,:);
OF7_SS(i,:) = SimOutput(58,:);
OF8_SS(i,:) = SimOutput(59,:);
OF9_SS(i,:) = SimOutput(60,:);
OF10_SS(i,:) = SimOutput(61,:);
Vcell_1_SS(i,:) = SimOutput(62,:);
Vcell_2_SS(i,:) = SimOutput(63,:);
Vcell_3_SS(i,:) = SimOutput(64,:);
Vcell_4_SS(i,:) = SimOutput(65,:);
Vcell_5_SS(i,:) = SimOutput(66,:);
Vcell_6_SS(i,:) = SimOutput(67,:);
Vcell_7_SS(i,:) = SimOutput(68,:);
Vcell_8_SS(i,:) = SimOutput(69,:);
Vcell_9_SS(i,:) = SimOutput(70,:);
Vcell_10_SS(i,:) = SimOutput(71,:);
PE_in_SS(i,:) = SimOutput(72,:);
H2_gen_1_SS(i,:) = SimOutput(73,:);
H2_gen_2_SS(i,:) = SimOutput(74,:);
H2_gen_3_SS(i,:) = SimOutput(75,:);
H2_gen_4_SS(i,:) = SimOutput(76,:);
```

```
    H2_gen_5_SS(i,:) = SimOutput(77,:);
    H2_gen_6_SS(i,:) = SimOutput(78,:);
    H2_gen_7_SS(i,:) = SimOutput(79,:);
    H2_gen_8_SS(i,:) = SimOutput(80,:);
    H2_gen_9_SS(i,:) = SimOutput(81,:);
    H2_gen_10_SS(i,:) = SimOutput(82,:);
    H2_diff_1_SS(i,:) = SimOutput(83,:);
    H2_diff_2_SS(i,:) = SimOutput(84,:);
    H2_diff_3_SS(i,:) = SimOutput(85,:);
    H2_diff_4_SS(i,:) = SimOutput(86,:);
    H2_diff_5_SS(i,:) = SimOutput(87,:);
    H2_diff_6_SS(i,:) = SimOutput(88,:);
    H2_diff_7_SS(i,:) = SimOutput(89,:);
    H2_diff_8_SS(i,:) = SimOutput(90,:);
    H2_diff_9_SS(i,:) = SimOutput(91,:);
    H2_diff_10_SS(i,:) = SimOutput(92,:);
    O2_gen_1_SS(i,:) = SimOutput(93,:);
    O2_gen_2_SS(i,:) = SimOutput(94,:);
    O2_gen_3_SS(i,:) = SimOutput(95,:);
    O2_gen_4_SS(i,:) = SimOutput(96,:);
    O2_gen_5_SS(i,:) = SimOutput(97,:);
    O2_gen_6_SS(i,:) = SimOutput(98,:);
    O2_gen_7_SS(i,:) = SimOutput(99,:);
    O2_gen_8_SS(i,:) = SimOutput(100,:);
    O2_gen_9_SS(i,:) = SimOutput(101,:);
    O2_gen_10_SS(i,:) = SimOutput(102,:);
    P_H2O_sat_SS(i,:) = SimOutput(103,:);
    AC_curt_SS(i) = SimOutput(104,end);
    %Convert mol/s to kg/sec
    H2Flowrate_SS(i,:) = H2Flowrate_SS(i,:).*(2.016/1000);
    %Convert W-hr to kW-hr
    sys_AC_cons_SS(i) =
trapz(Time_SS(i,:),ex_RE.*OF1_SS(i,:))+trapz(Time_SS(i,:),ex_RE.*OF2_SS(i,:))+trapz(T
ime_SS(i,:),ex_RE.*OF3_SS(i,:))+trapz(Time_SS(i,:),ex_RE.*OF4_SS(i,:))+trapz(Time_SS(
i,:),ex_RE.*OF5_SS(i,:))+trapz(Time_SS(i,:),ex_RE.*OF6_SS(i,:))+trapz(Time_SS(i,:),ex
_RE.*OF7_SS(i,:))+trapz(Time_SS(i,:),ex_RE.*OF8_SS(i,:))+trapz(Time_SS(i,:),ex_RE.*OF
9_SS(i,:))+trapz(Time_SS(i,:),ex_RE.*OF10_SS(i,:));
    sys_AC_cons_SS(i) = sys_AC_cons_SS(i)*(1000); %MW-hr to kW-hr
    ACPowerConsumption_SS(i) = ACPowerConsumption_SS(i)*(1/(1000)); %Total AC Power
Availible
    AC_curt_SS(i) = AC_curt_SS(i)*(1/(1000000)); %to MW-hr
    Stack1PowerConsumption_SS(i) = Stack1PowerConsumption_SS(i).*(1/(1000));
    Stack2PowerConsumption_SS(i) = Stack2PowerConsumption_SS(i).*(1/(1000));
    Stack3PowerConsumption_SS(i) = Stack3PowerConsumption_SS(i).*(1/(1000));
    Stack4PowerConsumption_SS(i) = Stack4PowerConsumption_SS(i).*(1/(1000));
    Stack5PowerConsumption_SS(i) = Stack5PowerConsumption_SS(i).*(1/(1000));
    Stack6PowerConsumption_SS(i) = Stack6PowerConsumption_SS(i).*(1/(1000));
    Stack7PowerConsumption_SS(i) = Stack7PowerConsumption_SS(i).*(1/(1000));
    Stack8PowerConsumption_SS(i) = Stack8PowerConsumption_SS(i).*(1/(1000));
    Stack9PowerConsumption_SS(i) = Stack9PowerConsumption_SS(i).*(1/(1000));
    Stack10PowerConsumption_SS(i) = Stack10PowerConsumption_SS(i).*(1/(1000));
    CompressorPowerConsumption_SS(i) = CompressorPowerConsumption_SS(i).*(1/(1000));
    CoolingPowerConsumption_SS(i) = CoolingPowerConsumption_SS(i).*(1/(1000));
    PE_loss_SS(i) = PE_loss_SS(i)*(1/(1000));
    %Convert mol to kg
```

```
    HydrogenProduced_SS(i,:) = HydrogenProduced_SS(i,:).*(2.016/1000);
    HydrogenLost_kg_SS(i,:) = HydrogenLost_SS(i,:).*(2.016/1000);
    H2_gen_kg_SS(i,:) = H2_gen_SS(i,:).*(2.016/1000);
    %System Specific Power Consumption
    SEC_SS1(i) =
(ACPowerConsumption_SS(i)+CompressorPowerConsumption_SS(i)+CoolingPowerConsumption_SS
(i))/HydrogenProduced_SS(i,end);
    SEC_SS2(i) =
(sys_AC_cons_SS(i)+CompressorPowerConsumption_SS(i)+CoolingPowerConsumption_SS(i))/Hy
drogenProduced_SS(i,end);
    Spec_H2Loss_kg_SS(i) = HydrogenLost_kg_SS(i,end)/H2_gen_kg_SS(i,end);
    perc_Stack1Power_SS(i) =
(Stack1PowerConsumption_SS(i)/HydrogenProduced_SS(i,end))/SEC_SS1(i);
    perc_Stack2Power_SS(i) =
(Stack2PowerConsumption_SS(i)/HydrogenProduced_SS(i,end))/SEC_SS1(i);
    perc_Stack3Power_SS(i) =
(Stack3PowerConsumption_SS(i)/HydrogenProduced_SS(i,end))/SEC_SS1(i);
    perc_Stack4Power_SS(i) =
(Stack4PowerConsumption_SS(i)/HydrogenProduced_SS(i,end))/SEC_SS1(i);
    perc_PowerElectronics_SS(i) =
(PE_loss_SS(i)/HydrogenProduced_SS(i,end))/SEC_SS1(i);
    perc_CompPower_SS(i) =
(CompressorPowerConsumption_SS(i)/HydrogenProduced_SS(i,end))/SEC_SS1(i);
    perc_CoolPower_SS(i) =
(CoolingPowerConsumption_SS(i)/HydrogenProduced_SS(i,end))/SEC_SS1(i);
    eta_total_SS1(i) = (1/SEC_SS1(i))*141.88/3.6;
    eta_total_SS2(i) = (1/SEC_SS2(i))*141.88/3.6;
    % Calculate the hydrogen molefraction in the anode (volume fraction)
    O2_gen_1_SS(i,O2_gen_1_SS(i,:)<600) = 0;
    O2_gen_2_SS(i,O2_gen_2_SS(i,:)<600) = 0;
    O2_gen_3_SS(i,O2_gen_3_SS(i,:)<600) = 0;
    O2_gen_4_SS(i,O2_gen_4_SS(i,:)<600) = 0;
    O2_gen_5_SS(i,O2_gen_5_SS(i,:)<600) = 0;
    O2_gen_6_SS(i,O2_gen_6_SS(i,:)<600) = 0;
    O2_gen_7_SS(i,O2_gen_7_SS(i,:)<600) = 0;
    O2_gen_8_SS(i,O2_gen_8_SS(i,:)<600) = 0;
    O2_gen_9_SS(i,O2_gen_9_SS(i,:)<600) = 0;
    O2_gen_10_SS(i,O2_gen_10_SS(i,:)<600) = 0;
    V_H2_1_SS(i,O2_gen_1_SS(i,:)>0) =
(abs(H2_diff_1_SS(i,O2_gen_1_SS(i,:)>0))./(abs(H2_diff_1_SS(i,O2_gen_1_SS(i,:)>0))+O2
_gen_1_SS(i,O2_gen_1_SS(i,:)>0)))*(1-P_H2O_sat_SS(i,end)/101325);
    V_H2_2_SS(i,O2_gen_2_SS(i,:)>0) =
(abs(H2_diff_2_SS(i,O2_gen_2_SS(i,:)>0))./(abs(H2_diff_2_SS(i,O2_gen_2_SS(i,:)>0))+O2
_gen_2_SS(i,O2_gen_2_SS(i,:)>0)))*(1-P_H2O_sat_SS(i,end)/101325);
    V_H2_3_SS(i,O2_gen_3_SS(i,:)>0) =
(abs(H2_diff_3_SS(i,O2_gen_3_SS(i,:)>0))./(abs(H2_diff_3_SS(i,O2_gen_3_SS(i,:)>0))+O2
_gen_3_SS(i,O2_gen_3_SS(i,:)>0)))*(1-P_H2O_sat_SS(i,end)/101325);
    V_H2_4_SS(i,O2_gen_4_SS(i,:)>0) =
(abs(H2_diff_4_SS(i,O2_gen_4_SS(i,:)>0))./(abs(H2_diff_4_SS(i,O2_gen_4_SS(i,:)>0))+O2
_gen_4_SS(i,O2_gen_4_SS(i,:)>0)))*(1-P_H2O_sat_SS(i,end)/101325);
    V_H2_5_SS(i,O2_gen_5_SS(i,:)>0) =
(abs(H2_diff_5_SS(i,O2_gen_5_SS(i,:)>0))./(abs(H2_diff_5_SS(i,O2_gen_5_SS(i,:)>0))+O2
_gen_5_SS(i,O2_gen_5_SS(i,:)>0)))*(1-P_H2O_sat_SS(i,end)/101325);
```

```
    V_H2_6_SS(i,O2_gen_6_SS(i,:)>0) =
(abs(H2_diff_6_SS(i,O2_gen_6_SS(i,:)>0))./(abs(H2_diff_6_SS(i,O2_gen_6_SS(i,:)>0))+O2
_gen_6_SS(i,O2_gen_6_SS(i,:)>0)))*(1-P_H2O_sat_SS(i,end)/101325);
    V_H2_7_SS(i,O2_gen_7_SS(i,:)>0) =
(abs(H2_diff_7_SS(i,O2_gen_7_SS(i,:)>0))./(abs(H2_diff_7_SS(i,O2_gen_7_SS(i,:)>0))+O2
_gen_7_SS(i,O2_gen_7_SS(i,:)>0)))*(1-P_H2O_sat_SS(i,end)/101325);
    V_H2_8_SS(i,O2_gen_8_SS(i,:)>0) =
(abs(H2_diff_8_SS(i,O2_gen_8_SS(i,:)>0))./(abs(H2_diff_8_SS(i,O2_gen_8_SS(i,:)>0))+O2
_gen_8_SS(i,O2_gen_8_SS(i,:)>0)))*(1-P_H2O_sat_SS(i,end)/101325);
    V_H2_9_SS(i,O2_gen_9_SS(i,:)>0) =
(abs(H2_diff_9_SS(i,O2_gen_9_SS(i,:)>0))./(abs(H2_diff_9_SS(i,O2_gen_9_SS(i,:)>0))+O2
_gen_9_SS(i,O2_gen_9_SS(i,:)>0)))*(1-P_H2O_sat_SS(i,end)/101325);
    V_H2_10_SS(i,O2_gen_10_SS(i,:)>0) =
(abs(H2_diff_10_SS(i,O2_gen_10_SS(i,:)>0))./(abs(H2_diff_10_SS(i,O2_gen_10_SS(i,:)>0)
)+O2_gen_10_SS(i,O2_gen_10_SS(i,:)>0)))*(1-P_H2O_sat_SS(i,end)/101325);
    V_H2_1_SS(i,O2_gen_1_SS(i,:)==0) = 0;
    V_H2_2_SS(i,O2_gen_2_SS(i,:)==0) = 0;
    V_H2_3_SS(i,O2_gen_3_SS(i,:)==0) = 0;
    V_H2_4_SS(i,O2_gen_4_SS(i,:)==0) = 0;
    V_H2_5_SS(i,O2_gen_5_SS(i,:)==0) = 0;
    V_H2_6_SS(i,O2_gen_6_SS(i,:)==0) = 0;
    V_H2_7_SS(i,O2_gen_7_SS(i,:)==0) = 0;
    V_H2_8_SS(i,O2_gen_8_SS(i,:)==0) = 0;
    V_H2_9_SS(i,O2_gen_9_SS(i,:)==0) = 0;
    V_H2_10_SS(i,O2_gen_10_SS(i,:)==0) = 0;
end
save_system("GHGS_MSA_v5")
%% Create Plots for Input Data
close all
TS = 7*24; %Plot Time Spans (# of days*24 hours)
figure('name','Scaled 100% wind/pv Generation vs. Load','position',[0 0 1080 720])
    p1 = plot(ERCOT_time(1:TS),sys_load(1:TS),'-
k',ERCOT_time(1:TS),sys_wind_gen(1:TS),'-b',ERCOT_time(1:TS),sys_pv_gen(1:TS),'-
y',ERCOT_time(1:TS),sys_RE_gen(1:TS),'-g');
    legend({'System Grid Load','System Wind Generation','System PV Generation','Total
System Generation'})
    xlabel('Time [hours]')
    xlim([0 TS])
    ylabel('Load/Generation [MW]')
    p1(1).Color = [0 0 0];
    p1(1).LineWidth = 4;
    p1(2).Color = [0 0.14118 0.8]; %Blue
    p1(2).LineWidth = 4;
    p1(3).Color = [1 .49804 0]; %Aggies Orange
    p1(3).LineWidth = 4;
    p1(4).Color = [0 .3 .08]; %CSU Green
    p1(4).LineWidth = 4;
    grid on
    ax = gca;
    set(ax,'Fontsize',20)
figure('name','Extra vs Short Generation','position',[0 0 1080 720])
    p2 = plot(ERCOT_time(1:8760),kWh_extra(1:8760),'-
g',ERCOT_time(1:8760),kWh_short(1:8760),'-r');
figure('name','Wind and PV Capacity Factors','position',[0 0 1080 720]);
```

```
    p3 =
plot(ERCOT_time(1:TS),ERCOT_wind_cf(1:TS),ERCOT_time(1:TS),ERCOT_pv_cf(1:TS));
    xlabel('Time [hours]')
    xlim([0 TS])
    ylabel('Capacity Factor [-]')
    ylim([0 1])
    legend({'Wind Capacity Factor','PV Capacity Factor'})
    p3(1).Color = [0 0.14118 0.8]; %Blue
    p3(1).LineWidth = 4;
    p3(2).Color = [1 .49804 0]; %Aggies Orange
    p3(2).LineWidth = 4;
    grid on
    ax = gca;
    set(ax,'Fontsize',20)
figure('name','Generation vs. Load','position',[0 0 1300 950])
    tl = tiledlayout(2,1);
    ax1 = nexttile;
    t = [1:1/1000:TS]; %Increase fidelity to make the plot look better
    RE_gen = interp1(sys_RE_gen,1:1/1000:TS);%Increase fidelity to make the plot look
better
    RE_load = interp1(sys_load,1:1/1000:TS);%Increase fidelity to make the plot look
better
    Lv = RE_gen >= RE_load;% Logical Vector when generation is greater than load
    hold on
    fill([t(Lv) fliplr(t(Lv))], [RE_gen(Lv)
fliplr(RE_load(Lv))],'g','edgecolor','none','FaceAlpha','0.5')
    fill([t(~Lv) fliplr(t(~Lv))], [RE_gen(~Lv)
fliplr(RE_load(~Lv))],'r','edgecolor','none','FaceAlpha','0.5')
    plot(t,RE_gen,'-ok','linewidth',4,'color',[0 .3
.08],'MarkerIndices',1:5000:length(RE_gen))
    plot(t,RE_load,'-k','linewidth',4)
    hold off
    title('A)')
    ax1.TitleHorizontalAlignment = 'left';
    xlim([0 TS])
    legend({'Excess Generation','Insufficient Generation','RE Generation','Grid
Load'},'location','bestoutside')
    ax = gca;
    set(ax,'Fontsize',20)
    xlabel('Time [hours]')
    ylabel({'Load/Generation','[MW]'})
    grid on

    ax2 = nexttile;
    p11 = plot(ERCOT_time(1:TS),ex_RE(1:TS),'-');
    title('B)')
    ax2.TitleHorizontalAlignment = 'left';
    p11(1).Color = [0 .3 .08]; %CSU Green
    p11(1).LineWidth = 4;
    yline(1.31*10,'--','label','Max Input - 13.1 MW','color',[0 0
0],'LineWidth',4,'Fontsize',20);
    yline(0.148,'--','label',{'Min Input -','148 kW'},'color',[0 0
0],'LineWidth',4,'Fontsize',20,'LabelHorizontalAlignment','left');
    xlim([0 TS])
    xlabel('Time [hours]')
```

```
    ylabel({'Excess RE Generation','[MW]'})
    legend('Excess Renewable Energy','location','bestoutside')
    grid on
    ax = gca;
    set(ax,'Fontsize',20)
figure('name','Scaled ERCOT Load/Generation Data','position',[0 0 1080 720])
    hold on
    fill([t(Lv) fliplr(t(Lv))], [RE_gen(Lv)
fliplr(RE_load(Lv))],'g','edgecolor','none','FaceAlpha','0.5')
    fill([t(~Lv) fliplr(t(~Lv))], [RE_gen(~Lv)
fliplr(RE_load(~Lv))],'r','edgecolor','none','FaceAlpha','0.5')
    plot(t,RE_gen,'-ok','linewidth',4,'color',[0 .3
.08],'MarkerIndices',1:5000:length(RE_gen))
    plot(t,RE_load,'-k','linewidth',4)
    hold off
    xlim([0 TS])
    legend({'Excess Generation','Insufficient Generation','RE Generation','Grid
Load'},'location','best')
    ax = gca;
    set(ax,'Fontsize',20)
    xlabel('Time [hours]')
    ylabel({'Load/Generation','[MW]'})
    grid on
figure('name','Scaled ERCOT Excess Generation Input','position',[0 0 1080 720])
    p11 = plot(ERCOT_time(1:TS),ex_RE(1:TS),'-');
    p11(1).Color = [0 .3 .08]; %CSU Green
    p11(1).LineWidth = 4;
    yline(1.31*10,'--','label','Max Input - 13.1 MW','color',[0 0
0],'LineWidth',4,'Fontsize',20);
    yline(0.148,'--','color',[0 0 0],'LineWidth',4);
    xlim([0 TS])
    xlabel('Time [hours]')
    ylabel({'Excess RE Generation','[MW]'})
    legend('Excess Renewable Energy','location','best')
    grid on
    ax = gca;
    set(ax,'Fontsize',20)
    annotation('textbox',...
        [0.746296296296298 0.128166669439938 0.147222218110606 0.106944441671173],...
        'String',{'Min Input -','148 kW'},...
        'FontSize',20,'EdgeColor','none');
figure('name','GHGS Model: Electrolyzer Operating Factors - Series
Loading','position',[0 0 1080 720])
    p4 = plot(ERCOT_time(1:TS),OF1_SL(1,1:TS),'-', ...
        ERCOT_time(1:TS),OF2_SL(1,1:TS),'-', ...
        ERCOT_time(1:TS),OF3_SL(1,1:TS),'-', ...
        ERCOT_time(1:TS),OF4_SL(1,1:TS),'-', ...
        ERCOT_time(1:TS),OF5_SL(1,1:TS),'-', ...
        ERCOT_time(1:TS),OF6_SL(1,1:TS),'-', ...
        ERCOT_time(1:TS),OF7_SL(1,1:TS),'-', ...
        ERCOT_time(1:TS),OF8_SL(1,1:TS),'-', ...
        ERCOT_time(1:TS),OF9_SL(1,1:TS),'-', ...
        ERCOT_time(1:TS),OF10_SL(1,1:TS),'-');
    xlim([0 TS])
```

```
figure('name','GHGS Model: Excess Renewable Energy and Hydrogen
Production','position',[0 0 1080 720])
    yyaxis left
    p5 = plot(ERCOT_time(1:TS),ex_RE(1:TS),'-');
    p5(1).Color = [0 .3 .08]; %CSU Green
    p5(1).LineWidth = 4;
    yyaxis right
    p6 = plot(Time_SL(1:TS),H2Flowrate_SL(1:TS),'-
*',Time_EL(1,1:TS),H2Flowrate_EL(1,1:TS),'-^');
    p6(1).Color = [0 0.14118 0.8]; %Blue
    p6(1).LineWidth = 4;
    p6(2).Color = [1 .49804 0]; %Aggies Orange
    p6(2).LineWidth = 4;
    xlim([0 TS])
    xlabel('Time [hours]')
    legend({'Excess Renewable Energy','Hydrogen Flowrate with SL Scheme','Hydrogen
Flowrate with PL Scheme'})
    grid on
    ax = gca;
    set(ax,'Fontsize',20)
    ax.YAxis(1).Color = [0 .3 .08];
    ax.YAxis(2).Color = [0 0 0];
figure('name','Average Stack Load SL vs PL','position',[0 0 1080 720])
    t = tiledlayout(2,1);
    ax1 = nexttile;
    p7 =
plot([1:10],avg_stack_load_SL(:,1),'o',[1:10],avg_stack_load_EL(:,3),'o',[1:10],avg_s
tack_load_EL(:,10),'^');
    title('A)')
    ax1.TitleHorizontalAlignment = 'left';
    p7(1).Color = [0 0.14118 0.8]; %Blue
    p7(1).MarkerFaceColor = [0 0.14118 0.8]; %Blue
    p7(1).MarkerSize = 10;
    p7(2).Color = [1 .49804 0]; %Aggies Orange
    p7(2).MarkerFaceColor = [1 .49804 0]; %Aggies Orange
    p7(2).MarkerSize = 10;
    p7(3).Color = [1 .49804 0]; %Aggies Orange
    p7(3).MarkerFaceColor = [1 .49804 0]; %Aggies Orange
    p7(3).MarkerSize = 10;
    ax = gca;
    set(ax,'Fontsize',20)
    grid on
    ylabel({'Average Electrolyzer','Power [MW]'})
    legend({'Series Loading - 10% Limit','Parallel Loading - 20% Limit','Parallel
Loading - 55% Limit'},'location','southeast')
    xticks([1:10])
    xlim([1 10])
    ylim([0.6 1.25])
    yticks([0.65:0.1:1.25])
    xticklabels({'Stack 1' 'Stack 2' 'Stack 3' 'Stack 4' 'Stack 5' 'Stack 6' 'Stack
7' 'Stack 8' 'Stack 9' 'Stack 10'})

    ax2 = nexttile;
    p12 = plot(1:length(AC_curt_SL),AC_curt_SL,'-
',1:length(AC_curt_EL),AC_curt_EL,'diamond');
```

```
    title('B)')
    ax2.TitleHorizontalAlignment = 'left';
    p12(1).Color = [0 0.14118 0.8]; %Blue
    p12(1).LineWidth = 4;
    p12(1).MarkerFaceColor = [0 0.14118 0.8]; %Blue
    p12(2).Color = [1 .49804 0]; %Aggies Orange
    p12(2).MarkerSize = 10;
    p12(2).MarkerFaceColor = [1 .49804 0]; %Aggies Orange
    xticks([1:length(AC_curt_SL)])
    xlim([1 15])
    xlabel('Min. Electrolyzer Power - % of Rated')
    xticklabels({'10%' '15%' '20%' '25%' '30%' '35%' '40%' '45%' '50%' '55%' '60%'
'65%' '70%' '75%' '80%'})
    ylabel({'Curtailed Renewable','Energy Input [MW-hr]'})
    legend({'Series Loading','Parallel Loading'},'location','best')
    ax = gca;
    set(ax,'Fontsize',20)
    ax.YAxis(1).Color = [0 0 0];
    grid on
figure('name','System Efficiency and H2 Gen Sequential Loading vs Even
Loading','position',[0 0 1080 720])
    yyaxis left
    p8 =
plot(1:length(eta_total_SL),eta_total_SL,'square',1:length(eta_total_EL),eta_total_EL
,'diamond');
    p8(1).Color = [1 .49804 0]; %Aggies Orange
    p8(1).MarkerSize = 10;
    p8(1).MarkerFaceColor = [1 .49804 0];
    p8(2).Color = [1 .49804 0]; %Aggies Orange
    p8(2).MarkerSize = 10;
    p8(2).MarkerFaceColor = [1 .49804 0];
    xticks([1:length(eta_total_EL)])
    xlim([1 15])
    xlabel('Min. Electrolyzer Power - % of Rated')
    xticklabels({'10%' '15%' '20%' '25%' '30%' '35%' '40%' '45%' '50%' '55%' '60%'
'65%' '70%' '75%' '80%'})
    ylabel('System Efficiency')

    yyaxis right
    p9 =
plot(1:length(eta_total_SL),HydrogenProduced_SL(:,end),'square',1:length(eta_total_EL
),HydrogenProduced_EL(:,end),'diamond');
    p9(1).MarkerSize = 10;
    p9(1).LineWidth = 2;
    p9(1).Color = [0 .3 .08]; %CSU Green
    p9(2).MarkerSize = 10;
    p9(2).LineWidth = 2;
    p9(2).Color = [0 .3 .08]; %CSU Green
    ylabel('Hydrogen Produced [kg]')
    legend({'System Efficiency - Parallel Loading','System Efficiency - Series
Loading','Hydrogen Produced - Parallel Loading','Hydrogen Produced - Series
Loading'},'location','northwest')
    ax = gca;
    set(ax,'Fontsize',20)
    ax.YAxis(1).Color = [1 .49804 0];
```

```
    ax.YAxis(2).Color = [0 .3 .08];
    grid on
figure('name','Excess RE Generation Input','position',[0 0 1300 720])
    p11 = plot(ERCOT_time(1:TS),ex_RE(1:TS),'-');
    p11(1).Color = [0 .3 .08]; %CSU Green
    p11(1).LineWidth = 4;
    yline(1.31*10,'--','label','Max Input-13.1 MW','color',[0 0
0],'LineWidth',4,'Fontsize',20);
    yline(0.148,'--','label','Min Input-148 kW','color',[0 0
0],'LineWidth',4,'Fontsize',20,'LabelHorizontalAlignment','left');
    xlim([0 TS])
    xlabel('Time [hours]')
    ylabel('Excess RE Generation [MW]')
    legend('Excess Renewable Energy','location','north')
    grid on
    ax = gca;
    set(ax,'Fontsize',20)
figure('name','System Efficiency Sequential Loading vs Even Loading','position',[0 0
1080 720])
    eta_total_SL_perc = eta_total_SL.*100;
    eta_total_EL_perc = eta_total_EL.*100;
    p8 =
plot(1:length(eta_total_SL_perc),eta_total_SL_perc,'o',1:length(eta_total_EL_perc),et
a_total_EL_perc,'diamond');
    p8(1).Color = [0 0.14118 0.8]; %Blue
    p8(1).LineWidth = 4;
    p8(1).MarkerFaceColor = [0 0.14118 0.8]; %Blue
    p8(2).Color = [1 .49804 0]; %Aggies Orange
    p8(2).MarkerSize = 10;
    p8(2).MarkerFaceColor = [1 .49804 0]; %Aggies Orange
    xticks([1:length(eta_total_EL)])
    xlim([1 15])
    xlabel('Min. Electrolyzer Power - % of Rated')
    xticklabels({'10%' '15%' '20%' '25%' '30%' '35%' '40%' '45%' '50%' '55%' '60%'
'65%' '70%' '75%' '80%'})
    ylabel('System Energy Conversion Efficiency - %')
    legend({'Series Loading','Parallel Loading'},'location','south')
    ax = gca;
    set(ax,'Fontsize',20)
    ax.YAxis(1).Color = [0 0 0];
    grid on
figure('name','System Efficiency Sequential Loading vs Even Loading','position',[0 0
1080 720])
    p12 =
plot(1:length(AC_curt_SL),AC_curt_SL,'o',1:length(AC_curt_EL),AC_curt_EL,'diamond');
    p12(1).Color = [0 0.14118 0.8]; %Blue
    p12(1).LineWidth = 4;
    p12(1).MarkerFaceColor = [0 0.14118 0.8]; %Blue
    p12(2).Color = [1 .49804 0]; %Aggies Orange
    p12(2).MarkerSize = 10;
    p12(2).MarkerFaceColor = [1 .49804 0]; %Aggies Orange
    xticks([1:length(AC_curt_SL)])
    xlim([1 15])
    xlabel('Min. Electrolyzer Power - % of Rated')
```

```
    xticklabels({'10%' '15%' '20%' '25%' '30%' '35%' '40%' '45%' '50%' '55%' '60%'
'65%' '70%' '75%' '80%'})
    ylabel('Curtailed Renewable Energy Input [kWh]')
    legend({'Series Loading','Parallel Loading'},'location','eastoutside')
    ax = gca;
    set(ax,'Fontsize',20)
    ax.YAxis(1).Color = [0 0 0];
    grid on
figure('name','Average Stack Load SL vs PL horizontal','position',[0 0 1080 720])
    t = tiledlayout(1,2);
    ax1 = nexttile;
    p7 =
plot([1:10],avg_stack_load_SL(:,1),'o',[1:10],avg_stack_load_EL(:,3),'o',[1:10],avg_s
tack_load_EL(:,10),'^');
    title('A)')
    ax1.TitleHorizontalAlignment = 'left';
    p7(1).Color = [0 0.14118 0.8]; %Blue
    p7(1).MarkerFaceColor = [0 0.14118 0.8]; %Blue
    p7(1).MarkerSize = 10;
    p7(2).Color = [1 .49804 0]; %Aggies Orange
    p7(2).MarkerFaceColor = [1 .49804 0]; %Aggies Orange
    p7(2).MarkerSize = 10;
    p7(3).Color = [1 .49804 0]; %Aggies Orange
    p7(3).MarkerFaceColor = [1 .49804 0]; %Aggies Orange
    p7(3).MarkerSize = 10;
    ax = gca;
    set(ax,'Fontsize',20)
    grid on
    ylabel({'Average Electrolyzer','Power [MW]'})
    legend({'Series Loading - 10% Limit','Parallel Loading - 20% Limit','Parallel
Loading - 55% Limit'},'location','southeast')
    xticks([1:10])
    xlim([1 10])
    ylim([0.6 1.25])
    yticks([0.65:0.1:1.25])
    xticklabels({'Stack 1' 'Stack 2' 'Stack 3' 'Stack 4' 'Stack 5' 'Stack 6' 'Stack
7' 'Stack 8' 'Stack 9' 'Stack 10'})

    ax2 = nexttile;
    p12 =
plot(1:length(AC_curt_SL),AC_curt_SL,'o',1:length(AC_curt_EL),AC_curt_EL,'diamond');
    title('B)')
    ax2.TitleHorizontalAlignment = 'left';
    p12(1).Color = [0 0.14118 0.8]; %Blue
    p12(1).LineWidth = 4;
    p12(1).MarkerFaceColor = [0 0.14118 0.8]; %Blue
    p12(2).Color = [1 .49804 0]; %Aggies Orange
    p12(2).MarkerSize = 10;
    p12(2).MarkerFaceColor = [1 .49804 0]; %Aggies Orange
    xticks([1:length(AC_curt_SL)])
    xlim([1 15])
    xlabel('Min. Electrolyzer Power - % of Rated')
    xticklabels({'10%' '15%' '20%' '25%' '30%' '35%' '40%' '45%' '50%' '55%' '60%'
'65%' '70%' '75%' '80%'})
    ylabel({'Curtailed Renewable','Energy Input [MW-hr]'})
```

```
    legend({'Series Loading','Parallel Loading'},'location','best')
    ax = gca;
    set(ax,'Fontsize',20)
    ax.YAxis(1).Color = [0 0 0];
    grid on
figure('name','Average Stack Load SL vs PL horizontal','position',[0 0 1080 720])
    p7 =
plot([1:10],avg_stack_load_SL(:,1),'o',[1:10],avg_stack_load_EL(:,3),'o',[1:10],avg_s
tack_load_EL(:,10),'^');
    p7(1).Color = [0 0.14118 0.8]; %Blue
    p7(1).MarkerFaceColor = [0 0.14118 0.8]; %Blue
    p7(1).MarkerSize = 10;
    p7(2).Color = [1 .49804 0]; %Aggies Orange
    p7(2).MarkerFaceColor = [1 .49804 0]; %Aggies Orange
    p7(2).MarkerSize = 10;
    p7(3).Color = [1 .49804 0]; %Aggies Orange
    p7(3).MarkerFaceColor = [1 .49804 0]; %Aggies Orange
    p7(3).MarkerSize = 10;
    ax = gca;
    set(ax,'Fontsize',20)
    grid on
    ylabel({'Average Electrolyzer','Power [MW]'})
    legend({'Series Loading - 10% Limit','Parallel Loading - 20% Limit','Parallel
Loading - 55% Limit'},'location','southeast')
    xticks([1:10])
    xlim([1 10])
    ylim([0.6 1.25])
    yticks([0.65:0.1:1.25])
    xticklabels({'Stack 1' 'Stack 2' 'Stack 3' 'Stack 4' 'Stack 5' 'Stack 6' 'Stack
7' 'Stack 8' 'Stack 9' 'Stack 10'})
figure('name','Curtailed RE Input SL vs PL','position',[0 0 1080 720])
    p12 =
plot(1:length(AC_curt_SL),AC_curt_SL,'o',1:length(AC_curt_EL),AC_curt_EL,'diamond');
    p12(1).Color = [0 0.14118 0.8]; %Blue
    p12(1).LineWidth = 4;
    p12(1).MarkerFaceColor = [0 0.14118 0.8]; %Blue
    p12(2).Color = [1 .49804 0]; %Aggies Orange
    p12(2).MarkerSize = 10;
    p12(2).MarkerFaceColor = [1 .49804 0]; %Aggies Orange
    xticks([1:length(AC_curt_SL)])
    xlim([1 15])
    xlabel('Min. Electrolyzer Power - % of Rated')
    xticklabels({'10%' '15%' '20%' '25%' '30%' '35%' '40%' '45%' '50%' '55%' '60%'
'65%' '70%' '75%' '80%'})
    ylabel({'Curtailed Renewable','Energy Input [MW-hr]'})
    legend({'Series Loading','Parallel Loading'},'location','best')
    ax = gca;
    set(ax,'Fontsize',20)
    ax.YAxis(1).Color = [0 0 0];
    grid on
figure('name','Hydrogen Produced SL vs PL','position',[0 0 1080 720])
    p =
plot(1:length(HydrogenProduced_SL(:,end)),HydrogenProduced_SL(:,end),'o',1:length(Hyd
rogenProduced_EL(:,end)),HydrogenProduced_EL(:,end),'diamond');
    p(1).Color = [0 0.14118 0.8]; %Blue
```

```
    p(1).LineWidth = 4;
    p(1).MarkerFaceColor = [0 0.14118 0.8]; %Blue
    p(2).Color = [1 .49804 0]; %Aggies Orange
    p(2).MarkerSize = 10;
    p(2).MarkerFaceColor = [1 .49804 0]; %Aggies Orange
    xticks([1:length(AC_curt_SL)])
    xlim([1 15])
    xlabel('Min. Electrolyzer Power - % of Rated')
    xticklabels({'10%' '15%' '20%' '25%' '30%' '35%' '40%' '45%' '50%' '55%' '60%'
'65%' '70%' '75%' '80%'})
    ylabel('Hydrogen Produced [kg]')
    legend({'Series Loading','Parallel Loading'},'location','best')
    ax = gca;
    set(ax,'Fontsize',20)
    grid on
figure('name','Number of Shutdowns SL Scheme - overlayed','position',[0 0 1080 720])
    hold on
    plot([1:length(MinStackSetpoint)],num_shutdowns1_SL,'-','Color',[0 0.14118 0.8
1],'LineWidth',4);
    plot([1:length(MinStackSetpoint)],num_shutdowns2_SL,'-','Color',[0 0.14118 0.8
.9],'LineWidth',4);
    plot([1:length(MinStackSetpoint)],num_shutdowns3_SL,'-','Color',[0 0.14118 0.8
.8],'LineWidth',4);
    plot([1:length(MinStackSetpoint)],num_shutdowns4_SL,'-','Color',[0 0.14118 0.8
.7],'LineWidth',4);
    plot([1:length(MinStackSetpoint)],num_shutdowns5_SL,'-','Color',[0 0.14118 0.8
.6],'LineWidth',4);
    plot([1:length(MinStackSetpoint)],num_shutdowns6_SL,'-','Color',[0 0.14118 0.8
.5],'LineWidth',4);
    plot([1:length(MinStackSetpoint)],num_shutdowns7_SL,'-','Color',[0 0.14118 0.8
.4],'LineWidth',4);
    plot([1:length(MinStackSetpoint)],num_shutdowns8_SL,'-','Color',[0 0.14118 0.8
.3],'LineWidth',4);
    plot([1:length(MinStackSetpoint)],num_shutdowns9_SL,'-','Color',[0 0.14118 0.8
.25],'LineWidth',4);
    plot([1:length(MinStackSetpoint)],num_shutdowns10_SL,'-','Color',[0 0.14118 0.8
.2],'LineWidth',4);
    xticks([1:length(MinStackSetpoint)])
    xlim([1 length(MinStackSetpoint)])
    ylabel('# of Shutdowns','Fontsize',20)
    xlabel('Min. Electrolyzer Power - % of Rated')
    xticklabels({'10%' '15%' '20%' '25%' '30%' '35%' '40%' '45%' '50%' '55%' '60%'
'65%' '70%' '75%' '80%'})
    legend({'Stack 1','Stack 2','Stack 3','Stack 4','Stack 5','Stack 6','Stack
7','Stack 8','Stack 9','Stack 10'},'location','eastoutside')
    ax = gca;
    set(ax,'Fontsize',20)
    grid on
figure('name','Number of Shutdowns EL Scheme - overlayed','position',[0 0 1080 720])
    hold on
    plot([1:length(MinStackSetpoint)],num_shutdowns1_EL,'-','Color',[1 .49804 0
1],'LineWidth',4);
    plot([1:length(MinStackSetpoint)],num_shutdowns2_EL,'-','Color',[1 .49804 0
.9],'LineWidth',4);
```

```
    plot([1:length(MinStackSetpoint)],num_shutdowns3_EL,'-','Color',[1 .49804 0
.8],'LineWidth',4);
    plot([1:length(MinStackSetpoint)],num_shutdowns4_EL,'-','Color',[1 .49804 0
.7],'LineWidth',4);
    plot([1:length(MinStackSetpoint)],num_shutdowns5_EL,'-','Color',[1 .49804 0
.6],'LineWidth',4);
    plot([1:length(MinStackSetpoint)],num_shutdowns6_EL,'-','Color',[1 .49804 0
.5],'LineWidth',4);
    plot([1:length(MinStackSetpoint)],num_shutdowns7_EL,'-','Color',[1 .49804 0
.4],'LineWidth',4);
    plot([1:length(MinStackSetpoint)],num_shutdowns8_EL,'-','Color',[1 .49804 0
.3],'LineWidth',4);
    plot([1:length(MinStackSetpoint)],num_shutdowns9_EL,'-','Color',[1 .49804 0
.25],'LineWidth',4);
    plot([1:length(MinStackSetpoint)],num_shutdowns10_EL,'-','Color',[1 .49804 0
.2],'LineWidth',4);
    xticks([1:length(MinStackSetpoint)])
    xlim([1 length(MinStackSetpoint)])
    ylabel('# of Shutdowns','Fontsize',20)
    xlabel('Min. Electrolyzer Power - % of Rated')
    xticklabels({'10%' '15%' '20%' '25%' '30%' '35%' '40%' '45%' '50%' '55%' '60%'
'65%' '70%' '75%' '80%'})
    legend({'Stack 1','Stack 2','Stack 3','Stack 4','Stack 5','Stack 6','Stack
7','Stack 8','Stack 9','Stack 10'},'location','eastoutside')
    ax = gca;
    set(ax,'Fontsize',20)
    grid on
figure('name','Total Number of Shutdowns SL Scheme','position',[0 0 1080 720])
    p = plot([1:length(MinStackSetpoint)],tot_shutdowns_SL,'-
o',[1:length(MinStackSetpoint)],tot_shutdowns_EL,'-diamond');
    p(1).LineWidth = 4;
    p(1).Color = [0 0.14118 0.8]; %Blue
    p(2).LineWidth = 4;
    p(2).Color = [1 .49804 0]; %Aggies Orange
    xticks([1:length(MinStackSetpoint)])
    xlim([1 length(MinStackSetpoint)])
    xlabel('Min. Electrolyzer Power - % of Rated')
    xticklabels({'10%' '15%' '20%' '25%' '30%' '35%' '40%' '45%' '50%' '55%' '60%'
'65%' '70%' '75%' '80%'})
    ylabel('# of Shutdowns')
    ax = gca;
    set(ax,'Fontsize',20)
    grid on
    legend({'Series Loading','Parallel Loading'},'location','northeast')
figure('name','System Efficiency vs System Scaling','position',[0 0 1080 720])
    eta_total_SS1p = eta_total_SS1.*100;
    eta_total_SS2p = eta_total_SS2.*100;
    p = plot([1:10],eta_total_SS1p,'o',[1:10],eta_total_SS2p,'diamond');
    p(1).LineWidth = 4;
    p(1).MarkerSize = 10;
    p(1).Color = [0 .3 .08]; %CSU Green
    p(2).LineWidth = 4;
    p(2).MarkerSize = 10;
    p(2).Color = [1 .49804 0]; %CSU Green
    xticks([1:10])
```

```
    xlim([1 10])
    xticklabels({'10 Stacks' '9 Stacks' '8 Stacks' '7 Stacks' '6 Stacks' '5 Stacks'
'4 Stacks' '3 Stacks' '2 Stacks' '1 Stacks'})
    xlabel('# of Electrolyzers in System')
    ylabel({'System Energy Conversion','Efficiency - %'})
    ax = gca;
    set(ax,'Fontsize',20)
    grid on
    legend({'Efficiency w/ Total AC Power Availible','Efficiency w/ Only Utilized AC
Power'},'location','best')
figure('name','System Efficiency vs System Scaling - method 1','position',[0 0 1080
720])
    p = plot([1:10],eta_total_SS1p,'-o');
    p(1).LineWidth = 4;
    p(1).MarkerSize = 10;
    p(1).Color = [0 .3 .08]; %CSU Green
    xticks([1:10])
    xlim([1 10])
    xticklabels({'10 Stacks' '9 Stacks' '8 Stacks' '7 Stacks' '6 Stacks' '5 Stacks'
'4 Stacks' '3 Stacks' '2 Stacks' '1 Stacks'})
    xlabel('# of Electrolyzers in System')
    ylabel({'System Energy Conversion','Efficiency - %'})
    ylim([10 50])
    yticks([10:5:50])
    ax = gca;
    set(ax,'Fontsize',20)
    grid on
figure('name','System Efficiency vs System Scaling - 0.3 scaling
factor','position',[0 0 1080 720])
    p = plot([1:10],eta_total_SS1p,'-o');
    p(1).LineWidth = 4;
    p(1).MarkerSize = 10;
    p(1).Color = [0 .3 .08]; %CSU Green
    xticks([1:10])
    xlim([1 10])
    xticklabels({'10 Stacks' '9 Stacks' '8 Stacks' '7 Stacks' '6 Stacks' '5 Stacks'
'4 Stacks' '3 Stacks' '2 Stacks' '1 Stacks'})
    xlabel('# of Electrolyzers in System')
    ylabel({'System Energy Conversion','Efficiency - %'})
    ylim([10 50])
    yticks([10:5:50])
    ax = gca;
    set(ax,'Fontsize',20)
    grid on
    annotation('textarrow',[0.356481481481482 0.305555555555556],...
        [0.733333333333333 0.877777777777778],...
        'String',{'Efficiency Peaks at 48.43%','with 8
Stacks'},'FontWeight','bold',...
        'FontSize',16);
figure('name','H2 Produced vs Installed Electrolyzer - method 1','position',[0 0 1080
720])
    insEZ = 1250*[10 9 8 7 6 5 4 3 2 1];
    p = plot(insEZ,HydrogenProduced_SS(:,end),'-o');
    p(1).LineWidth = 4;
    p(1).MarkerSize = 10;
```

```
    p(1).Color = [0 .3 .08]; %CSU Green
    xlabel('kW of Installed Electrolyzers')
    xlim([1250 12500])
    xticks(1250:1250:12500)
    ylabel('kg of H_2 Produced')
    ax = gca;
    set(ax,'Fontsize',20)
    ax.YAxis.Exponent = 0;
    ax.YAxis.TickLabelFormat = '%,.0f';
    ax.XAxis.TickLabelFormat = '%,.0f';
    grid on
%% Verify the zero hydrogen partial pressure in anode assumption
P_H2O_1 = 1.97e4;
P_O2_1 = 101325;
P_H2_1 = 3000000-P_H2O_1;
T = 60+273.15;
V_OC_1 = 1.2+(T*8.314)/(2*96485)*log((P_H2_1*sqrt(P_O2_1))/P_H2O_1);
P_O2_2 = 101325*(1-0.01);
V_OC_2 = 1.2+(T*8.314)/(2*96485)*log((P_H2_1*sqrt(P_O2_2))/P_H2O_1);
V_diff = V_OC_1-V_OC_2
%% Compare the amount of H2 produced with each strategy
xtra_H2 = HydrogenProduced_SL(:,end)-HydrogenProduced_EL(:,end)
```